MASSACHUSETTS INSTITUTE OF TECHNOLOGY

MVT-67-4

THE USE OF THE CHATTER MODE
IN SELF-ADAPTIVE SYSTEMS
by
Syozo Yasui

September, 1967

S.M. Thesis

MAN-VEHICLE CONTROL LABORATORY
CENTER FOR SPACE RESEARCH
MASSACHUSETTS INSTITUTE OF TECHNOLOGY
CAMBRIDGE, MASSACHUSETTS 02139

THE USE OF THE CHATTER MODE

IN SELF-ADAPTIVE SYSTEMS

by

SYOZO YASUI

E.B., University of Tokyo

(1963)

SUBMITTED IN PARTIAL FULFILLMENT

OF THE REQUIREMENTS FOR THE

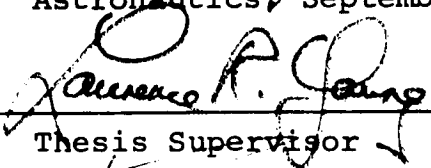DEGREE OF MASTER OF SCIENCE

at the

MASSACHUSETTS INSTITUTE OF TECHNOLOGY

September 1967

Signature of Author _____

Department of Aeronautics and
Astronautics September 1967

Certified by _____

Thesis Supervisor

Accepted by _____

Chairman, Departmental
Graduate Committee

THE USE OF THE CHATTER MODE
IN SELF-ADAPTIVE SYSTEMS

by

Syozo Yasui

Submitted to the Department of Aeronautics and
Astronautics on August 21, 1967, in partial fulfillment of
the requirements for the degree of Master of Science.

ABSTRACT

In an on-off relay control system under the chatter
mode, the average motion of the plant is completely determined
by the equation of the switching function. This fact has been
applied in self-adaptive control systems in which the switching
function describes the model dynamics, and the chatter mode
is reached. The proposed policy of forward gain (switching
level) adjustment takes into account the reduction of chatter
frequency and of the control force magnitude, in addition to
the sustenance of the chatter mode. A simple two dimensional
display is used for manual operation and/or monitoring.

Several examples are presented to demonstrate the
analog computer simulation. The results show satisfactory
performance of the gain adjustment mechanism.

Known self-adaptive control systems are outlined
with emphasis on those using a relay as a key element, and
extended application to a class of distributed parameter con-
trol systems is considered. As a byproduct of this study,
a numerical method without numerical integrations is proposed
for the solution of ordinary differential equations.

Thesis Supervisor: Laurence R. Young

Title: Associate Professor of
        Aeronautics and Astronautics

ACKNOWLEDGMENTS

TABLE OF CONTENTS

TABLE OF FIGURES

CHAPTER 1

INTRODUCTION

On-off control systems have been extensively studied and developed by a number of investigators; one can find many of these systems in operation in the field of aerospace technology, and at first glance the core of the controller, presumably a relay, is simple and relatively inexpensive. The discovery of the bang-bang principle of time optimality by Pontryalgin and his students increased the interest in these systems. This principle suggests that an on-off controller would permit time-optimum control, provided that the associated switching function is properly chosen. Unfortunately, a time-optimum switching function is difficult to obtain in a closed form, and even if obtained, its analytical expression would be too complex for practical usage.* For this reason, researchers have been developing near-time-optimal switching functions instead of exact ones.

Because of their simplicity, linear switching functions have been the most common candidates for the approximate

---

* Simple plants, such as stationary second order plants with no zero or the triple integrator plant, are exceptions. The switching functions for these are simple enough to implement with an analog computer (see ref. 12).

switching function. Most researchers have aimed at choosing

the coefficients of linear switching functions in such a way

that for a stable plant equilibrium is reached much faster

than when uncontrolled,[7,8] and for an unstable plant, the

region of stability is maximized.[10,11]

Lyapunov's second method is a powerful mathematical

tool in most of the studies related to near-optimal control.

When a switching function is non-optimum, chatter motion

or limit cycle oscillation usually occurs. Most works on

this aspect of on-off control systems, including the distin-

guished works of Flügge-Lotz and her co-workers, have been

done with non-optimum linear switching functions.[2,3,4,5,6,9]

The chatter mode will be the subject of this thesis.

Chatter motion is a singular behavior in which the state

point of the system "slides" along the switching surface,

if a perfect relay is assumed. However, since no physical

relay is perfect, the actual motion of the state point will

never actually be a sliding motion, but rather an oscillation

about the switching surface with a high frequency and a

small amplitude. Nevertheless, the average motion slides

along the switching surface. In other words, the system's

average motion is completely determined by the equation of

the switching surface, being independent of the plant's

dynamic characteristics and disturbances.

This fact leads to a self-adaptive control idea:

one may think of the equation of the switching surface as

that of the ideal model. The equation must describe stable

dynamics. The fundamental goal is to make the chatter mode dominate over the entire control envelope, or more specifically, to achieve the chatter mode as quickly as possible for any initial condition, and once it starts, to maintain it regardless of any change in operating conditions. An automatic adjustment device for the switching level or controllable gain has been developed in this thesis to meet this requirement.

The information required for this switching level adjustment device is (1) the instantaneous value of the switching function and (2) its time derivative. These two must always have opposite signs,* and the increment of the switching level is generated primarily to satisfy this requirement. The adjustment logic, however, must prevent the switching level from becoming too great. In the proposed system, a suitably designed adjustment logic would also reduce the chatter frequency.

There are two known self-adaptive control systems, described in Appendix A, which make use of a relay as a key element. The proposed system is different from both of these in its basic approach to self-adaptation. The central idea of the proposed system, the principle of using the chatter mode advantageously, may be applied in other areas, such as the control of distributed parameter systems (Appendix B) and a numerical solution for ordinary differential equations (Appendix C).

* A simple two dimensional display indicating these signs may be used for manual operation and/or monitoring.

CHAPTER 2

PRELIMINARIES: THE BEHAVIOR

OF NON-ADAPTIVE ON-OFF CONTROL SYSTEMS

2.1   General Description of Non-Adaptive Systems

A non-adaptive on-off control system is simply a

conventional on-off control system in which any parameter

of the controller is held constant. The examination of the

effects of the switching function, switching level, plant

characteristics, and the initial condition on the dynamic

behavior of the overall system will lead to the development

of the self-adaptive control system.

Figure 2.1 shows the general block diagram for the

non-adaptive on-off control system. For simplicity, the

system is assumed to be autonomous, and the standard nota-

tion, $e = x_1$, $\dot{e} = x_2$, . . . $e^{(n-1)} = x_n$, will be used for

the state variable representation, where e stands for the

output of the plant. The level of the relay is a positive

constant and is denoted by M. The input to the plant, con-

trol force u, can be written as

$$u = -M \text{ sgn } S \qquad\qquad (2.1)$$

The system can be the time optimum one, if the switching

function S is appropriate. However, the switching function

in which we are primarily interested is not optimum, but linear and stationary, and it can be written as

$$S(s) = 1 + d_1 s + d_2 s^2 + \ldots + d_m s^m \qquad (2.2a)$$

or, if the state variable representation is used,

$$S(x_1, x_2, \ldots, x_m) = x_1 + d_1 x_2 + d_2 x_3 \qquad (2.2b)$$

$$+ \ldots + d_m x_{m+1}$$

where the coefficients d_1, d_2, ..., d_m are all constant, and m is an integer.

2.2   Illustrative Examples of the Pure Inertia Plant

Let us consider first the pure inertia plant

$$G_p(s) = \frac{K}{s^2}$$

where K is a positive constant. Fig. 2.2a shows free trajectories in the phase plane x_1 - x_2 where there is no switching curve.[3,12] There are two sets of parabolic trajectories in the figure, corresponding to the polarity of the control force m, i.e., the solid trajectories are for m = -M and the dotted trajectories for m = +M. The trajectories PO and QO constitute the time optimum switching curve. A typical time optimum trajectory is sketched in fig. 2.2b.[12]

Now let us take a linear switching function:

$$S = x_1 + d_1 x_2$$

5

It is easy to conclude that the system is unstable for any initial condition if $d_1 < 0$. In fig. 2.3, the straight line MON represents the switching curve

$$S = x_1 + d_1 x_2 = 0$$

and the curve PQTR represents a dotted parabolic trajectory that is tangent to MON at T. Any solid trajectory such as AB that intersects MON at a point between T and N is immediately followed by an outgoing dotted trajectory such as BC after the switch. On the other hand, any solid trajectory such as DE that hits MON at a point between O and T is forced to remain on the switching line, and is therefore followed by a chatter motion proceeding toward T. At the instant when T is reached, the constraint is released, and the state point leaves the switching line along the dotted trajectory TR. Consequently, the system is unstable in all cases.

In the case of $d_1 = 0$, the behavior of the system is a kind of limit cycle dependent on the initial condition as shown in fig. 2.4.

For $d_1 > 0$, the switching function itself describes stable dynamics. In fig. 2.5, the straight line MON and the curve POQ represent the linear and the time optimum switching curves respectively. The two switching curves meet at U, O, and U'. The solid parabolic trajectory KTL is tangent to the switching line MON at T, and the dotted parabolic trajectory is tangent to K'T'L' at T'. The two solid

6

trajectories passing T' and U' intersect with the switching curve MON at V and W respectively. A dotted trajectory such as A_1A_2 intersecting MON at a point between T and T' is followed by a chatter motion immediately after the first switching. This chatter motion eventually brings the state point along the switching line to equilibrium, i.e., the origin, since the switching function is stable. As seen in the figure, however, other trajectories like $B_1B_2B_3$, $C_1C_2C_3$ and $D_1D_2D_3D_4$ need more than one switch to arrive somewhere between T and T' before starting the chatter motion. It should be pointed out that the system for this particular plant happens to be stable for any initial condition, but this may not be so for some other plant, even with a stable switching line and possible chatter motion.

The analytical version of the foregoing geometrical arguments is as follows. The dynamics of the system are described by a set of differential equations in terms of the state variables:

$$\dot{x}_1 = x_2$$

$$\dot{x}_2 = -M \, K \, \text{sgn} \, S$$

(2.3)

where

$$S = x_1 + d_1 x_2 \qquad (d_1 > 0) \qquad (2.4)$$

and

$$\text{sgn} \, S = \begin{cases} 1 & \text{if} \quad S > 0 \\ -1 & \text{if} \quad S < 0 \end{cases} \qquad (2.5)$$

7

Let us differentiate S with respect to time and use eq. (2.3) to obtain

$$\dot{S} = x_2 - d_1 M K \operatorname{sgn} S \qquad (2.6)$$

Multiplying both sides of this equation by sgn S and recalling that $(\operatorname{sgn} S)^2 = 1$ yields

$$\dot{S} \operatorname{sgn} S = x_2 \operatorname{sgn} S - d_1 M K \qquad (2.7)$$

This equation says that the following relation is always true whatever S may be:

$$\dot{S} \operatorname{sgn} S < 0 \qquad (2.8)$$

$$\text{if} \quad |x_2| < d_1 M K \qquad (2.9)$$

The interpretation of this is that a state point tends to approach the switching line in the strip region, $|x_2| < d_1 MK$, no matter which side of the switching line the state point is on. It follows that the segment of the switching line in that region is approachable from either side, and therefore the state point cannot cross the switching line but must "slide" along it. Any physical relay will be more or less imperfect, typically having delay and hysteresis. As a result, what actually occurs along the switching line is the chatter motion with small amplitude and high frequency. Inspecting either eq. (2.6) or eq. (2.7), it is also easy to see that the rest of the switching line belonging to the outer region, $|x_2| > d_1 MK$, is reachable only from one side as

8

indicated in fig. 2.6, and hence no chatter motion can occur there. The two terminal points of the switching line segment, namely $(-d_1^2 MK, d_1 MK)$ and $(d_1^2 MK, -d_1 MK)$, can be identified as T and T' in fig. 2.5 by a simple calculation.

During the chatter mode, the average motion of the state point is described by the equation of the switching line,

$$S = x_1 + d_1 x_2 = 0$$

or the overall system's dynamics can be expressed simply by a first order lag, $\frac{1}{1 + d_1 s}$. The amplitude of the chatter motion, depending on the degree of imperfection of the relay, may be quite small. For this reason, the instantaneous deviation of the state point from the average may also be very small. The theoretical value for sgn S during the sliding motion when the switching function S is identically zero can now be evaluated as follows.

For sliding mode,

$$S \equiv 0 \tag{2.10}$$

Then also

$$\dot{S} \equiv 0 \tag{2.11}$$

Thus from eq. (2.6)

$$\text{sgn } S = \frac{x_2}{d_1 MK} \tag{2.12}$$

For the chatter mode, this can be considered to be the average output of the physical relay.

2.3 Undesirable Phenomena

Suppose that the plant contains a zero, $S = -\alpha$. Then

$$G_p(s) = \frac{K(s + \alpha)}{s^2} \tag{2.13}$$

The dynamics of the system can be written

$$\dot{x}_1 = x_2$$

$$\dot{x}_2 = -MK(\text{sgn } S + \alpha \frac{d \text{ sgn } S}{dt}) \tag{2.14}$$

where the switching function is the same as in the last case of the foregoing section, namely

$$S = x_1 + d_1 x_2 \qquad (d_1 > 0) \tag{2.4}$$

We are now interested in seeing how the zero introduced in the plant will change the overall dynamics of the system. From eq. (2.4) and eq. (2.14) $\dot{S}$ becomes

$$\dot{S} = x_2 - d_1 MK \text{ sgn } S - \alpha d_1 MK \frac{d \text{ sgn } S}{dt} \tag{2.15}$$

This equation is the same as eq. (2.6) except that the last term on the right hand side has been added. Except for the exact moments of switching, the last term vanishes, and a trajectory in the phase plane belongs to the same parabolic family as before.

At each switching moment, on the other hand, $\frac{d}{dt}(\text{sgn } S)$ behaves like the delta function with polarity depending on the direction of the switch. This fact will result in a jumping phenomenon whenever the state point hits the switching line. The magnitude of each jump is given by $|\alpha|$ MK in the direction of x_2 or $|\alpha| d_1$MK in the direction perpendicular to the switching line.

Fig. 2.7a shows a possible motion when $\alpha > 0$, i.e., negative zero. The imperfection of the relay may be somewhat exaggerated in the figure. The motion is a high frequency oscillation which is one-sided with respect to the switching line. The magnitude of the jumping could be relatively large. Fig. 2.7b and fig. 2.7c show two different conceivable motions when $\alpha < 0$, i.e., positive zero.

The argument can be extended to show the possible existence of similar motions for higher order plants with one or more zeroes.[5] Furthermore, replacing the switching function

$$S = x_1 + d_1 x_2$$

with a second order switching function

$$S = x_1 + d_1 x_2 + d_2 x_3 \qquad (d_1, d_2 > 0)$$

instead of introducing a zero in the plant will cause similar jumping behavior, since $\dot{S}$ again will contain the factor $\frac{d}{dt}(\text{sgn } S)$. Needless to say, these phenomena are undesirable and should be avoided.
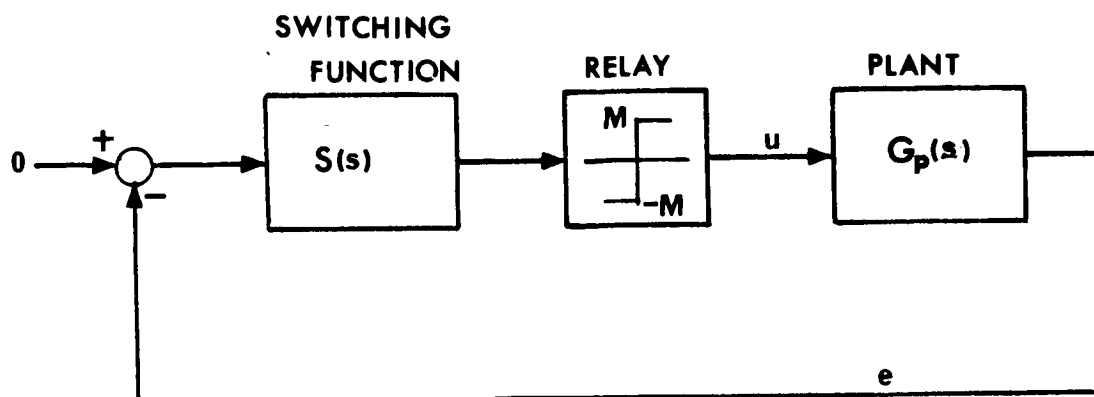
Fig. 2.1 Non-Adaptive On-Off Control System
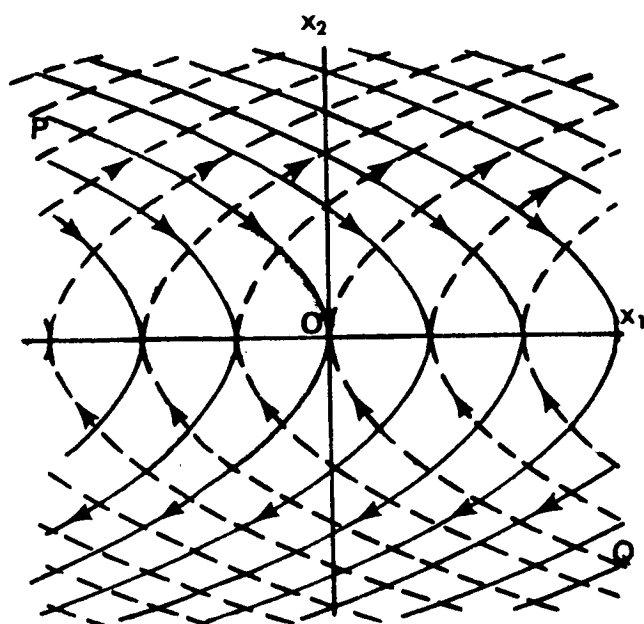
Fig. 2.2a Free Trajectories for
the Pure Inertia Plant
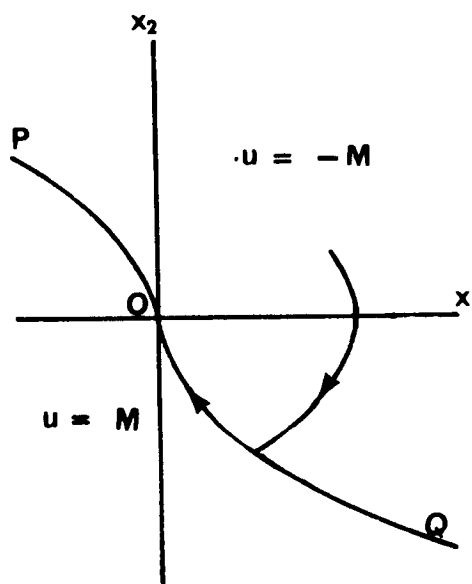
Fig. 2.2b A Time Optimum
Trajectory for the Pure
Inertia Plant
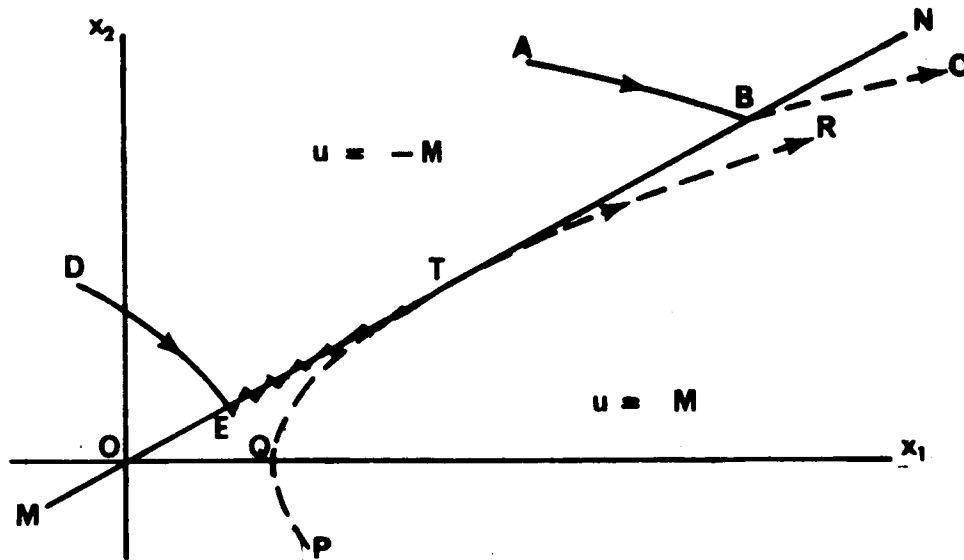
Fig. 2.3   Unstable Behavior of the Pure Inertia Plant
with $S = x_1 + d_1 x_2$ $(d_1 < 0)$
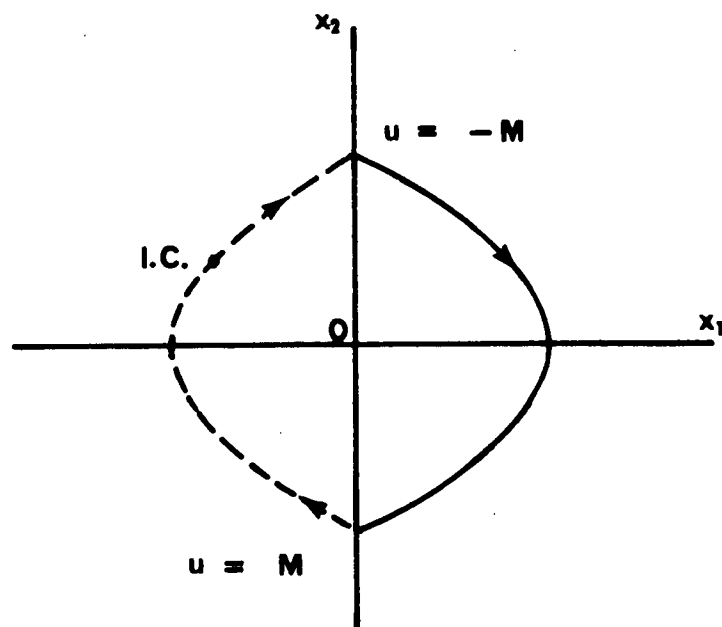
Fig. 2.4   Unstable Behavior of the Pure Inertia Plant
with $S = x_1$
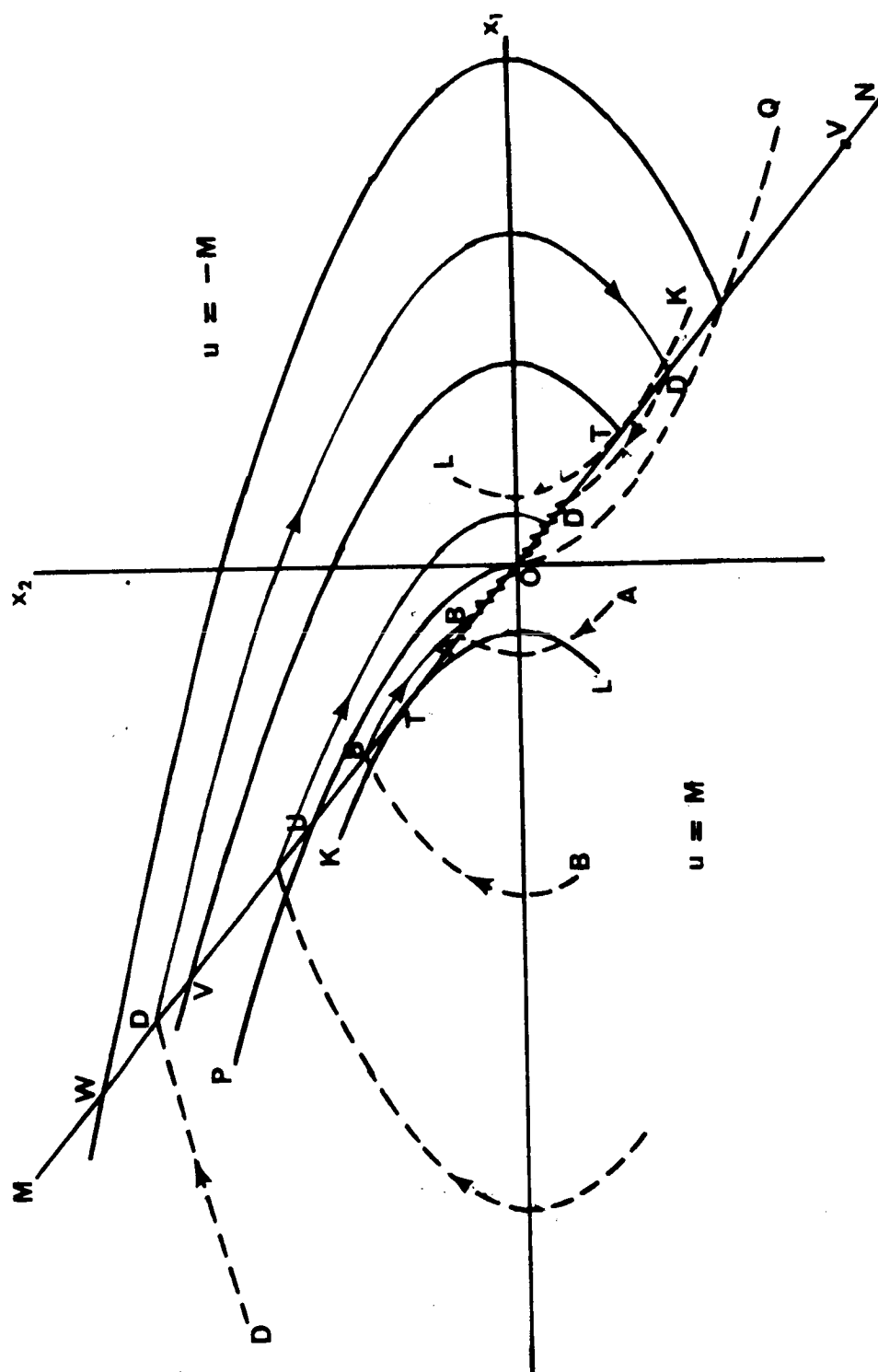
Fig. 2.5 Typical Trajectories for the Pure Inertia Plant
with $s = x_1 + d_1 x_2$ $(d_1 > 0)$

14
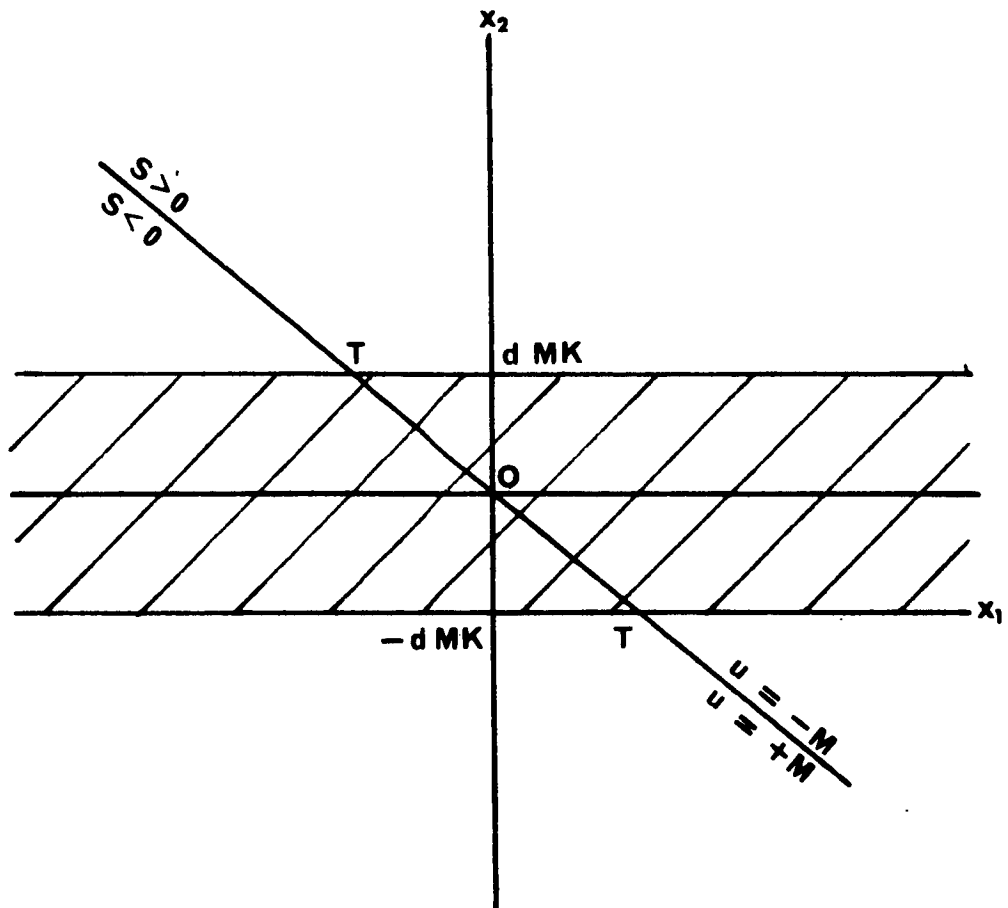
Fig. 2.6 Approaching Region of State (shaded)
and Departing Region (unshaded)
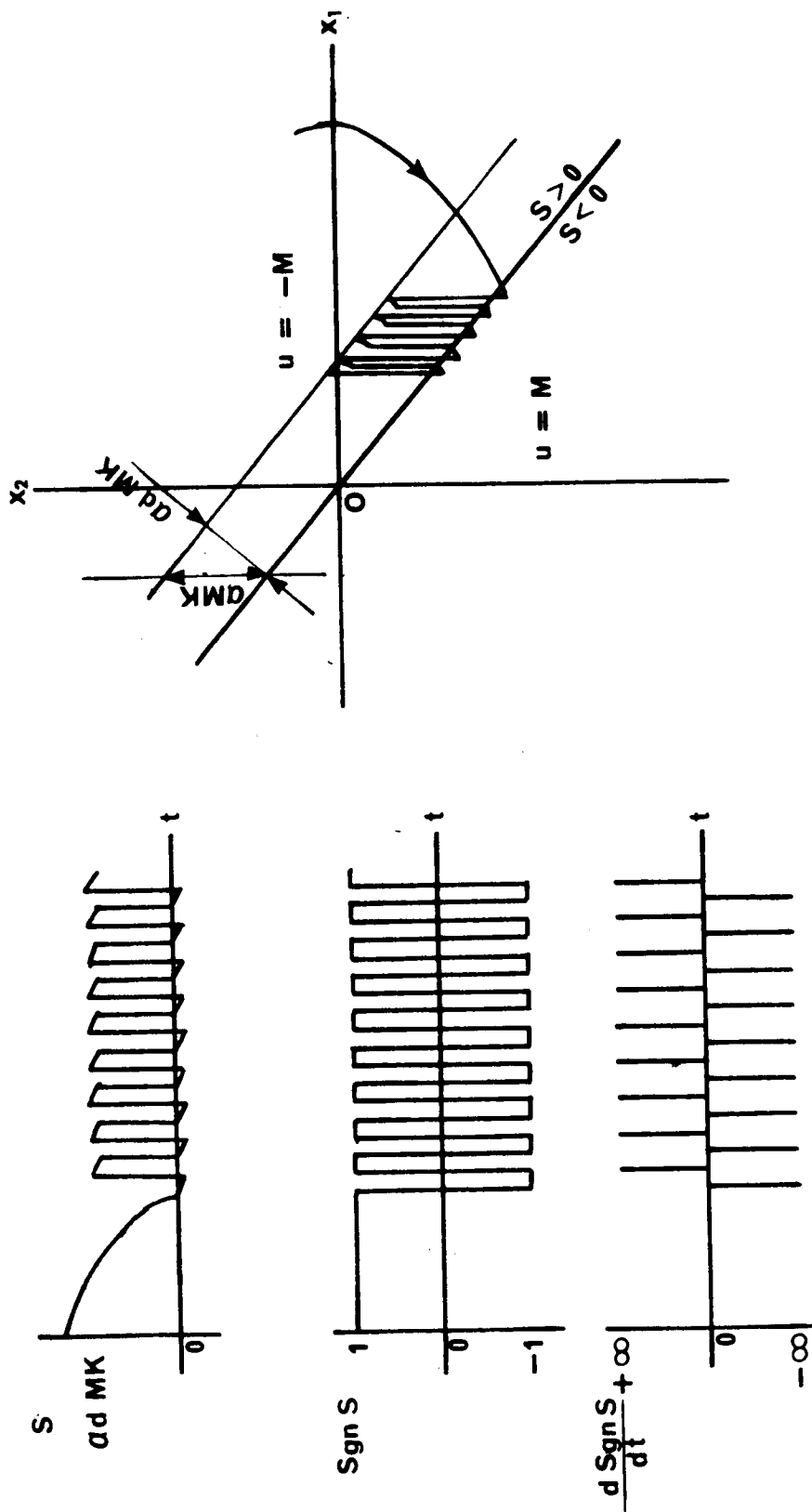
Fig. 2.7a A Typical Behavior when a Negative Zero
is Present (not to scale)
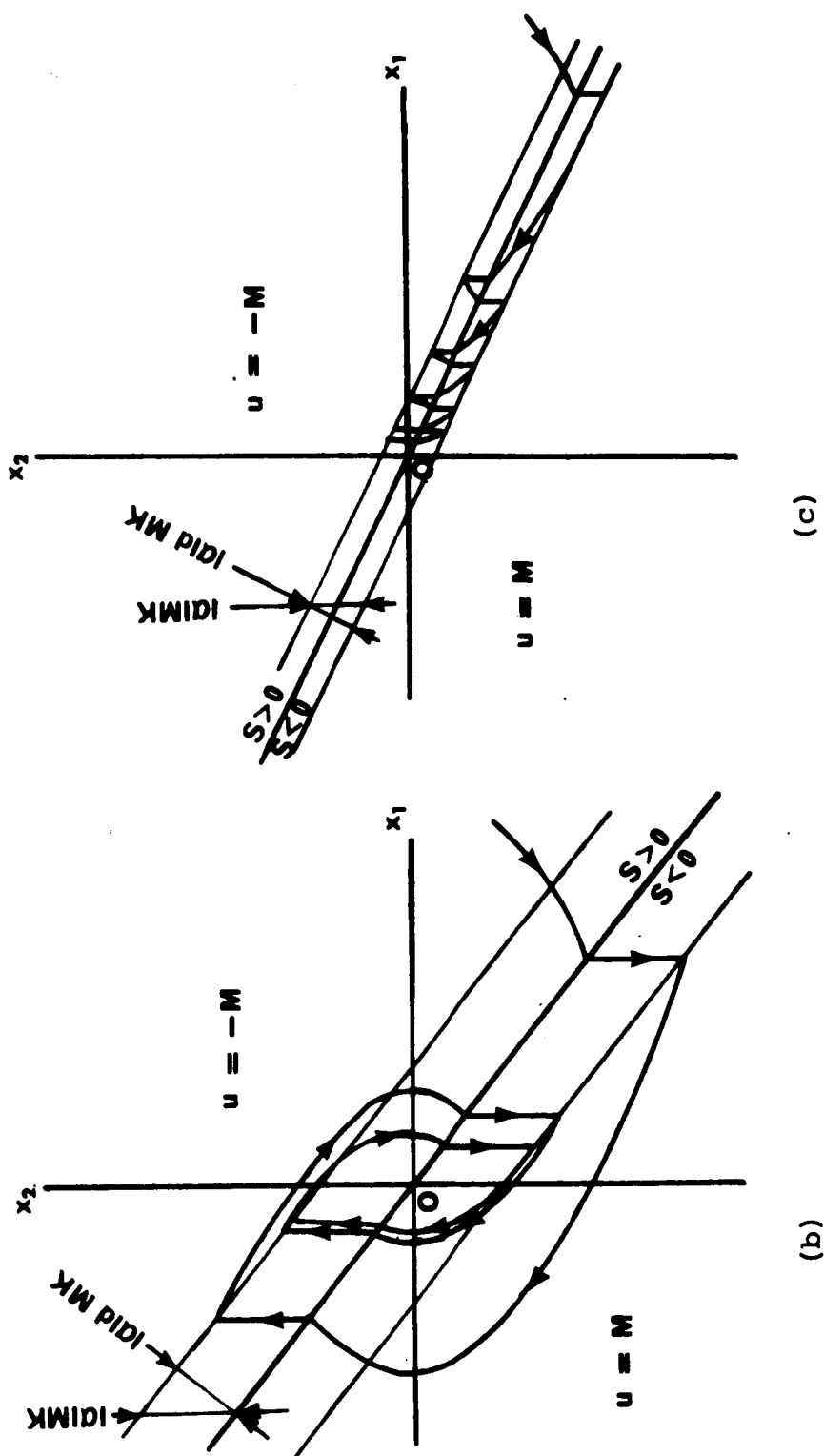
Fig. 2.7b, c Two Typical Behaviors when a Positive
Zero is Present (not to scale)

17

CHAPTER 3

PRINCIPLES OF SELF-ADAPTATION

3.1   Foundations

It was shown in Chapter 2 that undesirable jumping phenomena may occur if the plant equation contains any differential operation in the control input, or if the order of the switching function is not appropriate. When the plant and its dynamics are given, a compensation may be necessary in order to achieve a relationship of the form:

$$\dot{S} = F_1(\underline{x}, \ r, \ d, \ t) - MF_2(\underline{x}, \ t) \ \text{sgn} \ S \qquad (3.1a)$$

or equivalently

$$\dot{S} \ \text{sgn} \ S = F_1(\underline{x}, \ r, \ d, \ t) \ \text{sgn} \ S - MF_2(\underline{x}, t) \qquad (3.1b)$$

where

$\underline{x}$ = state vector

F_1 = some function of $\underline{x}$

r = reference command input

d = disturbance input

t = time

F_2 = a function of the state vector and time (presumably referring to the gain of the plant including the servo and the actuator)

18

The role of the compensation is to cancel any zero in the plant and/or to adjust the order of the plant in order to obtain $\dot{S}$ in the form of eq. (3.1).

The switching level M must now be adjusted so that the state point is always approaching the switching surface in the state space. This requirement is quantitatively stated by the inequality:

$$\dot{S} \text{ sgn } S < 0 \tag{3.2}$$

If the above condition is instantaneously satisfied, any initial condition will be followed by a trajectory which will always be approaching the switching surface. Once the switching surface is hit, the sustained chatter mode will follow. Combining (3.1b) and (3.2) when $F_2(\underline{x}, t)$ is assumed positive, the switching level M must be

$$M > \frac{F_1(\underline{x}, r, d, t)}{F_2(\underline{x}, t)} \tag{3.3}$$

Fig. 3.1 shows the general configuration of the self-adaptive system. The details of the switching function generator and the switching level adjustment mechanism are discussed in the following sections.

3.2 A Class of Applicable Systems

The following are some examples of systems which can be cast into the form of eq. (3.1) after some compensation:

19

$$\dot{x}_1 = x_2$$

$$\dot{x}_2 = x_3$$

$$\cdots$$

(3.4)

$$\dot{x}_{n-1} = x_n$$

$$\dot{x}_n = f_1(\underline{x}, d, t) + f_2(\underline{x}, t) u$$

where the control force u is expressed by -M sgn S, and the switching function must take the form

$$S = x_1 + d_1 x_2 + \cdots + d_{n-1} x_n$$

(3.5)

$$- (n_0 r + n_1 \dot{r} + \cdots + n_{n-2} r^{(n-2)})$$

That is, the model transfer function is of the n-1'th order for an n'th order system, i.e.,

$$\frac{x_{1_M}(s)}{r(s)} = \frac{n_0 + n_1 s + \cdots + n_{n-2} s^{n-2}}{1 + d_1 s + d_2 s^2 + \cdots + d_{n-1} s^{n-1}}$$

(3.6)

where

x_{1_M} = desired output

d_{n-1} = a positive constant

$d_1, d_2, \cdots d_{n-2}$: presumably non-negative constants

$n_0, n_1, \cdots n_{n-2}$: constants

20

Fig. 3.2 shows the mathematical switching function generator for this case. In eq. (3.4) f_1 and f_2 may be nonlinear functions of their arguments. f_2 may refer to the combined gain of the plant, servo, and actuator, and is assumed to be positive for simplicity. F_1 and F_2, which appeared in eq. (3.1), can now be evaluated for this system:

$$F_1(\underline{x}, r, d, t) = x_2 + d_1 x_3 + \ldots + \qquad (3.7)$$

$$+ d_{n-1} f_1(\underline{x}, d, t) - (n_0 r + n_1 \dot{r} + \ldots$$

$$+ n_{n-2} r^{n-2})$$

$$F_2(\underline{x}, t) = d_{n-1} f_2(\underline{x}, t) \qquad (3.8)$$

For example, if the combined transfer function is time-invariant, it is

$$\frac{K}{1 + a_1 s + a_2 s^2 + \ldots + a_n s^n} \qquad (3.9)$$

where

K, a_1, . . ., a_n are constants

then f_1 and f_2 can be easily identified

$$f_1(\underline{x}) = - \frac{a_{n-1} x_n + a_{n-2} x_{n-1} + \ldots + a_1 x_2 + x_1}{a_n} \qquad (3.10)$$

21

$$f_2(x) = \frac{K}{a_n} \qquad\qquad (3.11)$$

3.3   Switching Level Adjustment

One obvious switching level adjustment scheme would be to measure continuously each of the variables incorporating F_1 and F_2, and then to compute the right hand side of the inequality (3.3), generating the appropriate switching level. This "explicit adjustment scheme" may not lead to a genuine self-adaptive policy for the following reasons. First, the system would be complex and expensive, since a number of sensors, transducers and wires, in addition to an on-line computer would be necessary. Secondly, as mentioned in Appendix A, this type of system is in a sense open-loop and less self-adaptive since it depends on the anticipated explicit formulations of F_1 and F_2 necessary for the computer programming.

A better scheme is to make use of the higher control levels, which, as seen in eq. (3.1b), are more likely to satisfy the basic inequality condition given in eq. (3.2). The scheme sketched in fig. 3.3a is first proposed as a candidate for "implicit adjustment logic." Although the conditions $S \operatorname{sgn} \dot{S} < 0$, $\dot{S} \operatorname{sgn} S < 0$, $\operatorname{sgn} S \operatorname{sgn} \dot{S} = -1$ and $S \dot{S} < 0$ are all equivalent, the first one is most suitable for the abscissa, since its magnitude indicates the distance from the present position of the state point to the switching surface.

22

Suppose that the initial switching level M is not great enough to satisfy the condition S sgn $\dot{S}$ < 0. Starting from the initial condition 1 in fig. 3.4a, the state point will go away from the switching surface MN for a while. But the rate $\dot{S}$ will be rapidly decreasing in magnitude because of the increasing switching level. The turning point 2 is reached, and the state point begins to approach the switching surface. At the same time, the sign of S sgn $\dot{S}$ is reversed to the desired one, i.e., negative. This transition appears as a discontinuous jump from the right hand side to the left in fig. 3.3a. After the turning point, M is still increasing to accelerate the approach to the switching surface. As soon as the switching surface is finally hit at 3, the chatter motion starts, and the switching level stops increasing. The switching level remains constant thereafter as long as the chatter mode naturally continues. The control level, however, might not continue to sustain the chatter mode due to some later environmental changes. In such a case, S sgn $\dot{S}$ may become positive again, and the adjustment logic increases the level enough to pull S sgn $\dot{S}$ back to the left hand side. It should be noted that $\dot{M}$ is larger at greater distances from the switching surface in order to shorten the pre-chatter mode.

There may be many cases in which the lowest possible control level is desired in order to save electric or hydraulic power or fuel supply, or to avoid hardware limitations such as the saturation of an airplane's control surface deflection angle. The condition necessary for sustaining the

23

chatter mode is merely that S sgn $\dot{S}$ be negative, regardless
of its absolute value. Consequently, the level of M during
chatter mode need not be very high, as long as it is high
enough to make S sgn $\dot{S}$ negative. With this in mind, another
adjustment logic is proposed in fig. 3.3b. The greater the
switching level, the shorter the pre-chatter mode. Therefore,
at 3, the beginning of the chatter mode, the switching level
is presumably too great just to maintain the chatter mode. As
the chatter mode is established, the logic begins to remove
this excess switching level. When too much is removed, the
chatter mode will cease, pushing S Sgn $\dot{S}$ to the positive side.
Then, according to the logic, the switching level starts to
gain in magnitude again, resulting in a jump to the negative
side at 4 (fig. 3.3b). After the jump, the state point approaches
the switching surface as before, and the system will repeat
this cycle, 3-4-3. With an appropriately designed logic, the
trajectory in the state space might be of the form shown either
in fig. 3.4b or 3.4c. The frequency of the cyclic repetition
could undoubtedly be much lower than that of the original
chatter mode, while the maximum magnitude of the deviation or
error determined by S at 4 could be kept sufficiently small.

Whatever the order of the system might be, the desired
condition is simply a matter of the sign of the S and $\dot{S}$.
Therefore, a simple two dimensional visual display would be
possible for manual adjustment or for manual monitoring pur-
poses. Fig. 3.5 shows an example of such a display. The
second and fourth quadrant are shaded to indicate the target
area or acceptable region.

24
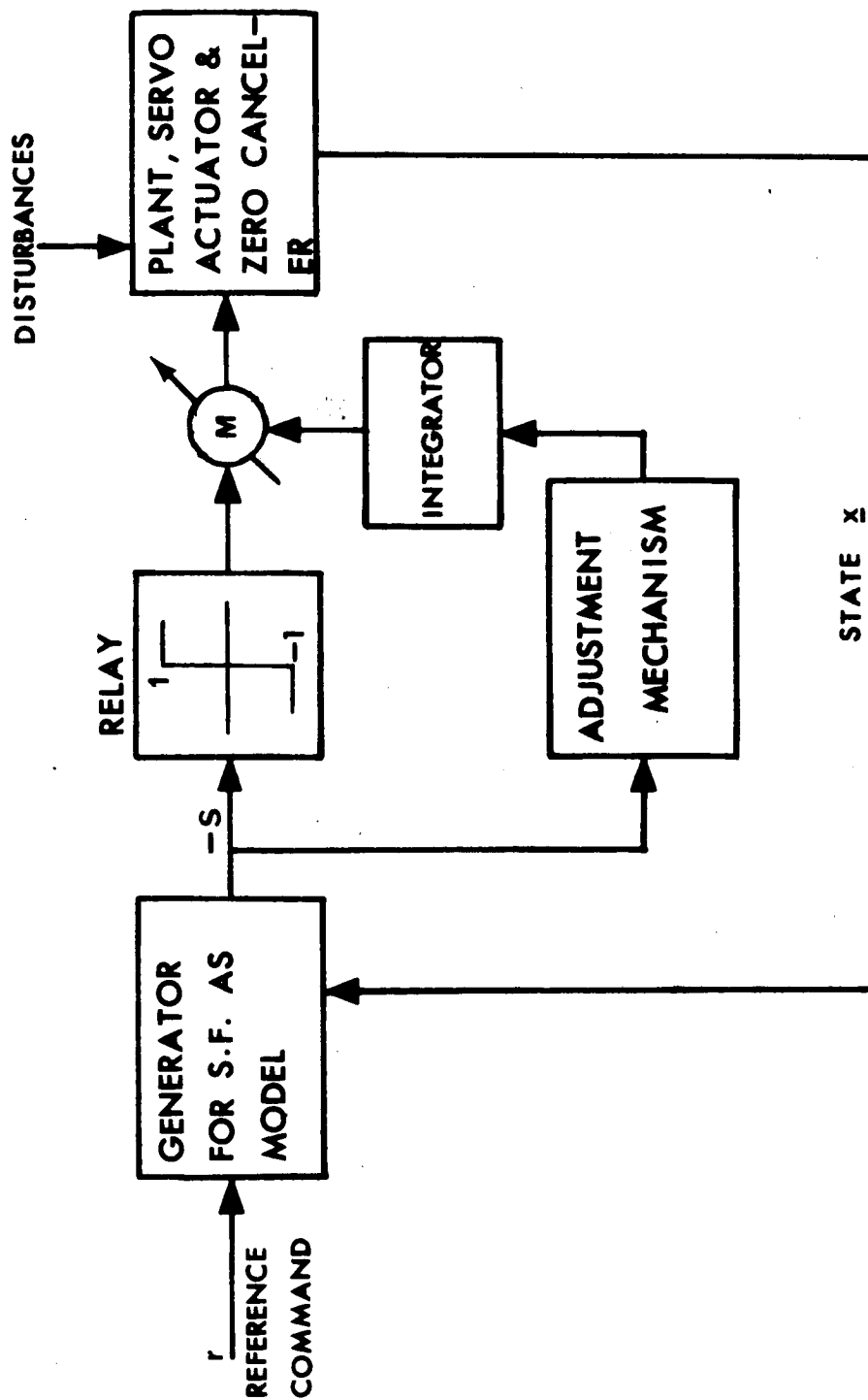
Fig. 3.1 Functional Block Diagram of the Proposed
Self-Adaptive System

Input labeled:

$\dfrac{r}{\text{COMMAND}}$

feeds into a block: $n_0 + n_1 s + \cdots + n_{n-2}s^{n-2}$

Input labeled:

$\dfrac{x}{\text{PLANT'S STATE}}$

feeds into a block: $1 + d_1 s + \cdots + d_{n-1}s^n$

Both blocks feed into a summing junction (with $-$ and $+$ inputs) producing output:
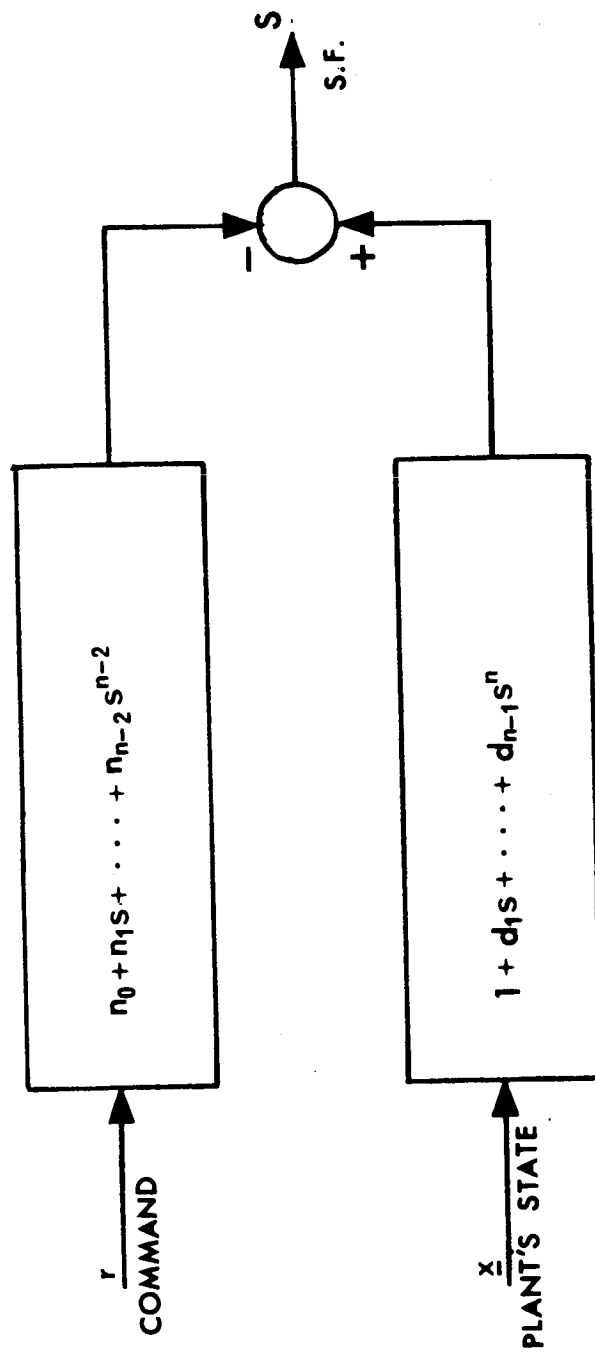
S

S.F.

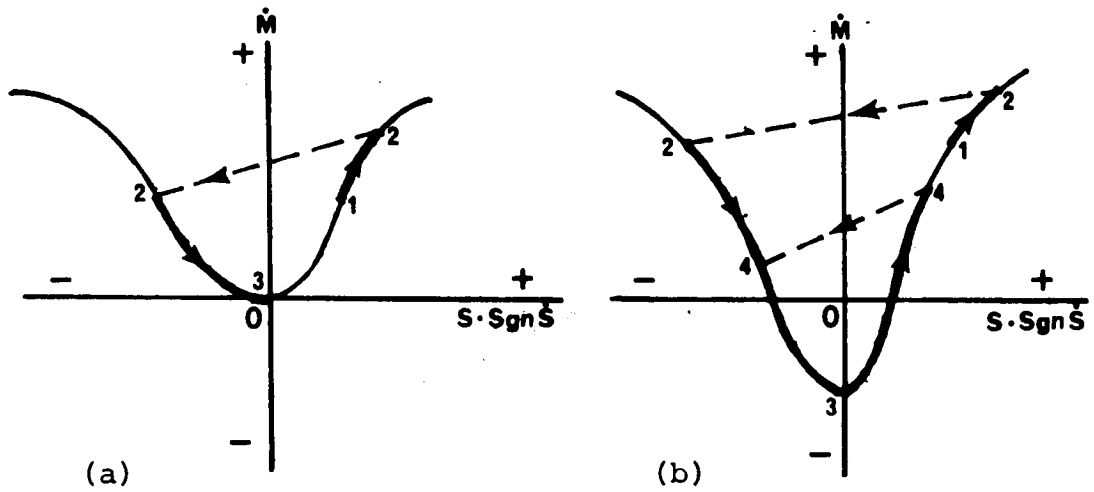Fig. 3.2 Mathematical Switching Function Generator

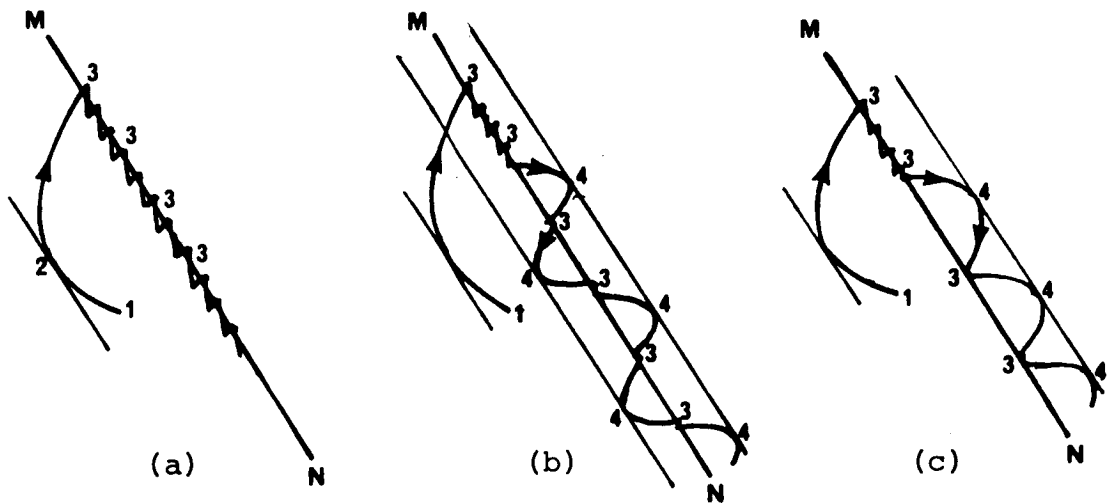Fig. 3.3 Switching Level Adjustment Logics

Fig. 3.4 Trajectories Near the Switching
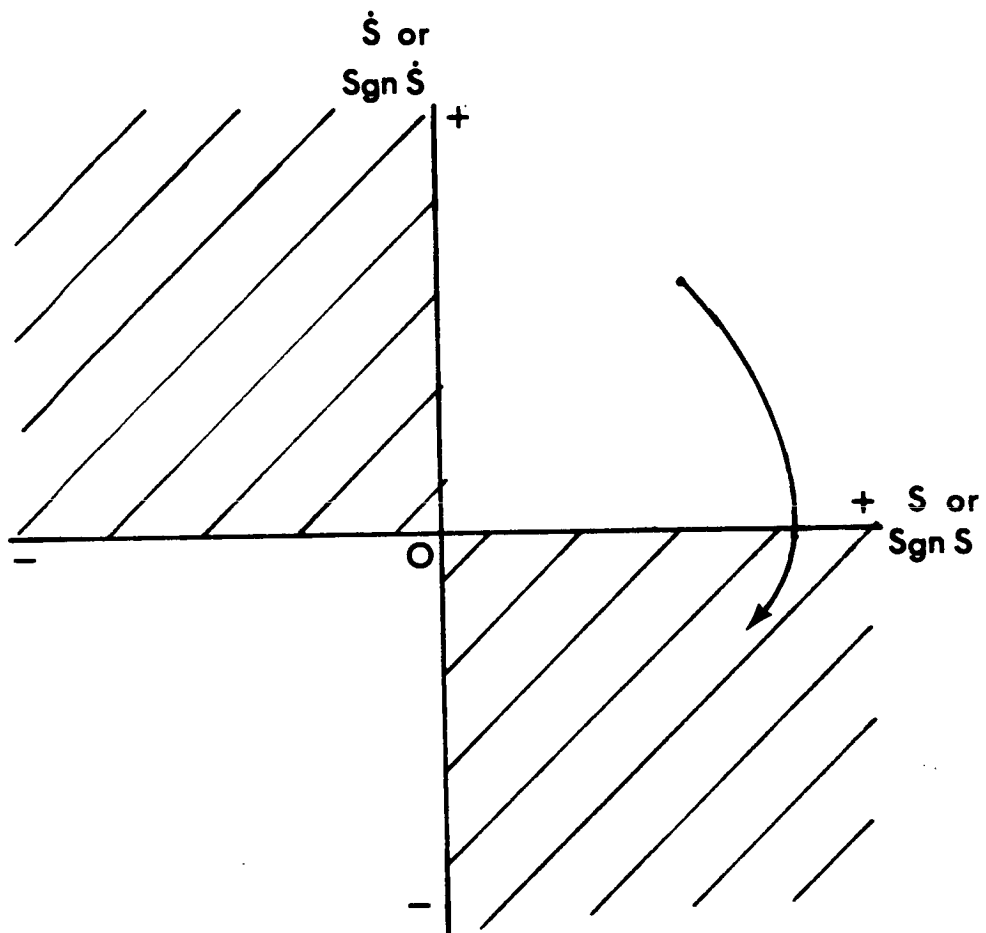Surface (Not to scale)

Fig. 3.5   A Display for Manual Use

CHAPTER 4

EXPERIMENTAL RESULTS

4.1   Preparations

The experiments were performed using the TR-48
analog computer in the Department of Aeronautics and Astro-
nautics at M.I.T.   Three different switching level adjustment
logics were employed, mechanized by the diode function gen-
erator.   The M-S sgn $\dot{S}$ characteristics of the logics are
recorded in fig. 4.1.   Logic B (fig. 4.1b) has smaller values
of $\dot{M}$ for large magnitudes of S sgn $\dot{S}$, and narrower and
sharper notch characteristics over small magnitudes of S sgn $\dot{S}$
than those of logic A (fig. 4.1a).   The characteristics of
logic C (fig. 4.1c) are almost the same as those of B, but
the former is symmetric with respect to the ordinate.

Electronic switches were used to realize the sign
functions.   It should be noted that the data recorded on the
strip chart for a control force u = -M sgn S during the
chatter mode do not accurately represent the actual control
force.   The actual control force is the output of the elec-
tronic switch which is essentially an unbiased rectangular
wave like the one shown in fig. 4.2.   Its frequency was high
enough to dominate the plotting pen's mechanical dynamics.
As a result of the filtering, the recorded data may look like

the data shown in fig. 4.2 with a bias equal to the average of the actual control force and with an amplitude and frequency determined by the pen's dynamics as well as the actual control force.

4.2   Example 1

The plant is of the pure inertia type. The equation for the dynamics is

$$\ddot{x} = -d + u \qquad\qquad (4.1)$$

where

$$u = -M \text{ sgn } S$$

and d is a parameter. The switching function S is

$$S = x + _\tau \dot{x}$$

The system is autonomous, i.e., there is no command input. The objective is first to bring the state point $(x,\dot{x})$ from an initial location $(x_0,\dot{x}_0)$ to the switching line quickly, and then to continue towards the final state $(0,0)$ along the switching line, In short, the overall approach to the goal is to be exponential, like $e^{-\tau t}$.

A corresponding practical example would be a lunar soft-landing mission with bang-bang thrust control in the lunar vertical direction. For such a case,

x = the lunar altitude h

d = the lunar gravitational acceleration, g_ℓ

M = the thrust acceleration, i.e., $\frac{T}{M}$, the thrust divided by the mass of the lunar module

30

Three initial conditions were assumed:

I.C.1 $x_0 = 8.0$ volts $\dot{x} = -1.0$ volts

I.C.2 $x_0 = 8.0$ volts $\dot{x}_0 = 2.0$ volts

I.C.3 $x_0 = 8.0$ volts $\dot{x}_0 = -4.0$ volts

The input parameter d was set at 0.081 volts. If the scaling correspondence

2 km $\leftrightarrow$ 1 volt

100 m/sec $\leftrightarrow$ 1 volt

10 m/sec^2 $\leftrightarrow$ 1 volt

is made, the value of d represents that of g_ℓ, 1.622 m/sec^2, and each run gives the simulation, condensed ten times, for the soft-landing mission from the lunar altitude 16 km. Fig. 4.3 shows a possible mechanization of such a lunar soft-landing guidance system.

The results for I.C.1, 2, and 3 with adjustment logic A are shown in fig. 4.4. For each initial condition, the time history of x(h), u $(\frac{T}{m}$, thrust acceleration), and S sgn $\dot{S}$ are recorded. In addition, the trajectory in the M $\sim$ S sgn $\dot{S}$ plane is recorded in order to see how the adjustment logic actually worked.

The value of τ was chosen to be 2.6 sec^{-1}. The initial value of the switching magnitude M_0 was arbitrarily set at 0.50 volts for all these runs. Fig. 4.4a and 4.4b represent the results when S sgn $\dot{S}$ was initially negative. The switching level kept increasing, accelerating the

31

approach to the switching line. At the very beginning of the

chatter mode, at about 1.5 sec, the increased M read 1.15

volts. During the chatter mode, M was gradually decreased

because of the slightly negative value of $\dot{M}$ at S sgn $\dot{S}$ = 0.

When M was reduced to 0.1 volts at 17 sec, this value of M

was insufficient to sustain the chatter, because of the small

value of $\dot{x}$ (see eq. (4.3)). The chatter ceased, and S sgn $\dot{S}$

tended toward the positive. But logic A acted immediately to

increase M and to draw S sgn $\dot{S}$ back to the negative. Again,

M was reduced to render S sgn $\dot{S}$ positive. From 20 sec on,

this cycle was repeated. The system's behavior during this

interval was not chatter. The switching function S was kept

barely negative, though $\dot{S}$ changed its sign repeatedly, keeping

the control force u positive. Specifically, u constantly

remained at 0.081 volts, balancing -d, or the gravity accelera-

tion. The offset error in x arose because S was not precisely

zero for this interval.

In fig. 4.5a and 4.5b are shown the results for I.C.2.

The initial S sgn $\dot{S}$ was on the "bad side," the positive.

Nevertheless, it jumped almost instantly to the negative side,

because of the logic. Shortly afterwards, the chatter motion

started and continued until 34 sec. M was gradually reduced

from 2.5 volts to 0.1 volts during the chatter. Unfortunately,

for the reason noted in section 4.1, the record for u does

not show the history of the decreasing M itself.

Fig. 4.6a and fig. 4.6b show the results for I.C.3.

The initial S sgn $\dot{S}$ was again positive, but this time, S sgn $\dot{S}$

traveled away for a while until M was large enough to make the jump to the negative side. Fig. 4.7 shows the trajectories in the phase plane for the above cases.

Next, logic B instead of A was employed for I.C.1. The results are shown in fig. 4.8a, b, and c. Since $\dot{M}$ for S sgn $\dot{S} = 0$ was now further negative, the excess magnitude was removed more promptly. The post-chatter regular mode beginning at 5 sec lasted until 14 sec, when the new chatter mode started. This second chatter motion is different from the first one. It is caused by the behavior of S sgn $\dot{S}$ periodically moving back and forth around its null value. Therefore, it may be reasonable that its frequency should be much lower than that of the first chatter motion.

Since the notch was so narrow, S sgn $\dot{S}$ was virtually held at zero after the first chatter mode started, so there remained no offset error in the output x. The microscopic plot shown in fig. 4.8c revealed the cyclic behavior in the vicinity of the origin.

Lastly, logic C was employed for I.C.1. The results are shown in fig. 4.9a, b, and c. The remarkable feature in this case is the constant cyclic behavior closing the entire narrow symmetric notch which resulted in a time history of u with a much reduced frequency, about 0.35 c/sec. There was a short high frequency chatter motion in every period. It occurred each time S sgn $\dot{S}$ crossed the abscissa from the left hand side to the right in the $\dot{M}$-S sgn $\dot{S}$ plane. The offset error in x could have been greatly reduced if the notch had been made narrower.

4.3   Example 2

The plant is second order and time-varying. The equation of the dynamics is

$$\ddot{x} + a(t)\, x = u \qquad (4.4)$$

where

$$u = -M \text{ sgn } S$$

and the initial magnitude M_0 was arbitrarily set at 0.20 volts. Fig. 4.10 shows the functional block diagram of this system. The parameter $a(t)$ was

$$a(t) = \exp(-0.05t) - 0.5 \text{ volts} \qquad (4.5)$$

This time history is shown in fig. 4.11. The uncontrolled plant would be obviously unstable. The first order model transfer function

$$\frac{x(s)}{r(s)} = \frac{1}{1 + \tau s} \qquad (4.6)$$

$$\tau = 2.6 \text{ sec}^{-1}$$

was assumed.

It follows that the switching function S is

$$S = x + \tau \dot{x} - r \qquad (4.7)$$

The command input r was a near step, as shown in fig. 4.12. The model response x_m to the command is also shown in the same figure. All initial conditions were null throughout the experiment.

In fig. 4.13a are shown the actual plant's output x_a, the error, $e = x_a - x_m$, u, S, and S sgn $\dot{S}$, when logic B was used. The plot of M-S sgn $\dot{S}$ is shown in fig. 4.13 b. Through the entire run, S was held slightly negative, while S sgn $\dot{S}$ was mostly negative with occasional impulsive changes to positive whenever S approached the zero line. Thus there was neither chatter motion nor single switching. Note that the only change in the polarity of u occured at 13 sec; it was attributed to the polarity change of the continuously decreasing M. From then on, M was negative. At any rate, the error remained sufficiently small.

It should also be noted that M is assumed to be positive in the theory. In fact, the characteristics of the adjustment logics were originally decided by the properties described in the inequality (3.3), which is valid only under such assumptions. However, M may be negative in the vicinity of the origin of the M-S sgn $\dot{S}$ plane for adjustment logics such as that shown in fig. 3.3b. As long as M is negative, the cyclic behavior around the origin is clockwise; when positive, the motion is counterclockwise.

It remains to be demonstrated that the above results are practically the same as the "sliding motion" by the ideal perfect relay. The analysis is similar to that in the last part of section 2.2. For sliding mode, the switching function would be null:

$$S \equiv 0 \qquad\qquad\qquad (4.8a)$$

Thus, from eq. (4.7)

$$S = x + \tau \dot{x} - r = 0 \qquad (4.8b)$$

$\dot{S}$ should also be indentically zero

$$\dot{S} \equiv 0 \qquad (4.9a)$$

Thus

$$\ddot{x} + \tau \dot{x} - r = 0 \qquad (4.9b)$$

Eliminating $\dot{x}$ and $\ddot{x}$ from eq. (4.4), (4.8b), and (4.9b)

$$u = [a(t) + \frac{1}{\tau 2}] \, x + \frac{1}{\tau}(r - \frac{r}{\tau}) \qquad (4.10)$$

This is the continuous control force which would be obtained by using the ideal perfect relay. Using the model output data, the above time history of the ideal control force was calculated and plotted as the dotted curve in fig. 4.13a, where the actual control force is recorded. Little difference is observed between the two. The evidence indicates that adjustment logic B effectively made the actual relay be the perfect ideal relay, and made the sliding motion real.

From another point of view, the continuous form of the control force given by eq. (4.10) might suggest the linear equivalent system shown in fig. 4.14. However, this is based on the explicit formulation for u, and the precise measurement of the plant's parameter a(t), would be less adaptive and less practical. In other words, it refers to the programming adaptive system discussed in Appendix A.

Secondly, logic C was employed. Discussion of the results, shown in fig. 4.15a and b, would be similar to that in section 2.2.

4.4 Example 3

This plant is second order and nonlinear. The equation of the dynamics is

$$\ddot{x} - x\dot{x} - x = u \qquad (4.11)$$

where

$$u = -M \, \text{sgn} \, S$$

and the initial magnitude M_0 was arbitrarily set at 0 volts. The uncontrolled plant would be unstable. The command input and the model are exactly the same as in example 2.

Fig. 4.16 shows the results when logic B was used; fig. 4.17, logic C. These results are similar in nature to the corresponding results in the last example.

4.5 Example 4

The last experimental example consists of the application of a roll control system to a supersonic transport. For simplicity, one degree of freedom roll dynamics are assumed, neglecting the coupling effect due to side slip and yaw motion. This assumption may be reasonable in practice, if a suitable damper is provided for the Dutch roll mode. The SST's transfer function $G_a(s)$ from aileron deflection angle δ_a to roll angle ϕ is then

$$G_a(s) = \frac{\phi}{\delta_a} = \frac{K}{(s(1 + \tau s)} \tag{4.12}$$

where

K = gain

τ = time constant

The aileron servo actuator is assumed to have the transfer function

$$G_A(s) = \frac{\delta a}{u} = \frac{1}{1 + 0.1s} \tag{4.13}$$

See reference 22 for further treatment of this SST.

Two representative flight conditions and their corresponding values for K and are shown below.

Flight Condition I

Mach: 0.4, Altitude: 5,000 ft.

$$K = 4.74$$

$$\tau = 1.18 \text{ sec}^{-1}$$

Flight Condition II

Mach: 3.0, Altitude: 70,000 ft.

$$K = 6.83$$

$$\tau = 5.30 \text{ sec}^{-1}$$

The model transfer function $G_m(s)$ relating the model output x_m to the command input r is the second order function that has been taken for granted as the ideal model for human pilots, namely

$$G_m(s) = \frac{1}{\frac{s^2}{W_m^2} + 2\frac{\zeta_m}{W_m} s + 1} \tag{4.14}$$

38

where

$$\zeta_m = 0.7$$

$$w_m = 3.0 \text{ rad/sec}$$

Thus the switching function is

$$S = \frac{\ddot{x}}{w_m^2} + 2\frac{\zeta_m}{w_m} \dot{x} + x - r \qquad (4.15)$$

where

$$x = \phi$$

Fig. 4.18 shows the time history for the command and the model output.

Before being equipped with the proposed self-adaptive system, the SST had a conventional adaptive system using the classical follow-up principle illustrated in Appendix A, with lead compensation in the forward loop. Fig. 4.19 shows the block diagram and fig. 4.20 the results.

The parameters involved in the lead network were selected so that an adequate response under Flight Condition I was possible. As seen in the figure, however, this system with the parameters so selected proved unstable under Flight Condition II. On the other hand, the proposed self-adaptive system, whose possible implementation is suggested in fig. 4.21, gave satisfactory results for both Flight Condition I and II, as shown in fig. 4.22 and 4.23 respectively, when adjustment logic B was employed.
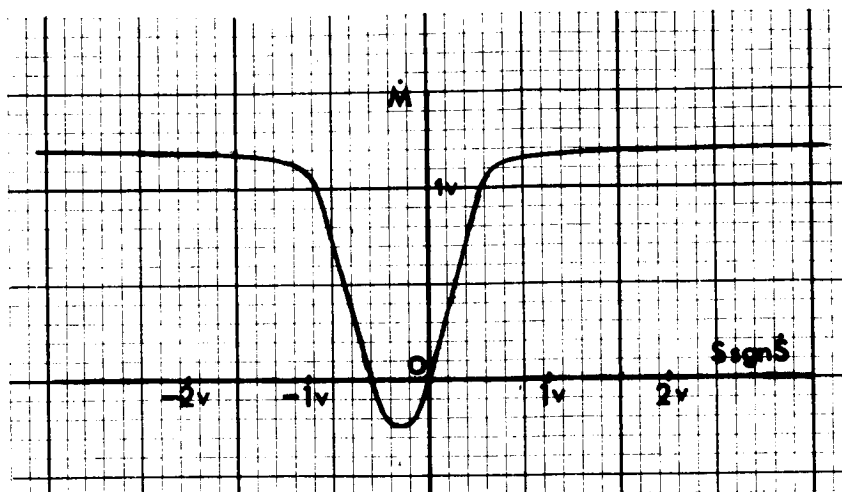
(a)
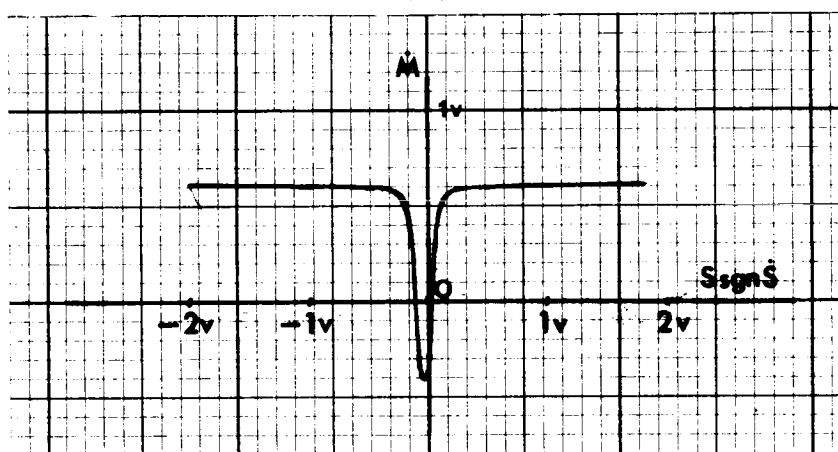
(b)
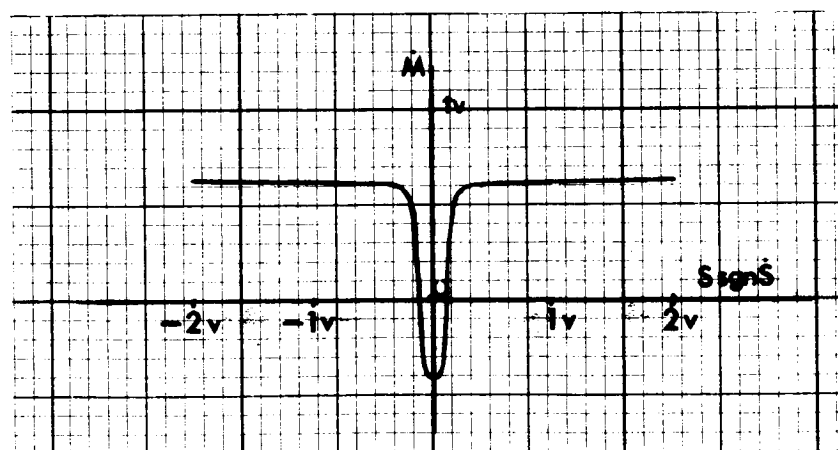
(c)

Fig. 4.1 Three Different Switching Logics
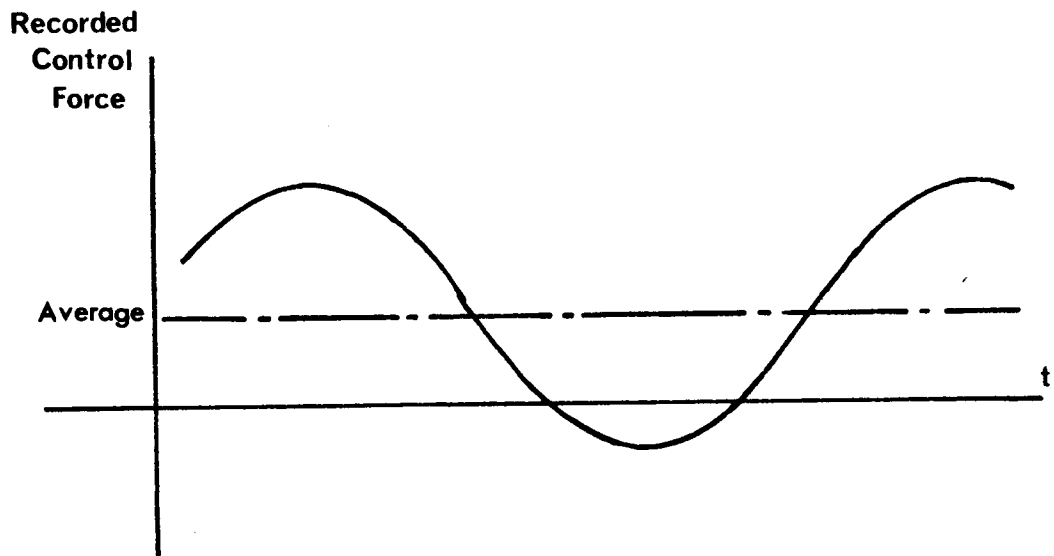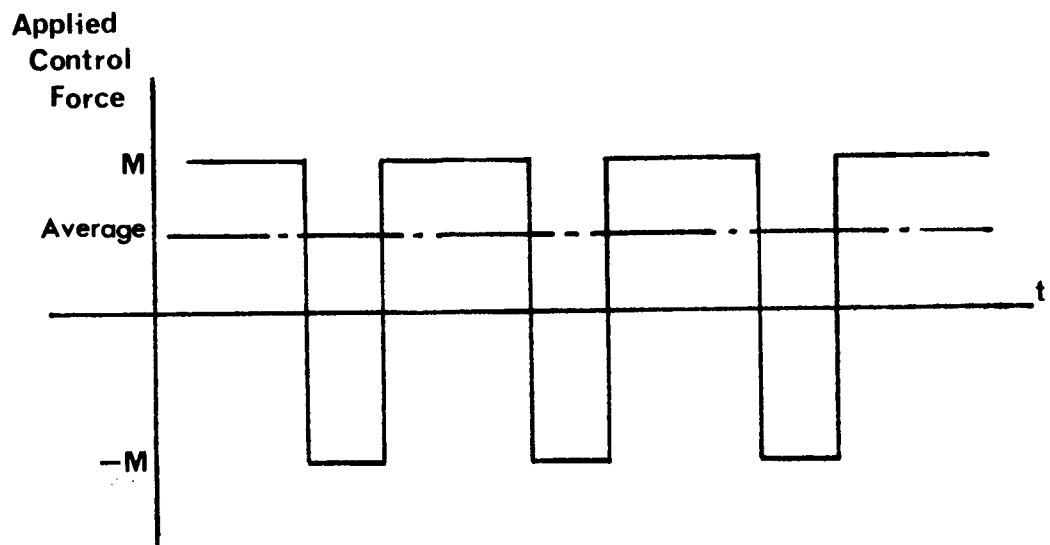Used in the Experiment
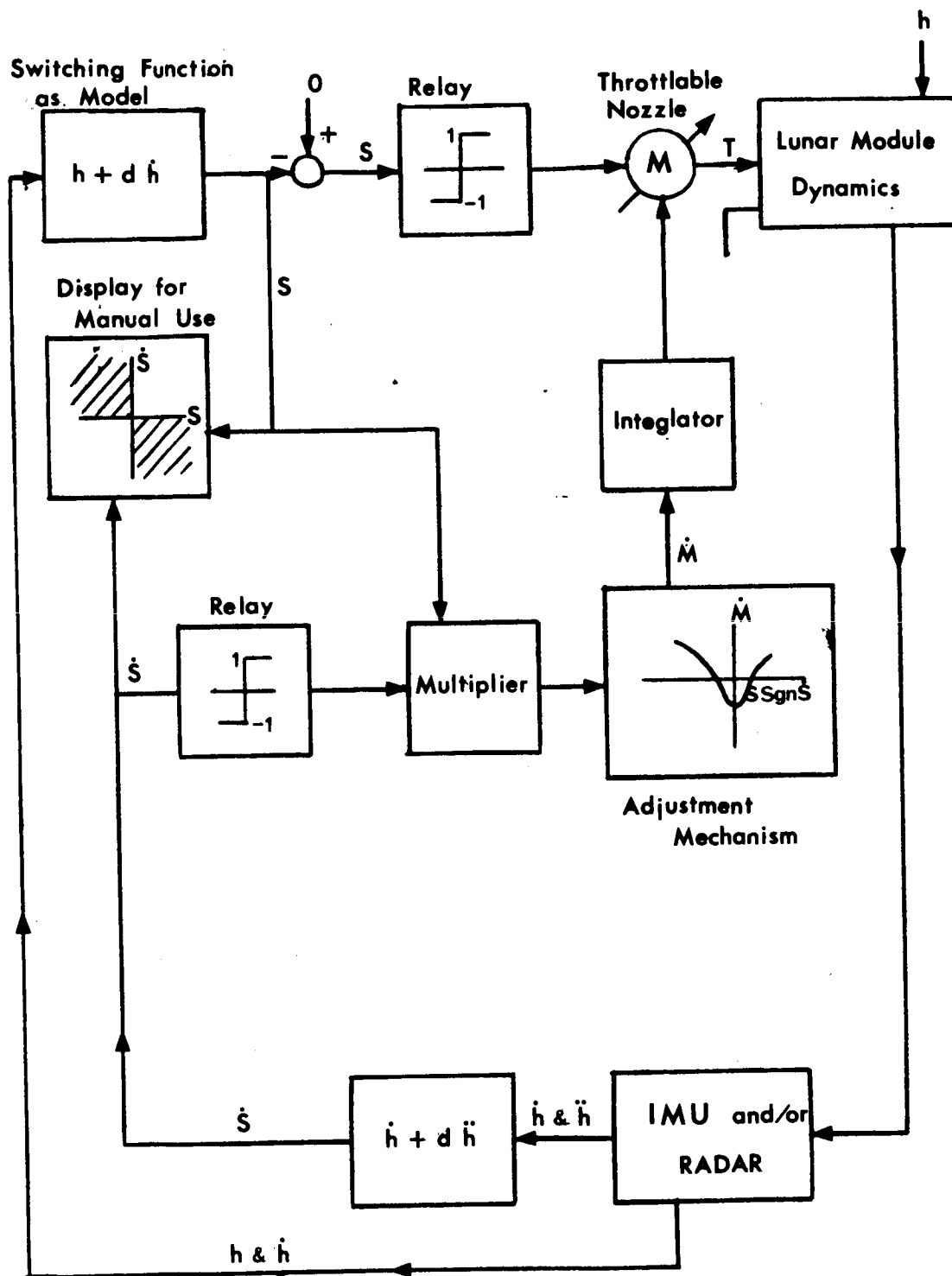
40

Fig. 4.2 Applied and Recorded Control Forces

Fig. 4.3 A Possible Implementation for
the Lunar Soft Landing Guidance System
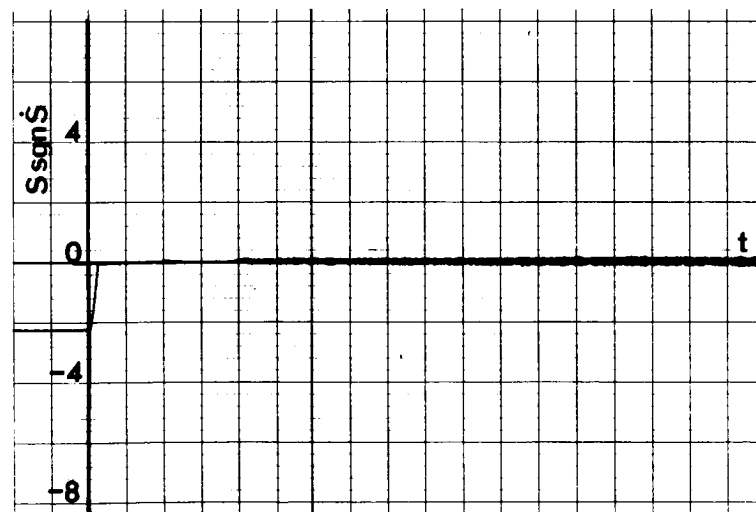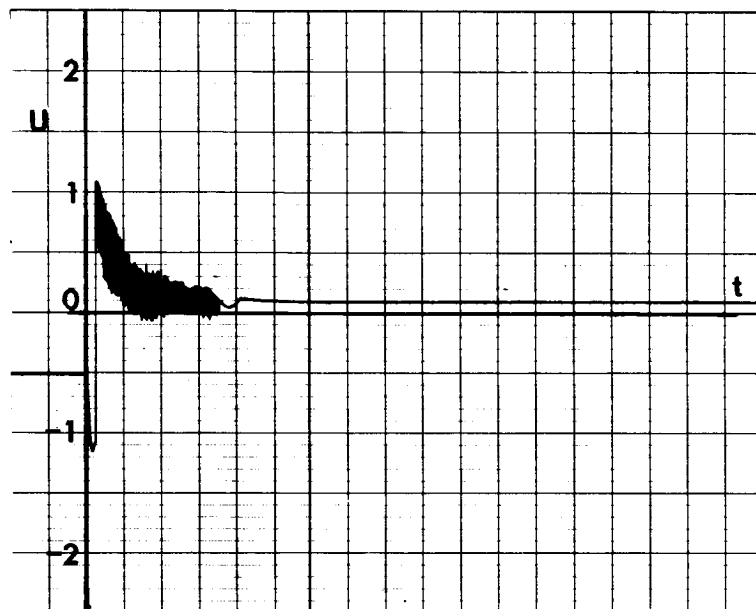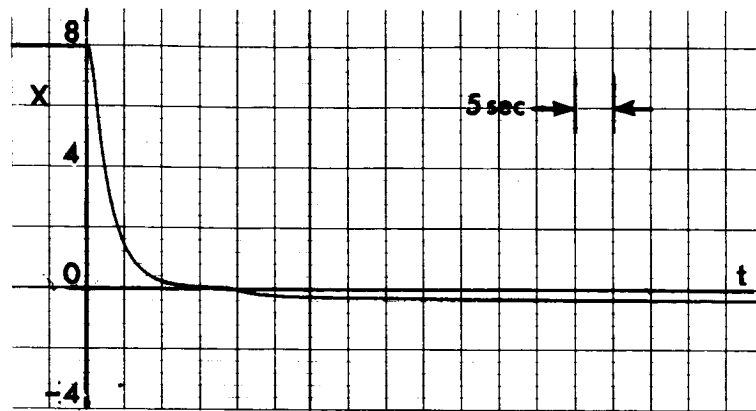
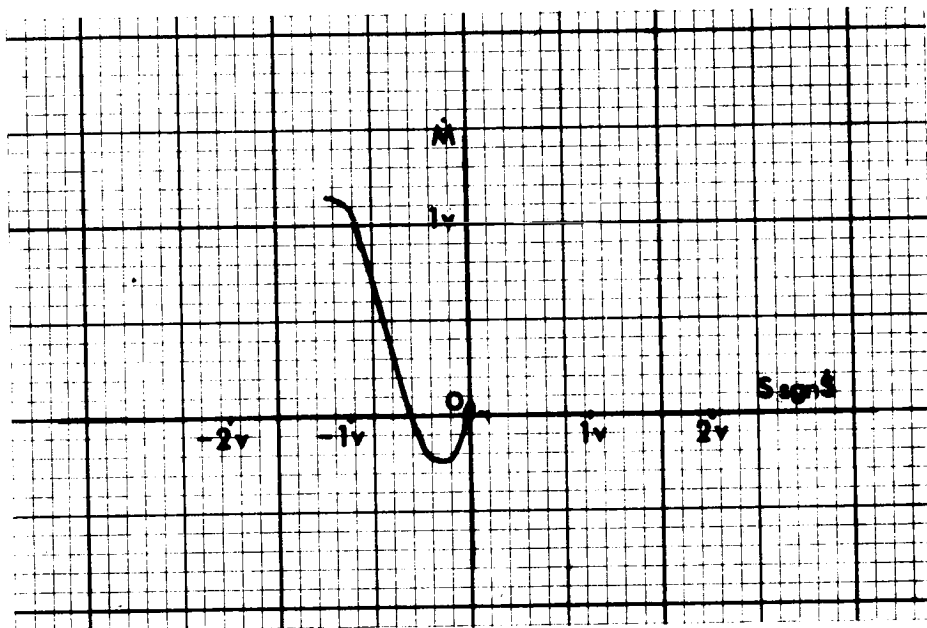Fig. 4.4a   Example 1 for I.C.I with
            Adjustment Logic A

Fig. 4.4b Example 1 for I.C.1 with
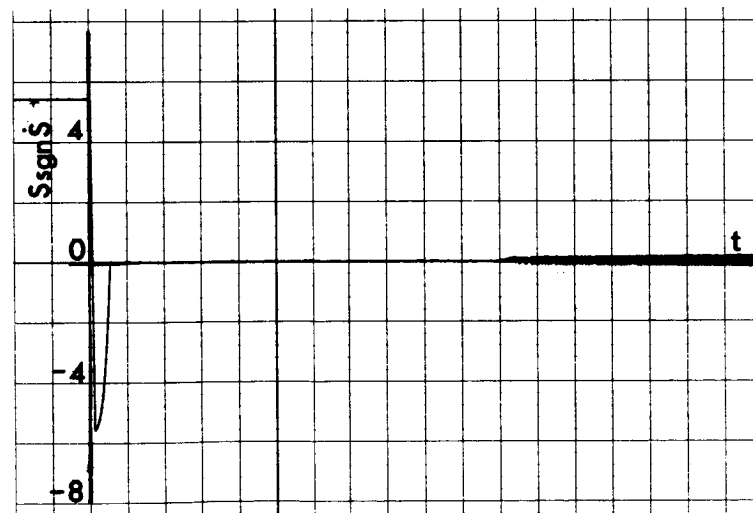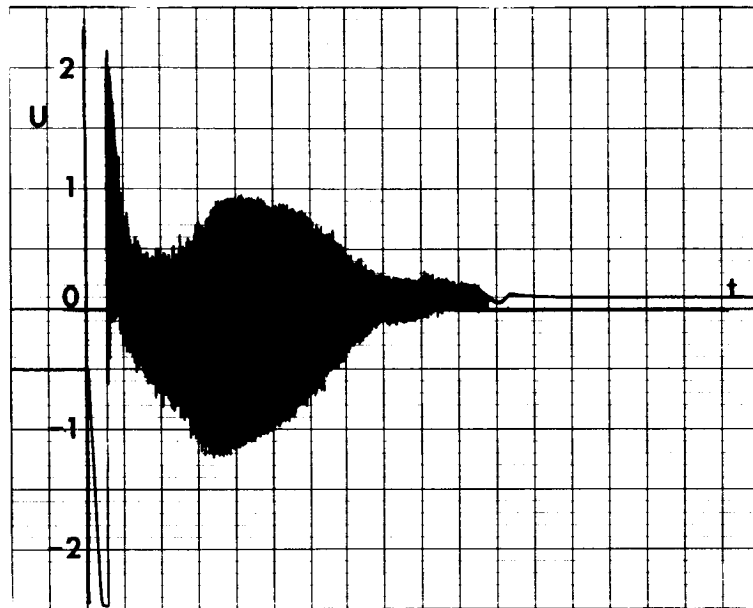Adjustment Logic A

44

Fig. 4.5a   Example 1 for I.C.2 with
Adjustment Logic A

45

Fig. 4.5b Example 1 for I.C.2 with
Adjustment Logic A

46
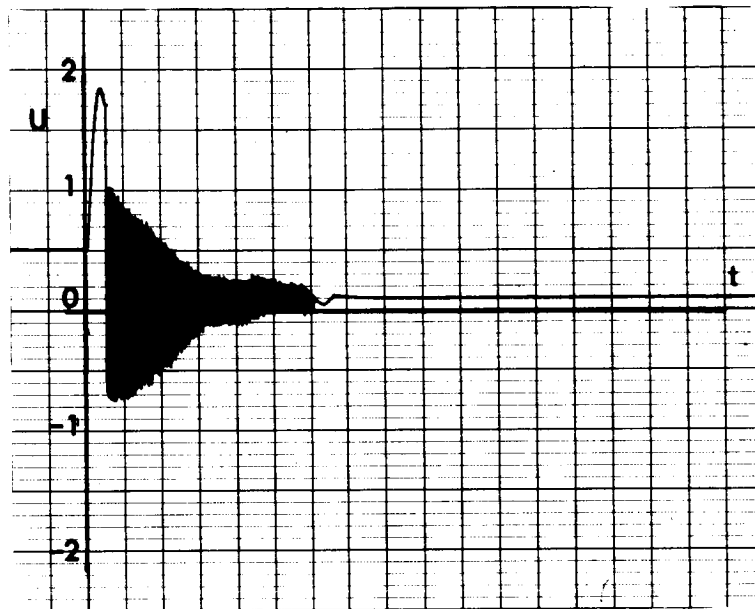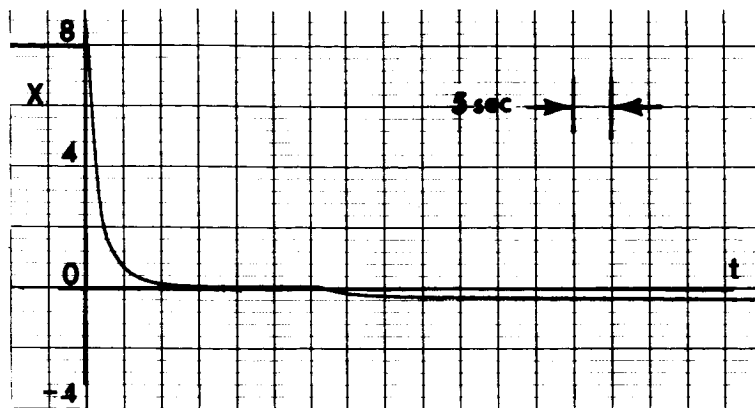
Fig. 4.6a   Example 1 for I.C.3 with
Adjustment Logic A

47

Fig. 4.6b   Example 1 for I.C.3 with
         Adjustment Logic A
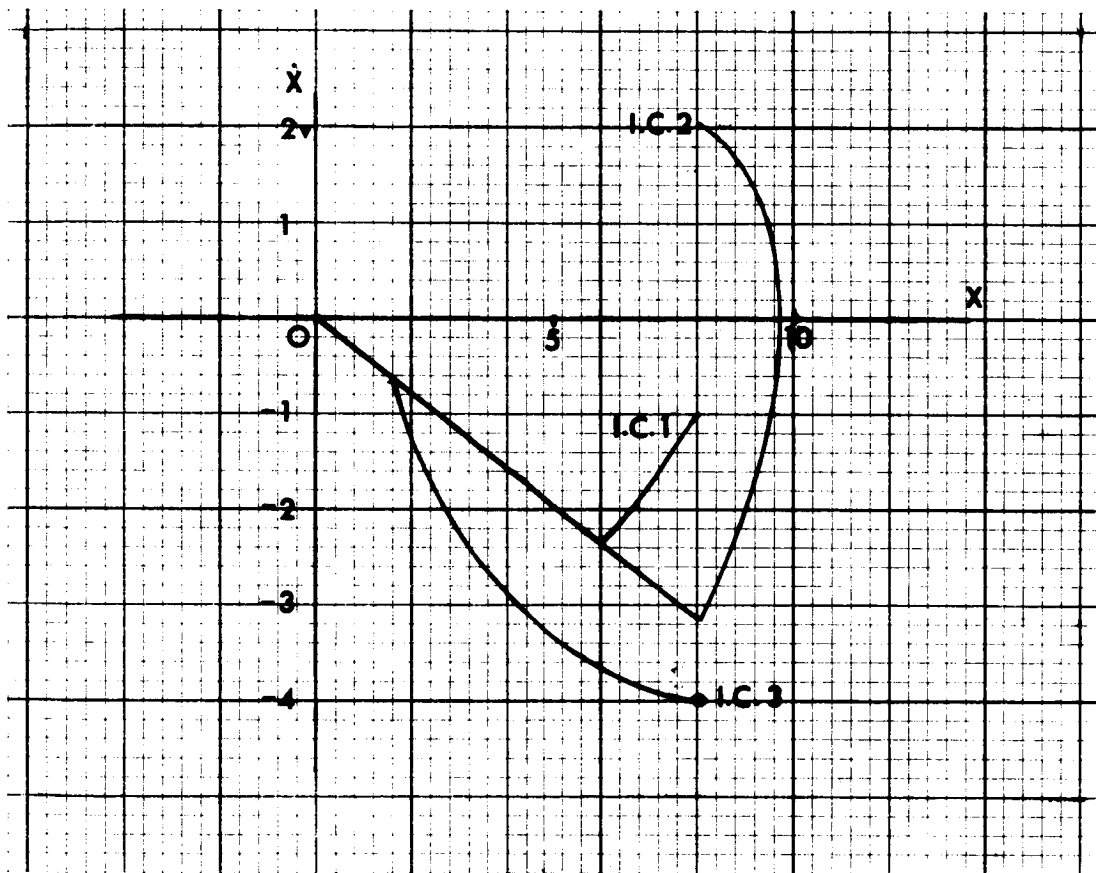
Fig. 4.7 Trajectories in the Phase Plane
for Example 1
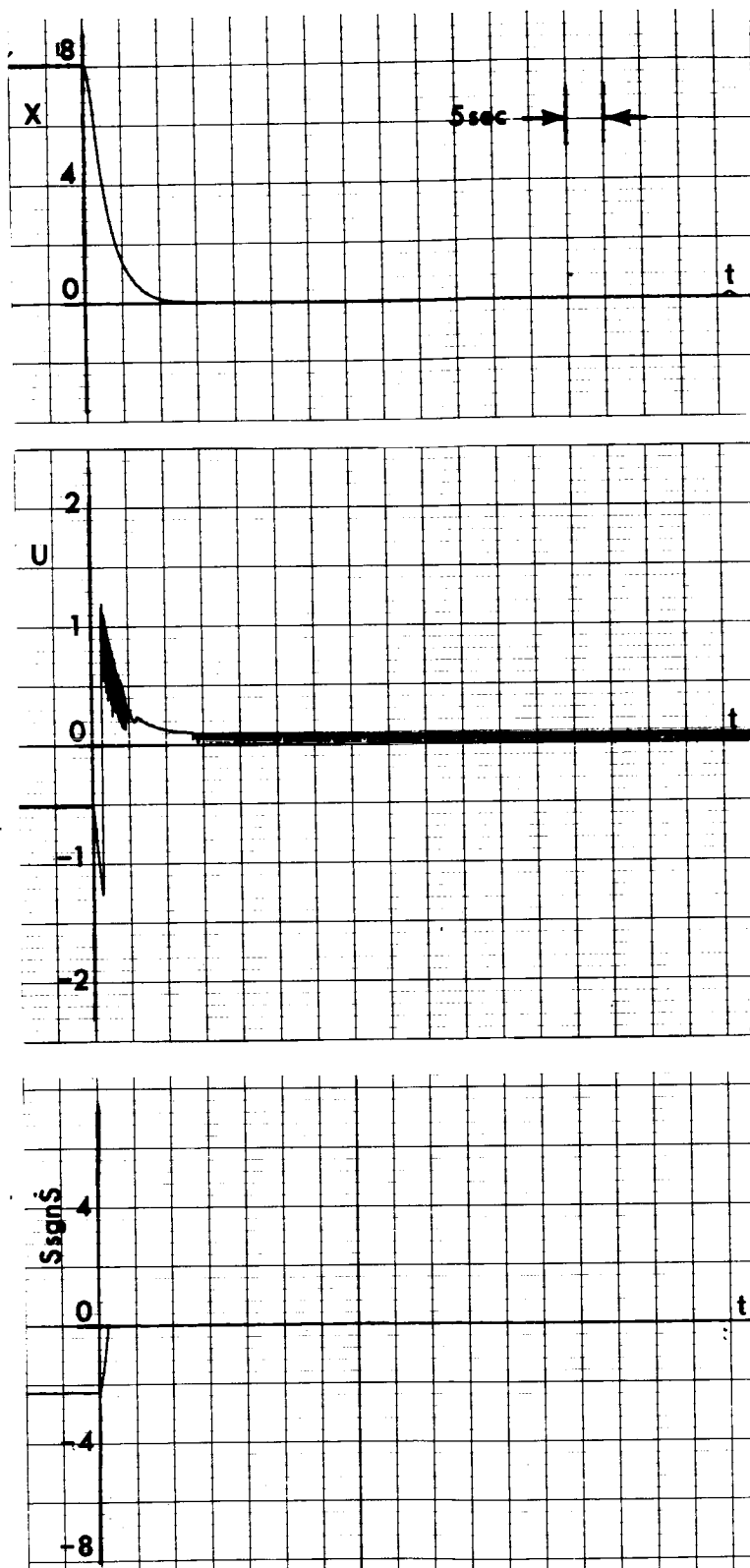
Fig. 4.8a   Example 1 for I.C.1 with
Adjustment Logic B
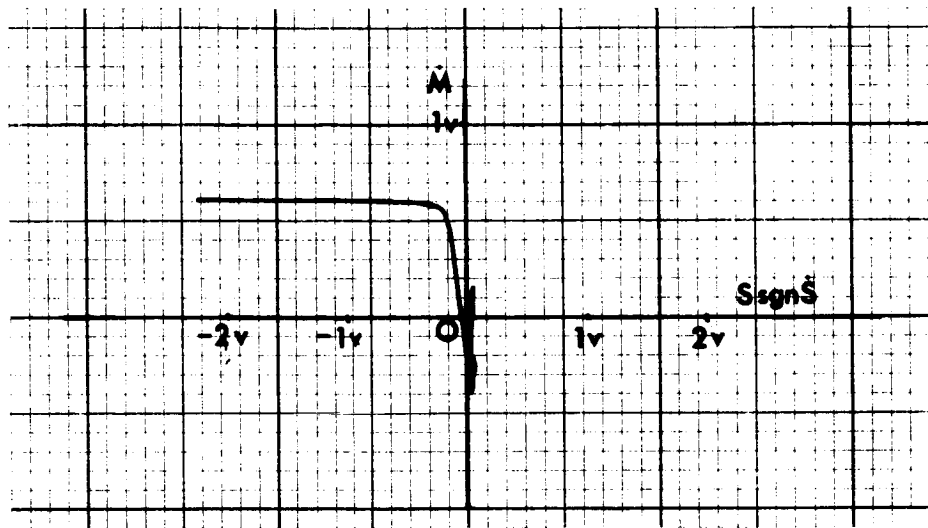
Fig. 4.8b   Example 1 for I.C.1 with
Adjustment Logic B
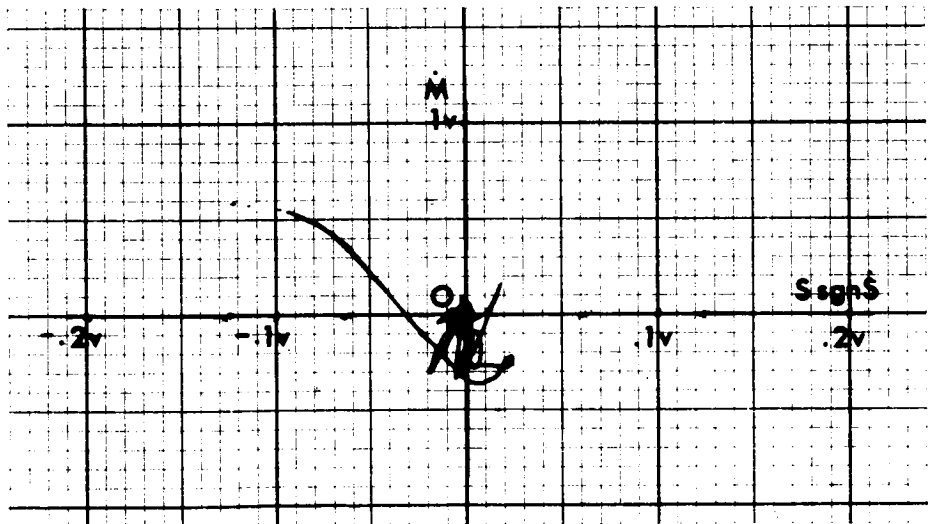
Fig. 4.8c   Enlargement of Fig. 4.8b
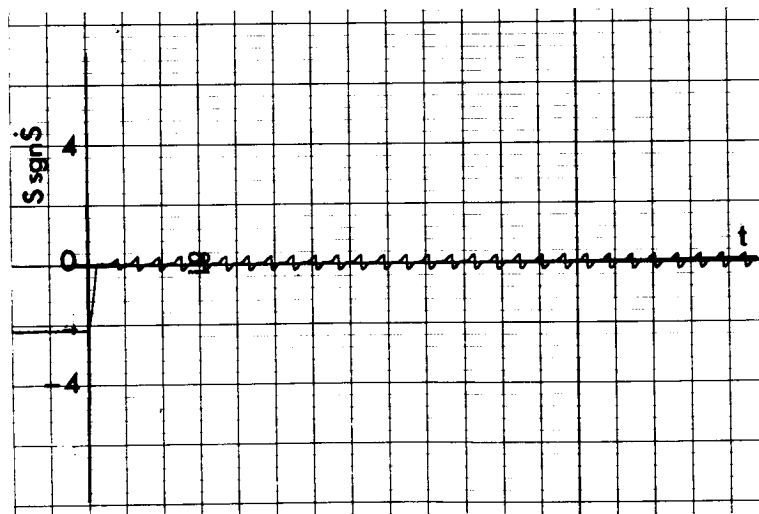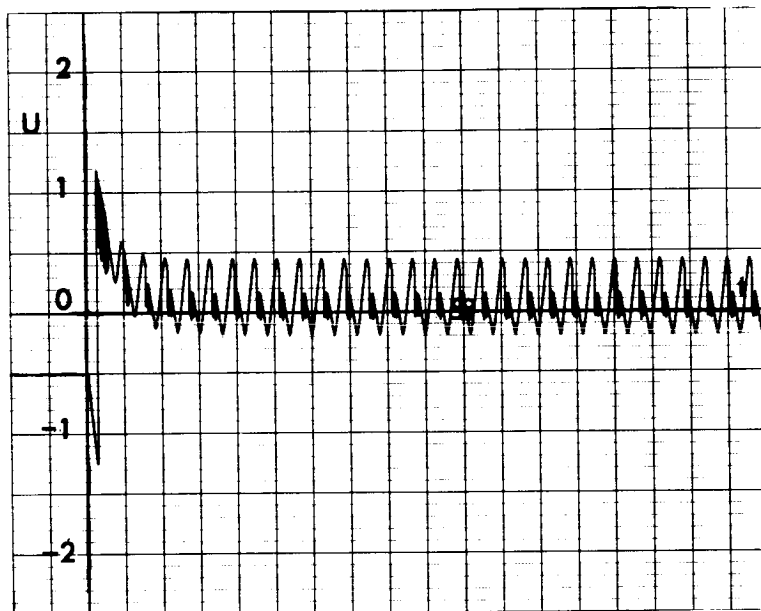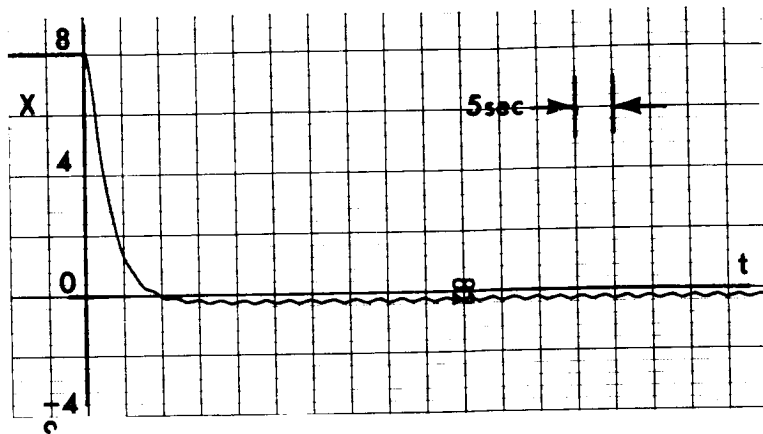
Fig. 4.9a Example 1 for I.C.1 with
Adjustment Logic C
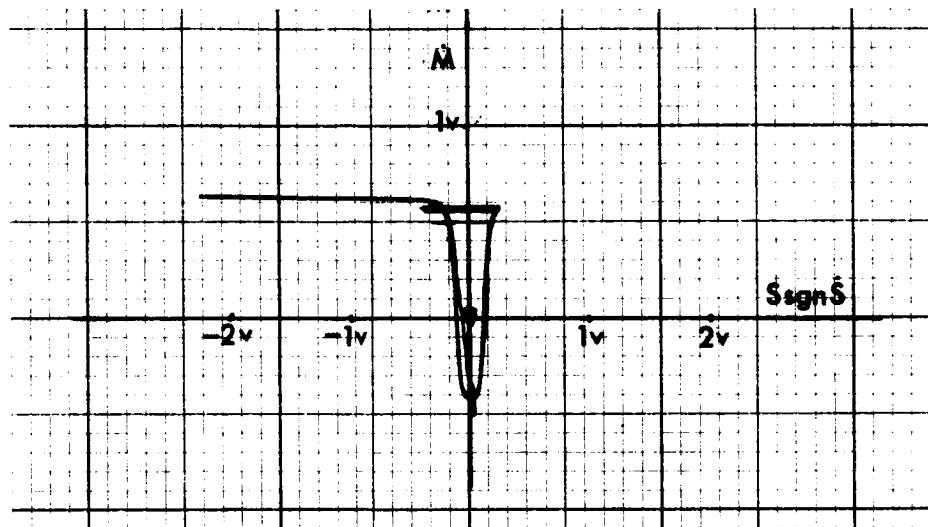
Fig. 4.9b   Example 1 for I.C.1 with
Adjustment Logic C
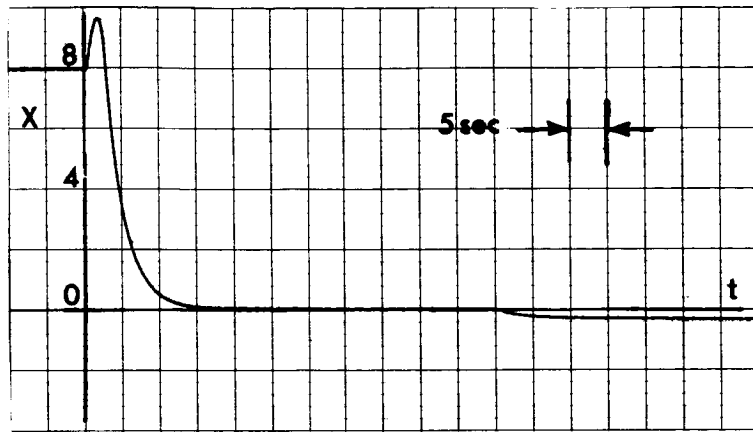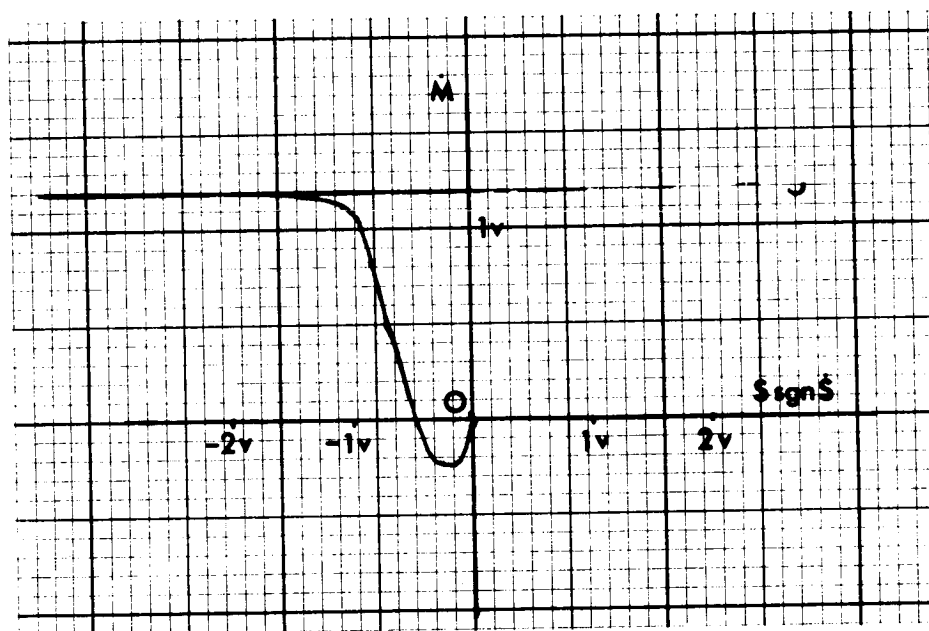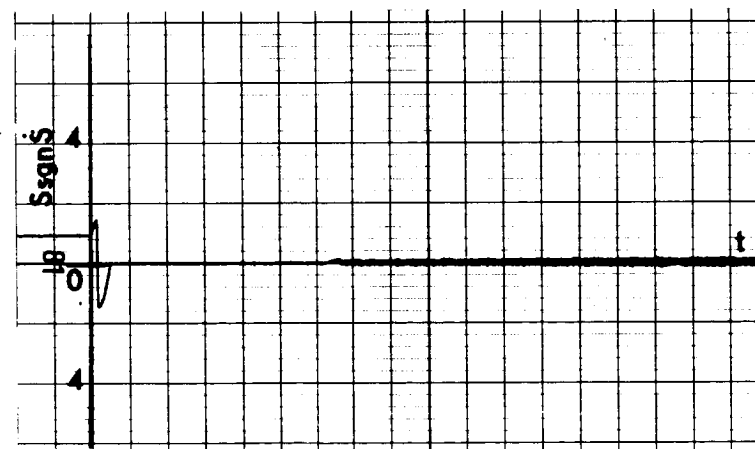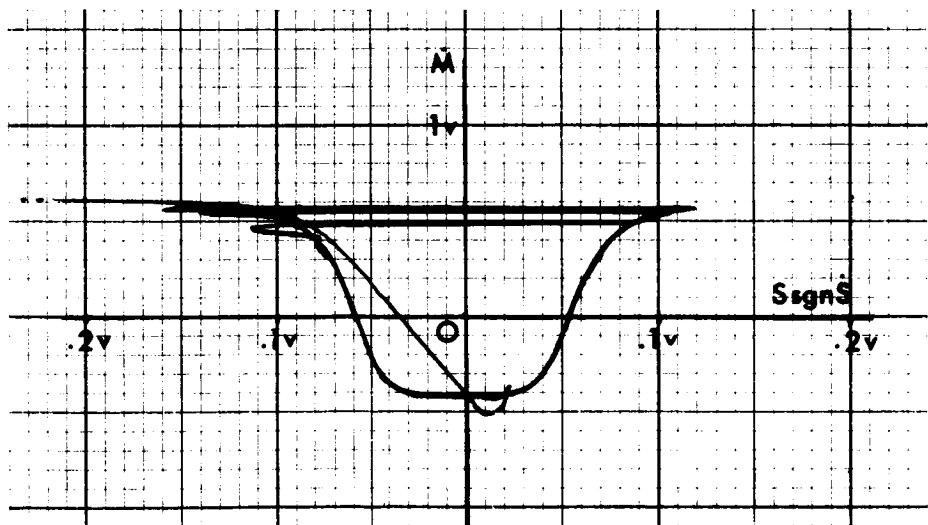

Fig. 4.9c   Enlargement of Fig. 4.9b
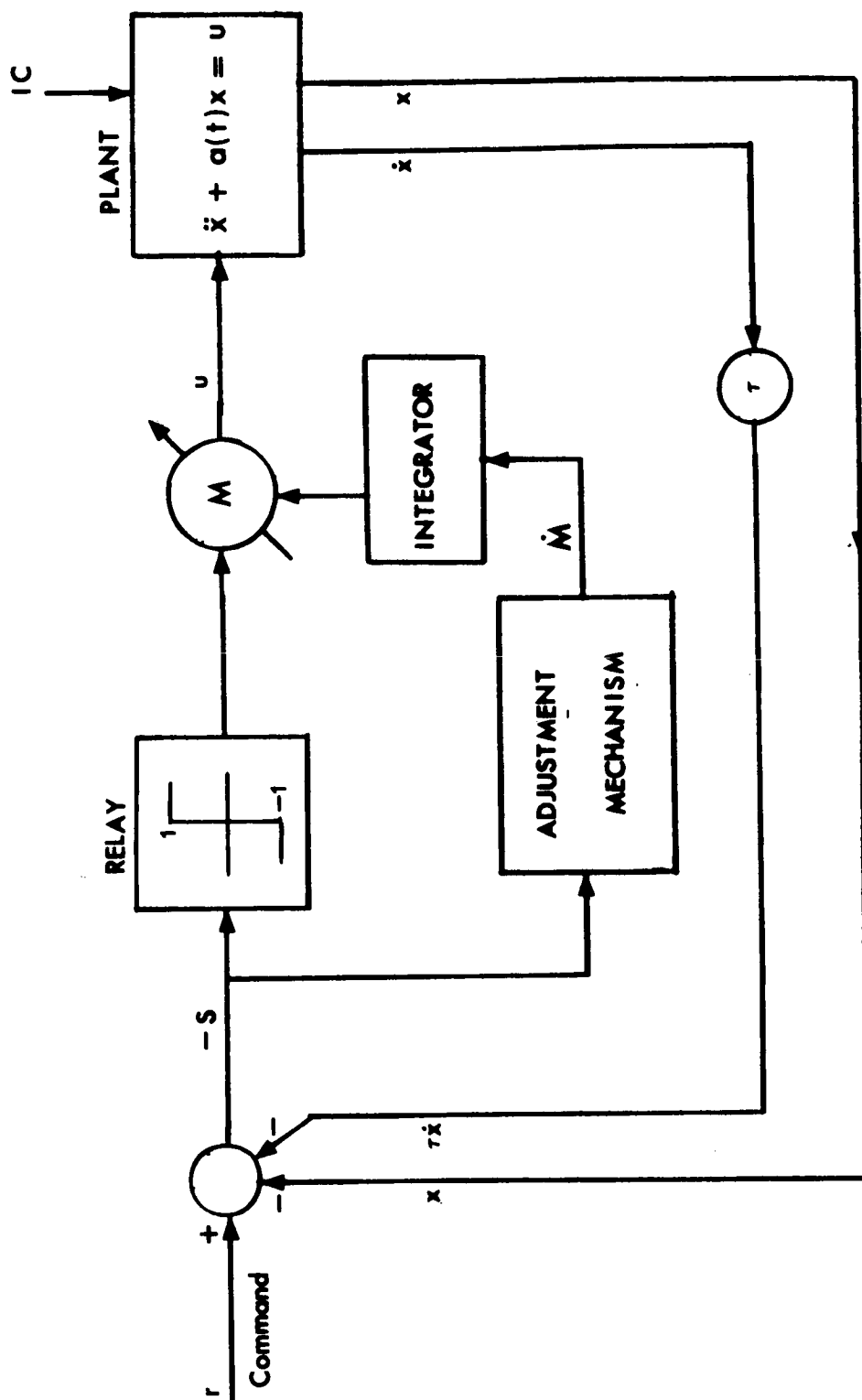
Fig. 4.10 Functional Block Diagram
for Example 2
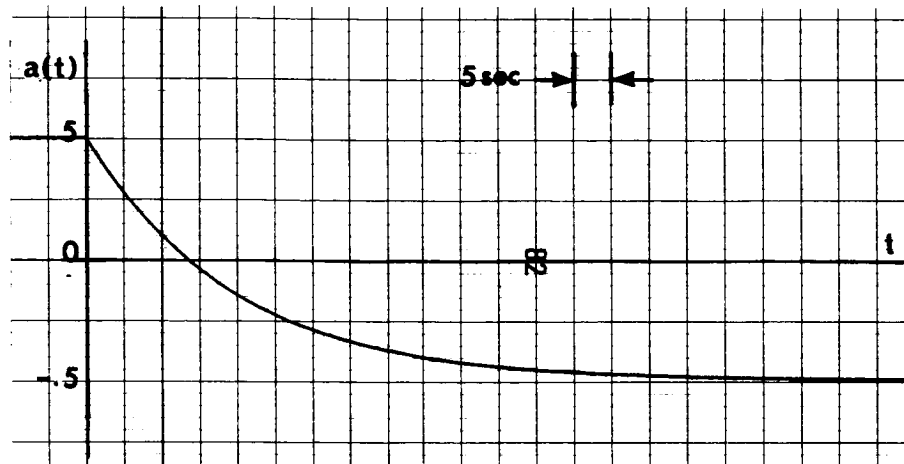
Fig. 4.11 Time History of Plant's Parameter a(t)
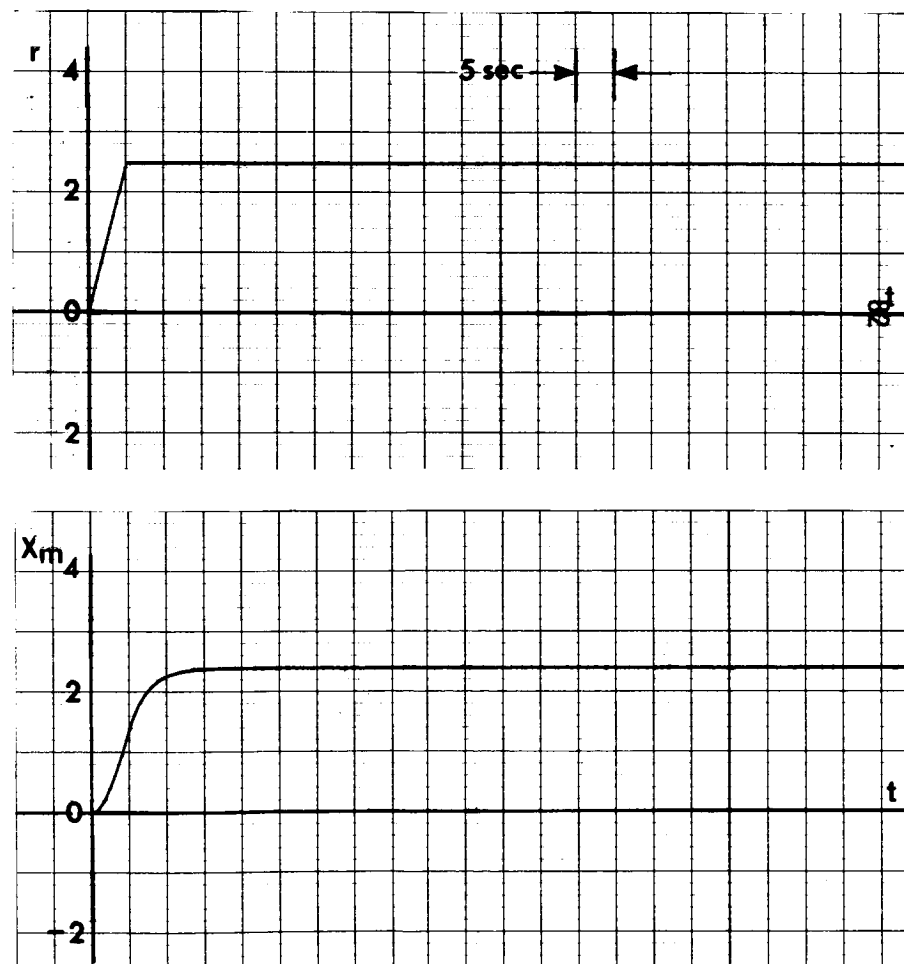
Fig. 4.12 Command Input r and Model Response x_m
for Example 2 and 3
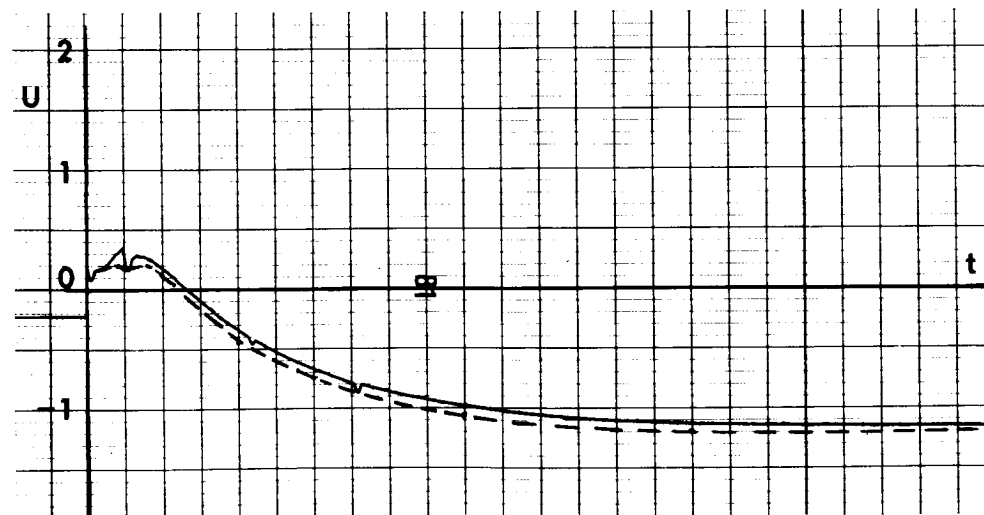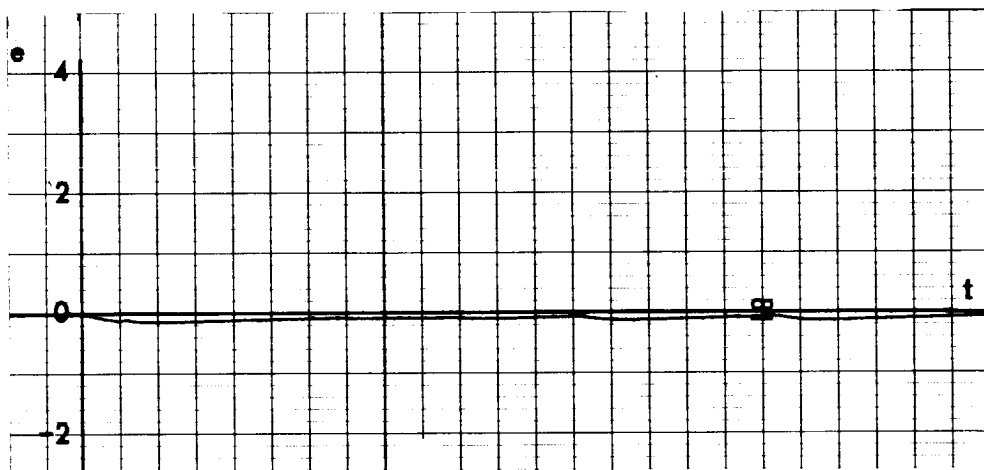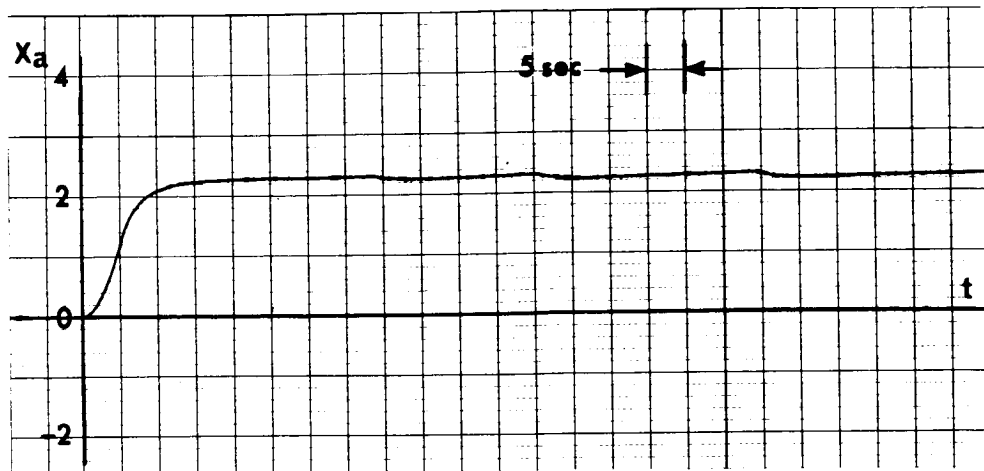
Fig. 4.13a   Example 2 with
Adjustment Logic B

56
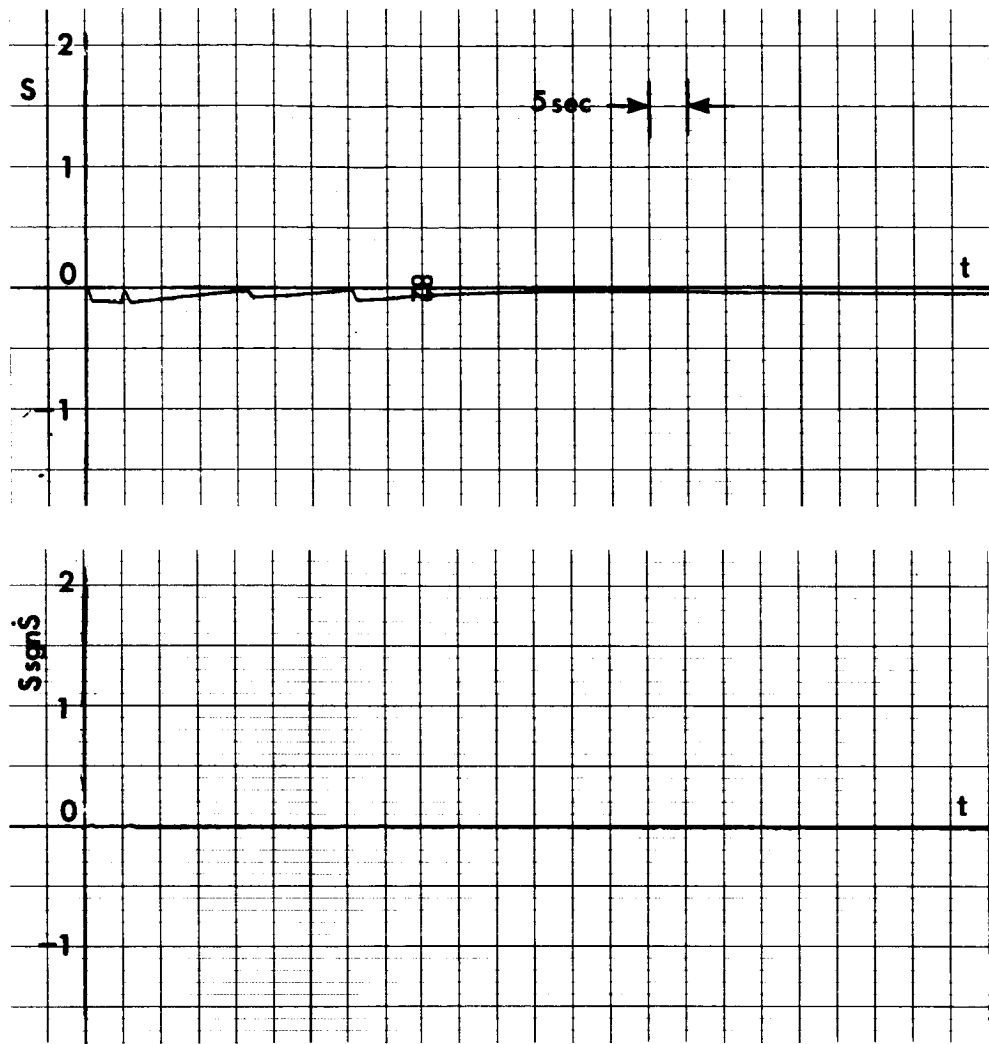
Fig. 4.13a (continued)
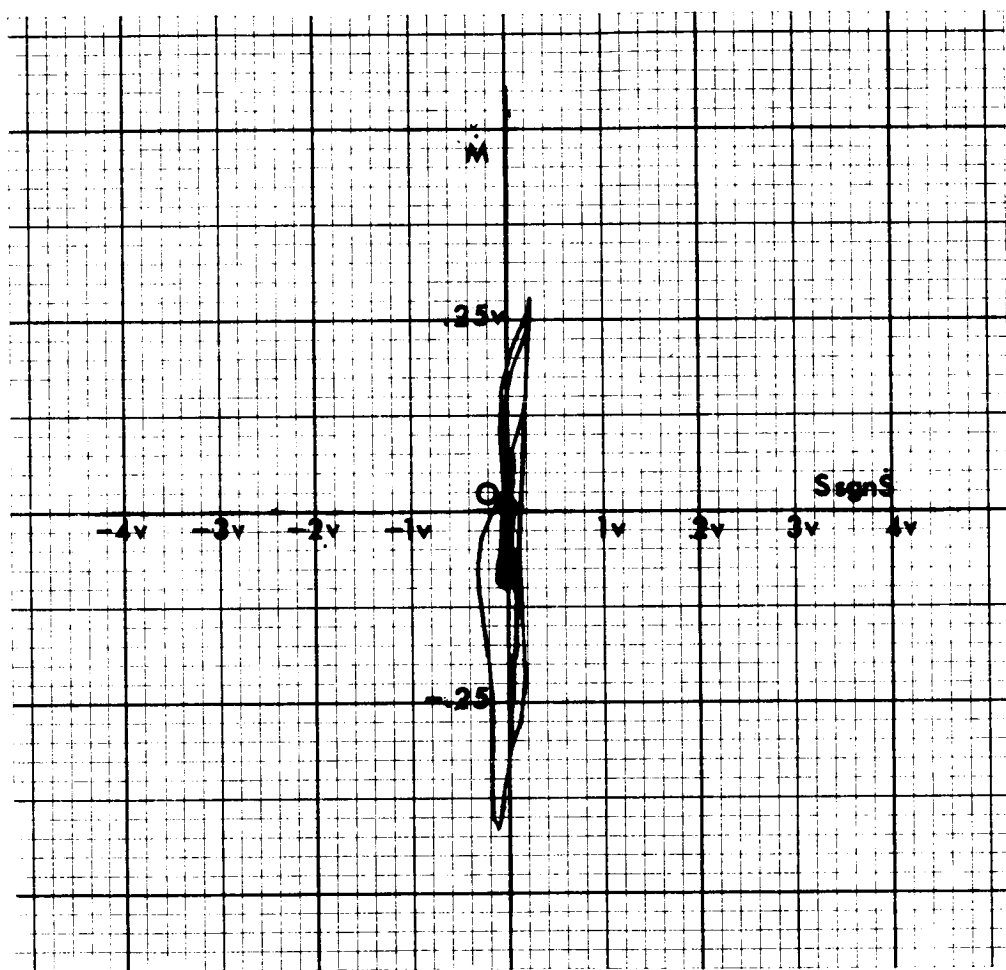
Fig. 4.13b Example 2 with
Adjustment Logic B
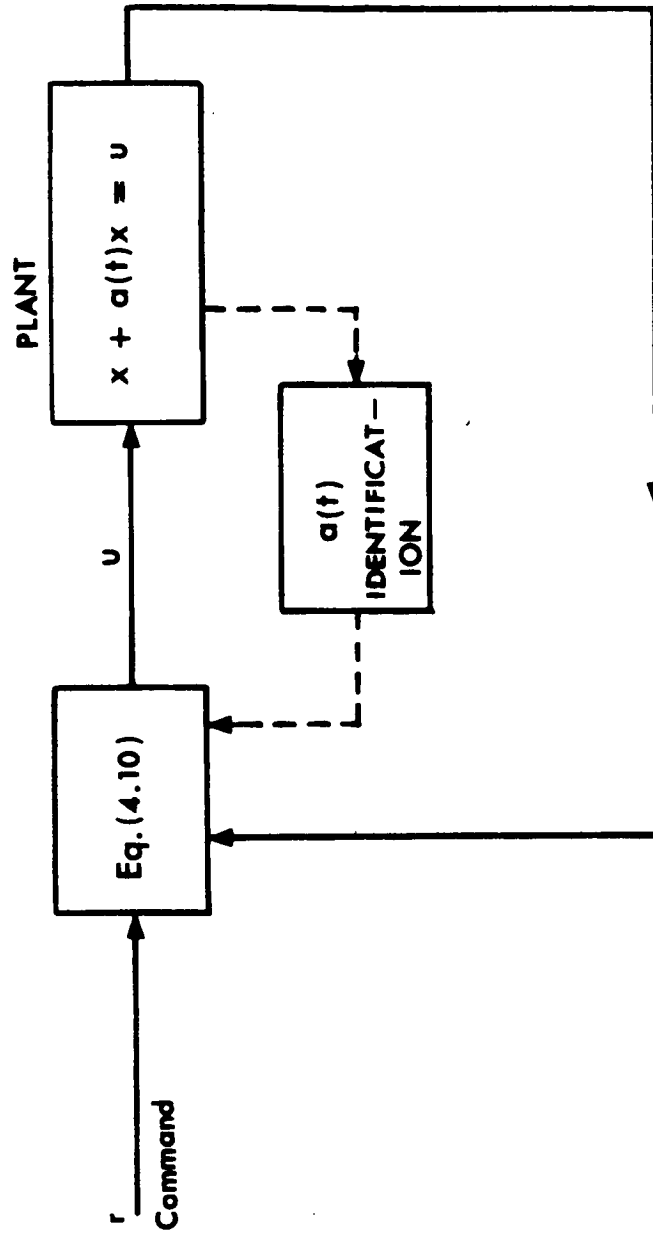
Fig. 4.14 Linear Equivalent System for Example 2
with Adjustment Logic B
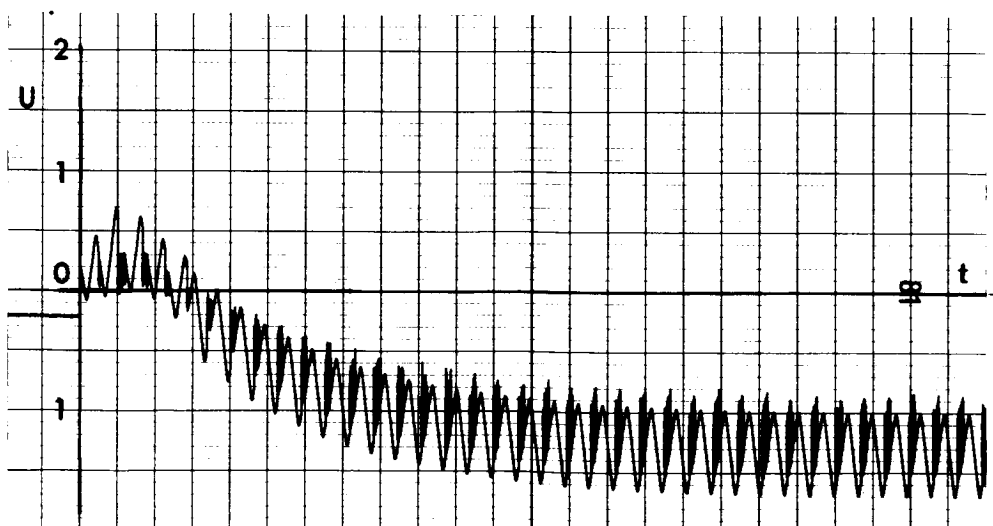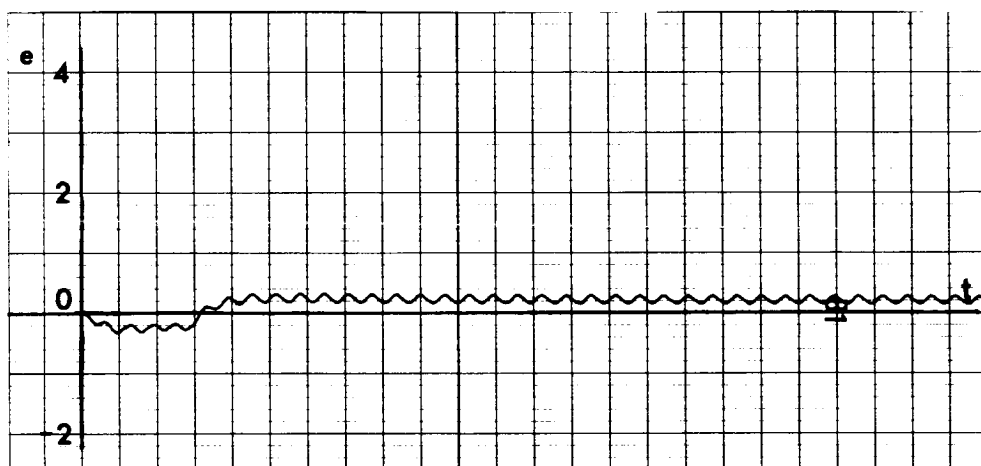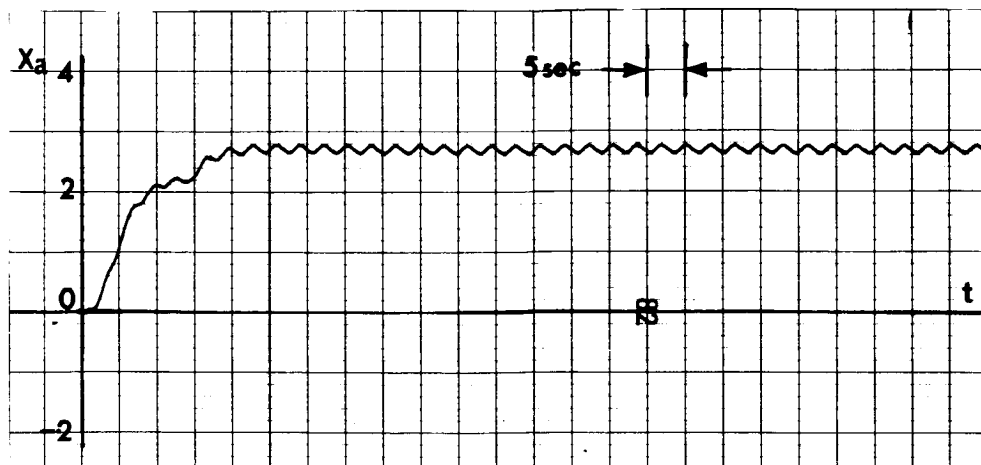
Fig. 4.15a   Example 2 with
Adjustment Logic C

60
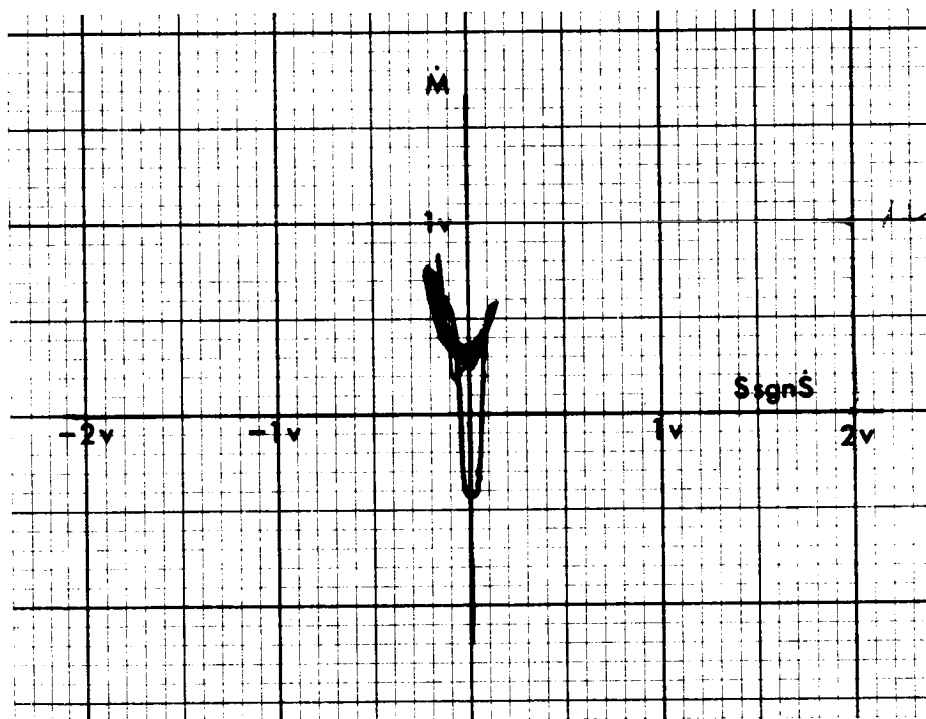
Fig. 4.15a (continued)

Fig. 4.15b Example 2 with
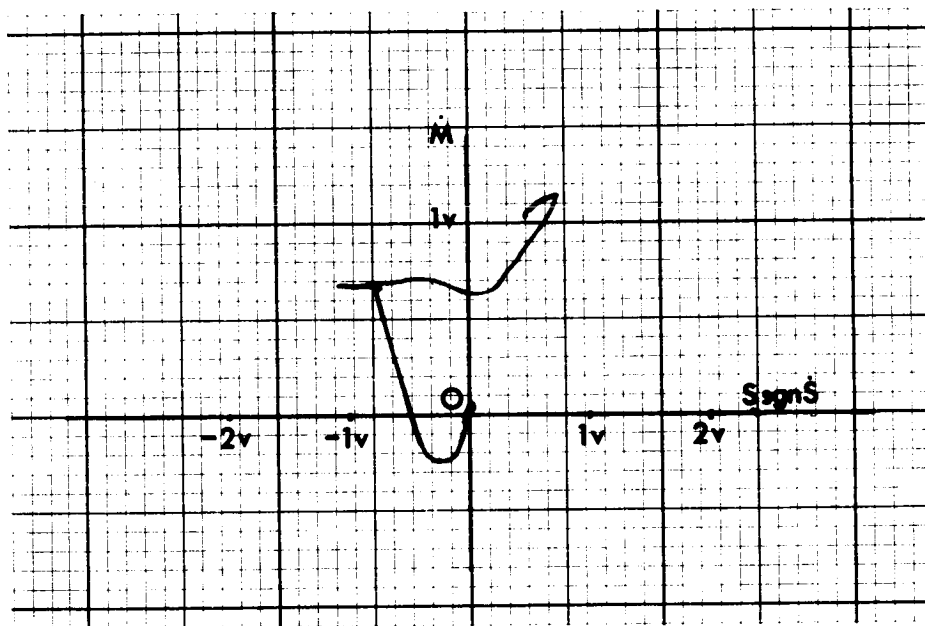Adjustment Logic C
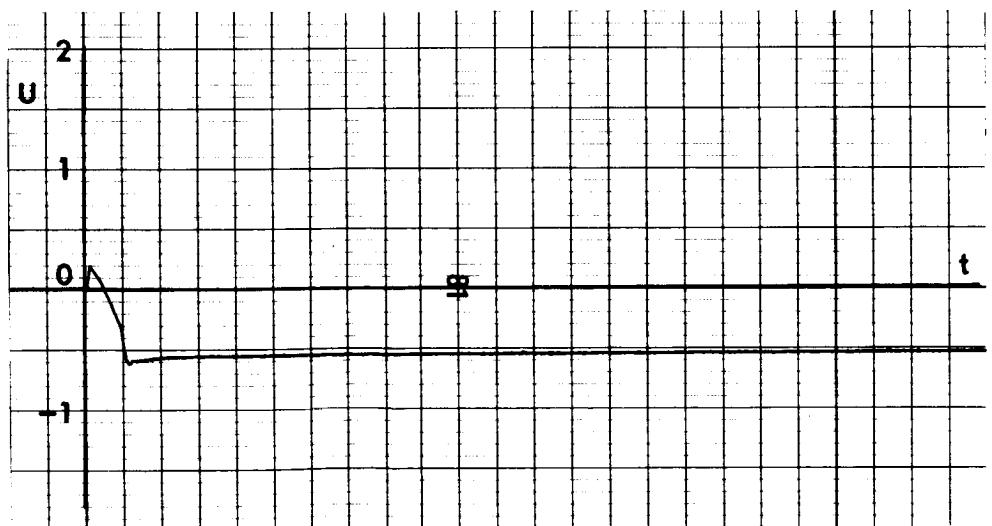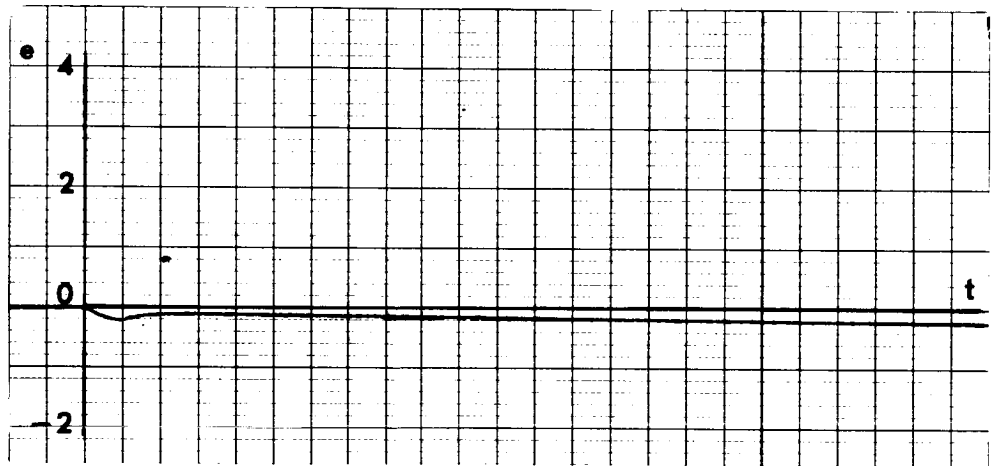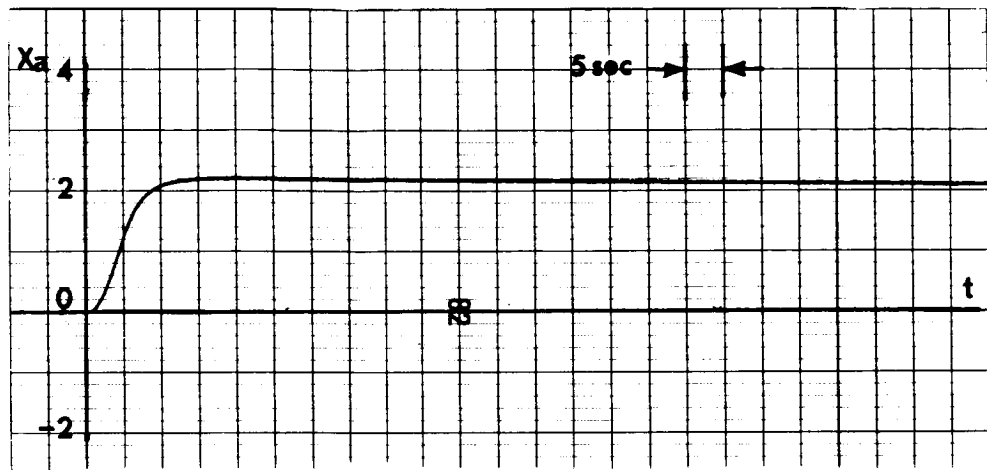
Fig. 4.16   Example 3 with
Adjustment Logic B

Fig. 4.16 (continued)

64
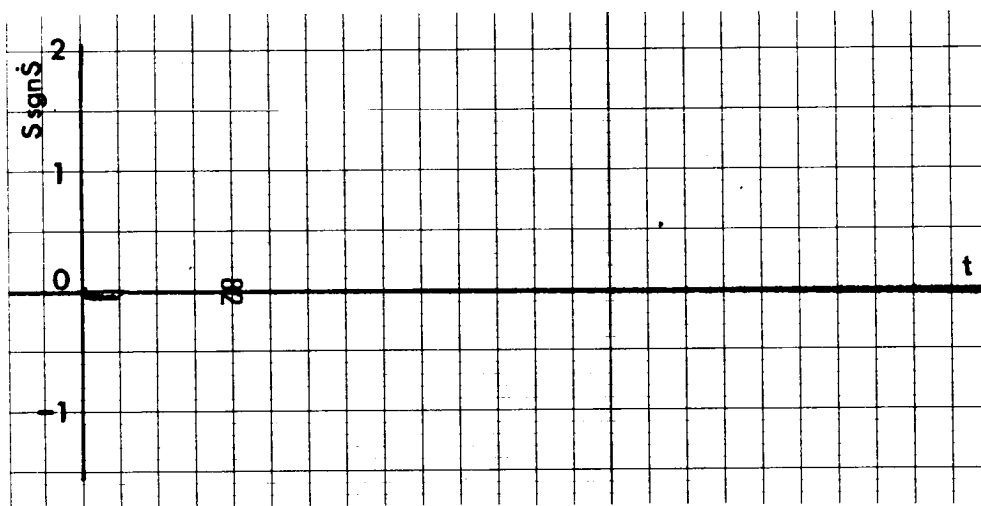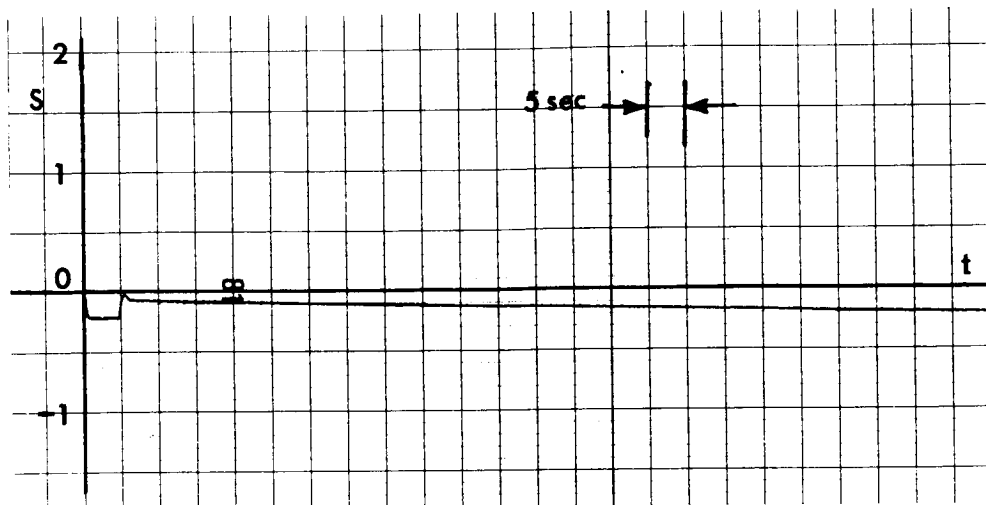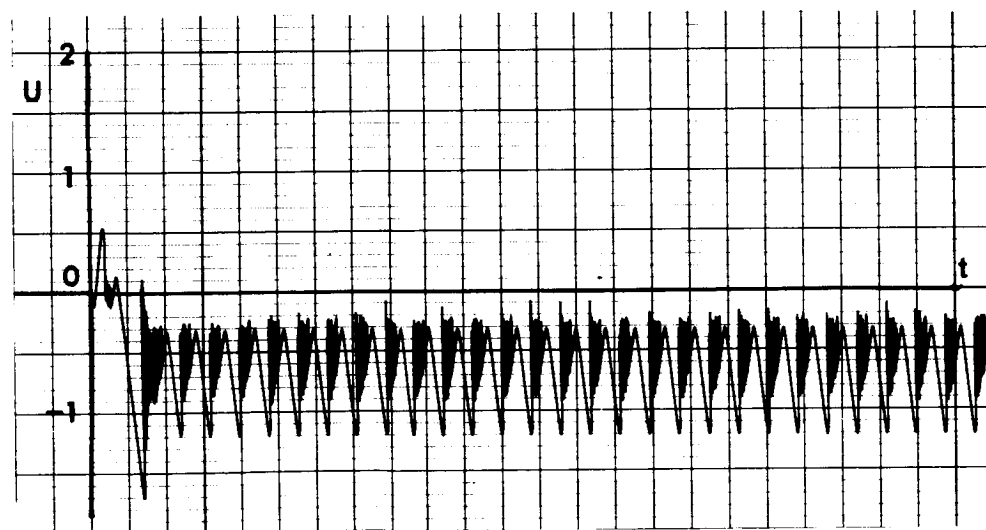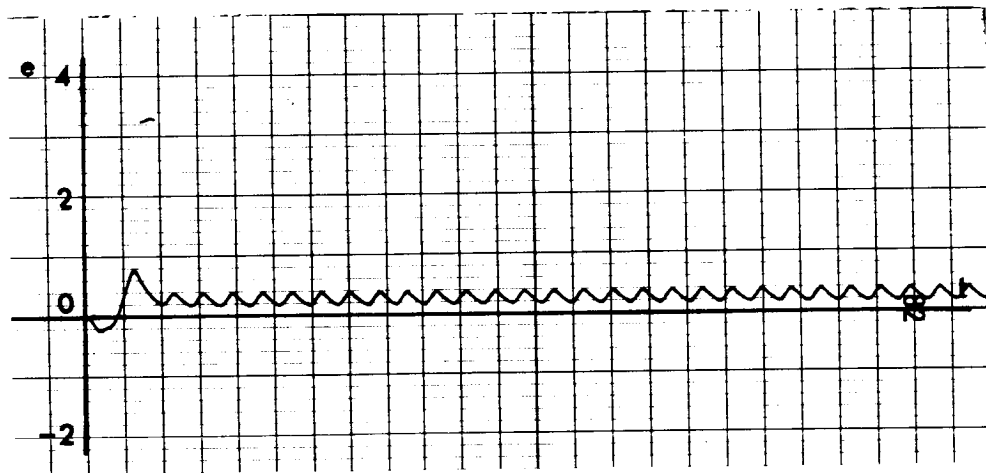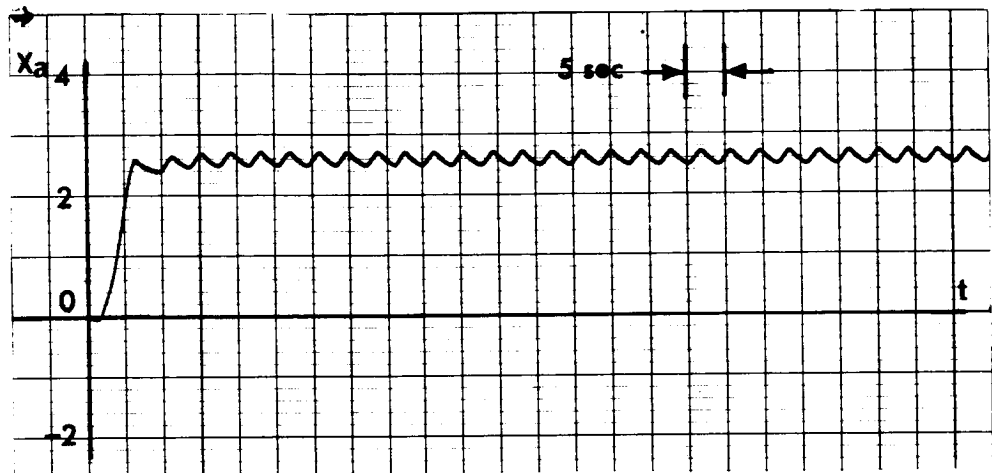
Fig. 4.17 Example 3 with Adjustment
Logic C
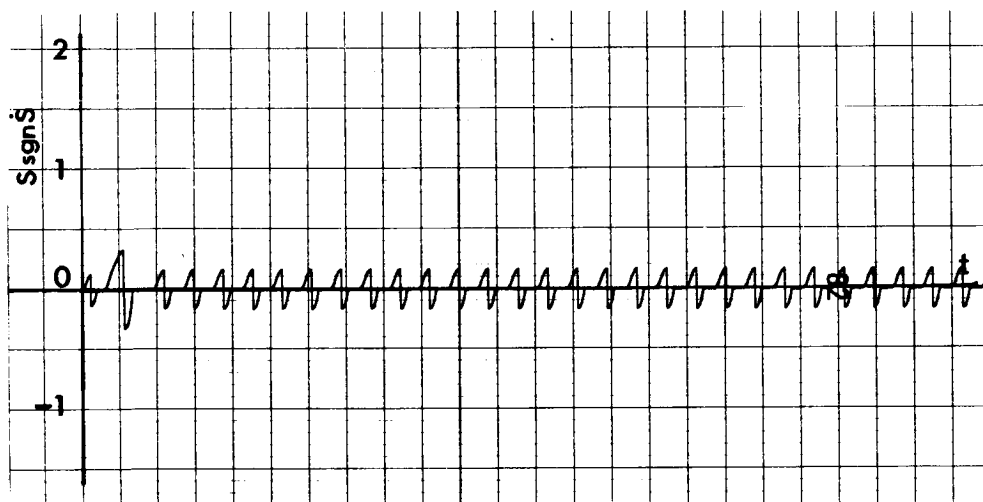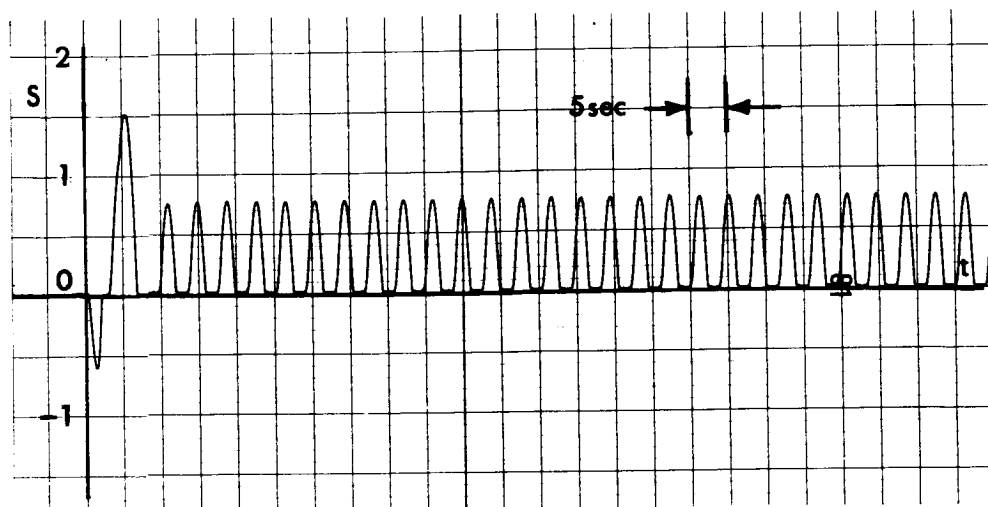
Fig. 4.17 (continued)
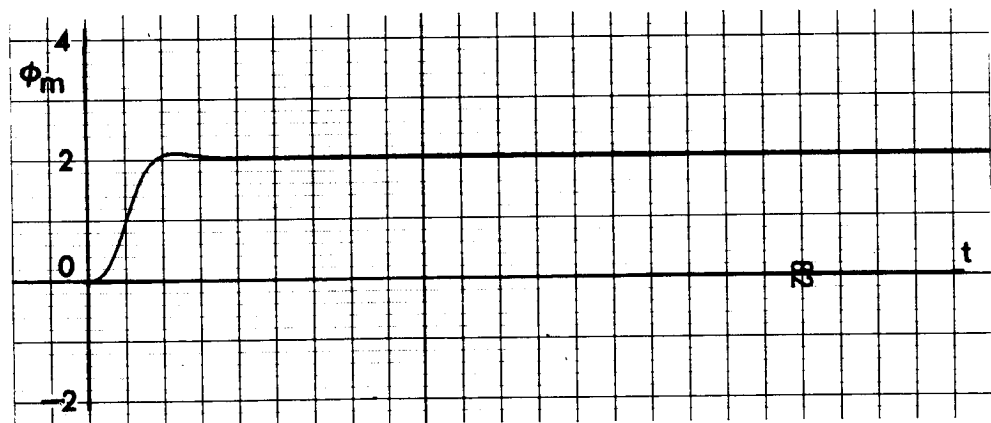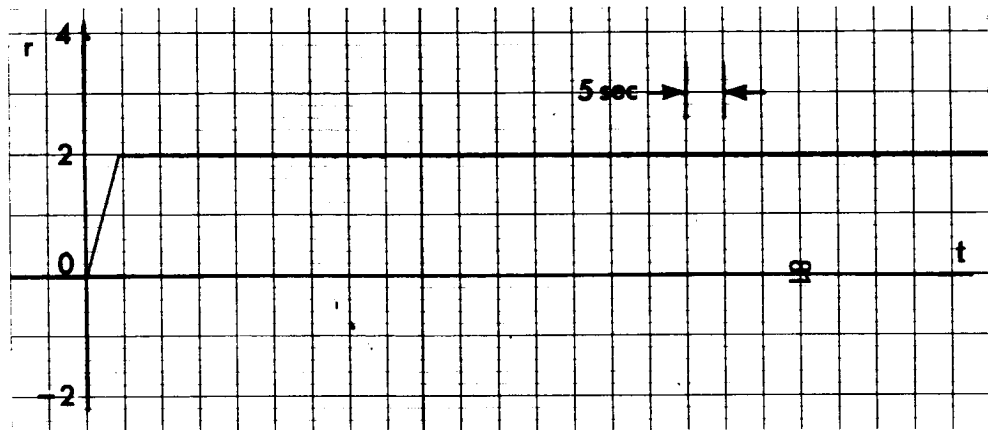
Fig. 4.18   Command r and Model Output
for Example 4

67
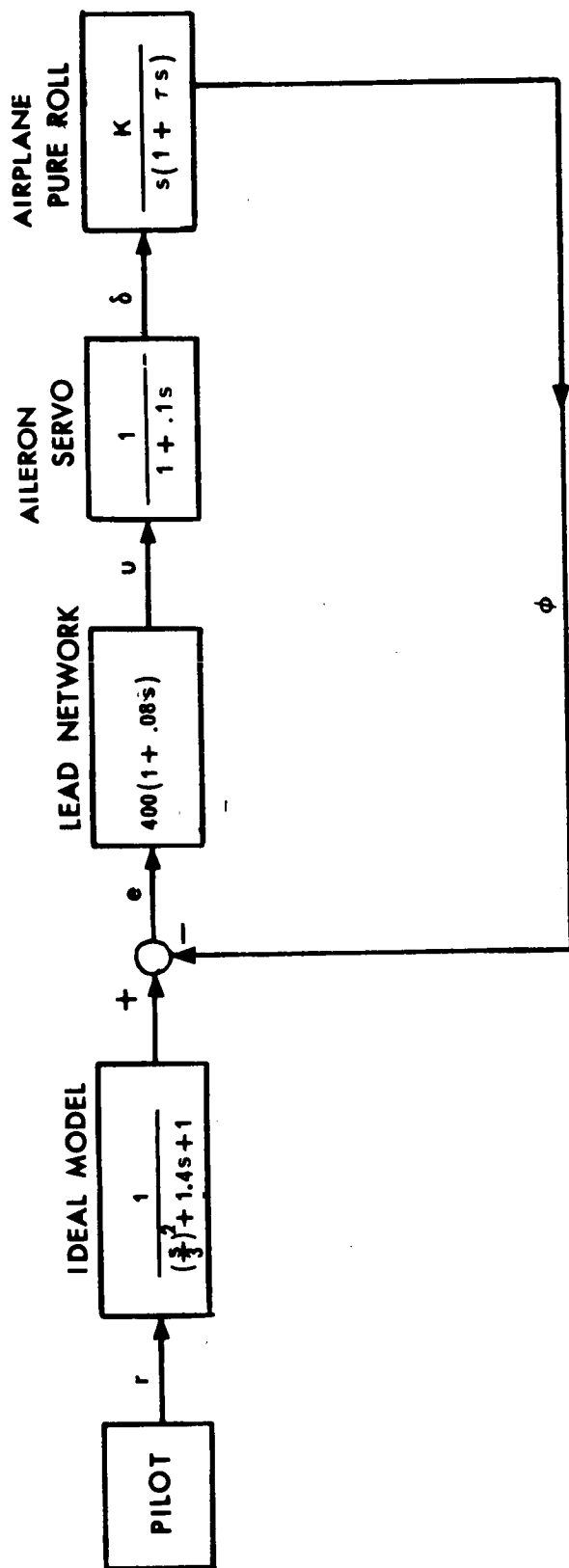
Fig. 4.19 Block Diagram of the Linear Self-Adaptive
Roll Control System for Example 4
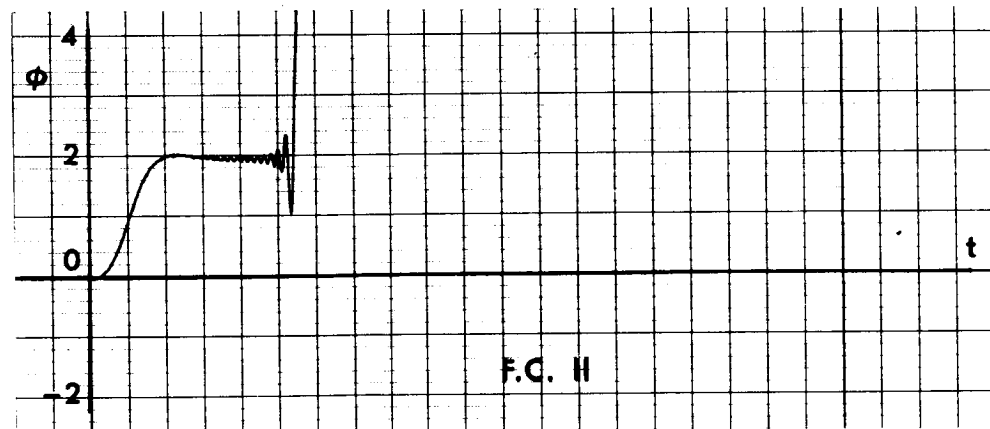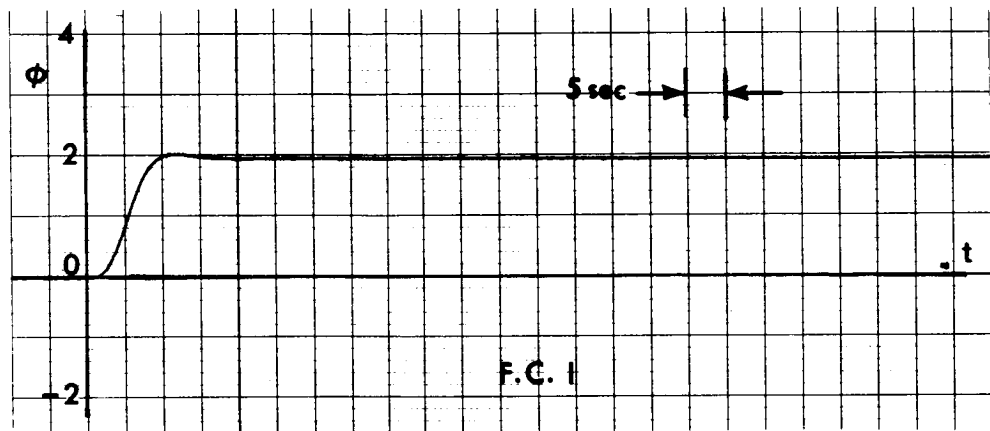
Fig. 4.20 Results of the Linear System
for Two Different Flight Conditions

69
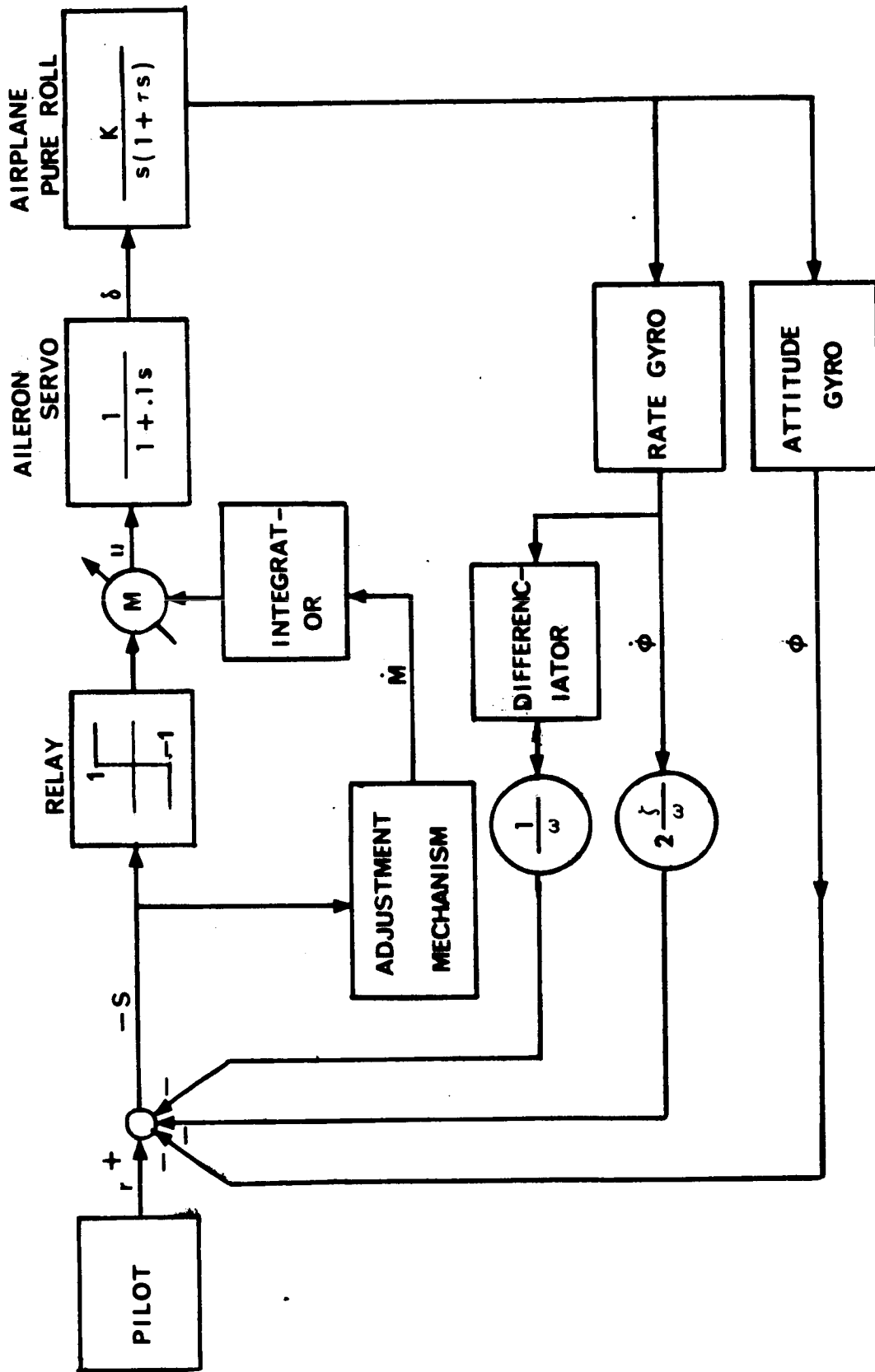
Fig. 4.21 A Suggested Implementation of the Proposed
Self-Adaptive System for Example 4
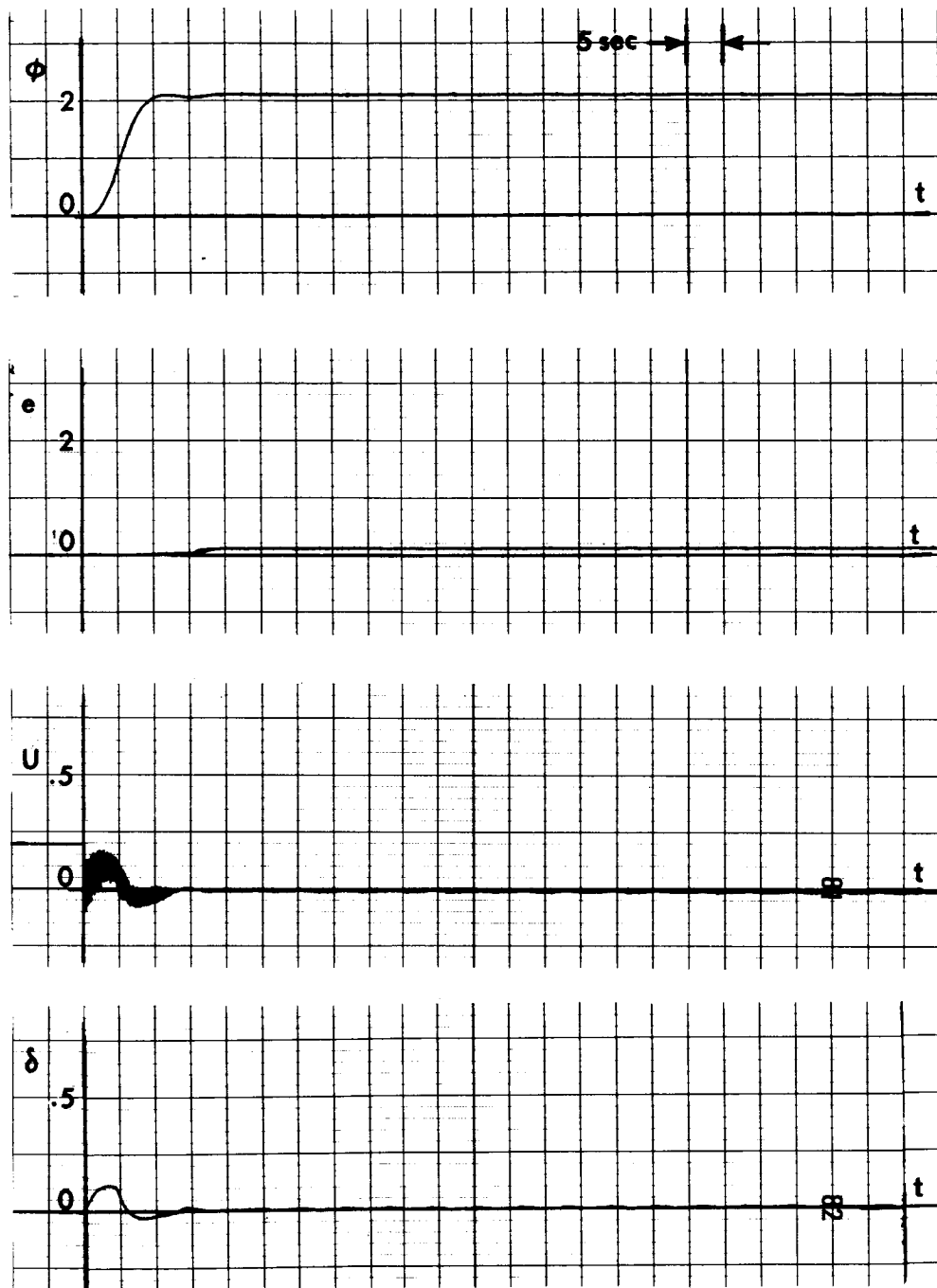
Fig. 4.22 Example 4 with Adjustment
Logic B (Flight Condition I)

71
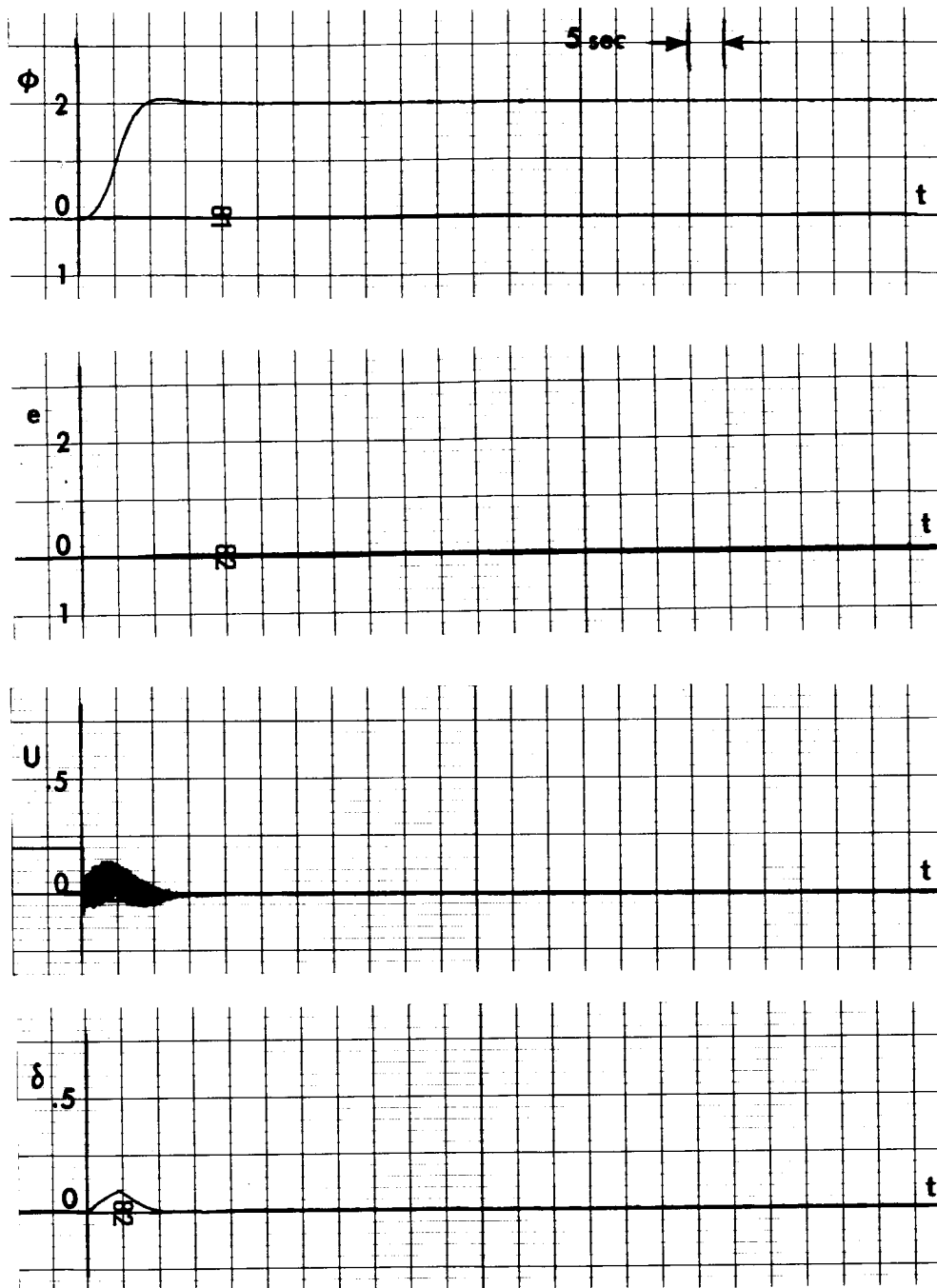
Fig. 4.23 Example 4 with Adjustment
Logic B (Flight Condition II)

CHAPTER 5

CONCLUSIONS AND RECOMMENDATIONS

FOR FURTHER STUDY

5.1 Conclusions

The chatter mode can be advantageously used for self-adaptive control systems, if the following basic requirements are met:

(1) There must be a switching function to describe the ideal model dynamics

(2) The chatter mode must be reached quickly and then be sustained

(3) The chatter frequency must be reduced

(4) Any zero in the plant transfer function must. be cancelled

Under the chatter mode, the average motion of the plant is determined by the equation of the switching function. Requirements (1) and (2) are thus essential first of all.

Requirement (2) reflects a need for some suitable forward gain (switching level) adjustment. The proposed scheme for the adjustment is simple, requiring only two pieces of information, the instantaneous switching function

and its time derivative. Furthermore, it can remove any excess amount of gain, and reduce the high chatter frequency as well. In particular, the experiment (example 2, logic B) suggests that well designed adjustment logics will realize "the sliding mode with <u>physical relay</u>" rather than the chatter mode, eliminating the frequency problem altogether.

The conditions for applying this self-adaptive system are

(1) There must be no zero in the plant transfer function

(2) The model transfer function must be of $n-1$'th order for an n'th order plant

Zeroes may be common in most on-off control systems, but an appropriate compensation network could effectively eliminate these zeroes to fulfill condition (1). Either compensating the original plant or slightly modifying the ideal model by compromising the base somewhate, could adjust the order of the transfer function to fulfill condition (2).

5.2   Recommendations for Further Study

The following topics are recommended for future study in this area:

(1)   Examination of anti-disturbance performance

(2)   More quantitative investigation of the dynamics of the adjustment logic for design purposes

(3)   Manual experiments using the suggested visual display

(4) Extended application of the basic idea in areas other than self-adaptive control systems, including those suggested in Appendices B and C*

---

* Experimental verification of the theory given in Appendix C is in progress using a digital computer.

APPENDIX A

THE STATE OF THE ART OF SELF-ADAPTIVE CONTROL SYSTEMS

A.1 The Need for Self-Adaptive Systems

This section first discusses and justifies the general philosophy underlying self-adaptive control systems, and then outlines the basic ideas in the well-known self-adaptive control systems. In particular, two self-adaptive control systems, in which a relay plays a crucial role will be discussed for purposes of comparison with the proposed system.

An adaptive control system may be defined as one which can maintain satisfactory performance of the plant over a wide range of changing conditions, either external or internal. The terms "adaptive control systsm" and "self-adaptive control system" are not clearly distinguished in the literature. Yet, if one'wants to insist on the distinction, a self-adaptive control system could be defined as an adaptive control system which organizes itself to accomplish its objective through internal processes of measurement, evaluation, adjustment, etc.[13,19]

Any conventional control system is adaptive to some extent. The limitation is that it need not or cannot cope with a wide range of environmental conditions. It can deal

with only a limited range of plant parameter variations, and limited kinds of external disturbances and command reference inputs which are anticipated in the design stage.

Fig. A.1 shows a follow-up servo system. First suppose that the system is a conventional one, i.e., the plant with transfer function $G_p(s)$ can be considered virtually stationary. The closed loop transfer function relating the output to the command input is

$$\frac{\text{Output}}{\text{Input}} = \frac{G_c(s) \ G_p(s)}{1 + G_c(s) \ G_p(s)} \simeq 1$$

for $G_c(s) \ G_p(s) >> 1$

The transfer function to the disturbance input is

$$\frac{\text{Output}}{\text{Disturbance}} = \frac{G_p(s)}{1 + G_c(s) \ G_p(s)} \simeq \frac{1}{G_c(s)}$$

Forgetting about the stability problem for a moment, it is necessary to make the controller transfer function, $G_c(s)$, great enough to satisfy both $G_c(s) >> 1$ and $G_c(s) \ G_p(s) >> 1$ in order to achieve good follow-up performance and insensitivity to disturbance input.

This follow-up principle leads directly to an adaptive control system whose functional block diagram is shown in fig. A.2. Unfortunately, however, such a high forward gain tends to introduce instability, and furthermore, the extremely high gain is practically impossible to realize by linear components. The conventional linear design must take this conflict into account.

77

Various advanced vehicles in modern aviation encounter tremendous changes in flight conditions. For instance, the parameters of a re-entry vehicle vary by two orders of magnitude. When a supersonic fighter with a VTOL capability is hovering at zero speed, the aerodynamic damping disappears and the transfer function from the stick movement for the stabilizing jets to the aircraft's longitudinal attitude becomes merely a double integration. Even under such sharply changing conditions, the vehicle dynamic response must remain relatively constant to provide the pilot or autopilot with almost invarying handling characteristics over the entire flight regime.

A controller designed for a fixed condition can never accomplish this; it would yield either poor performance or instability under some other flight condition. One obvious solution is to predict all possible flight conditions and program the parameters of the controller as functions of the appropriate parameters representing such flight conditions. In fact, until recently, such an approach had not been uncommon for missile autopilots. The adjustment of controller gain, for instance, is basically scheduled according to altitude and Mach number. When this system works, it works well with the distinct advantage of the fastest adaptation to the new environmental changes among all types of adaptive control systems. However, the following disadvantages were fatal:

1. The system is an open loop system in a certain sense. The operational strategies are based upon the mathe-

matically modelled plant for off-line analysis, not upon the real one. the controller would not know if an unprepared environmental condition arose. Using the terminology, it may be an adaptive control system, but clearly may not be a self-adaptive one.

2. Its versatility could be increased only by costly and time consuming processes. A series of wind tunnel tests would be needed to discover all the aerodynamic derivatives' profiles, and extensive systems analysis and simulations on the ground would be necessary in order to find out the optimum parameter programming. Finally a number of actual flight tests would have to be made to take account of pilot opinion.

3. Furthermore, a high performance vehicle might be so dominated by its nonlinear and time-varying characteristics that the usual Laplace transformed plant modeling would not be allowed. An advanced interceptor, for instance, can climb from the ground up to the stratosphere in one minute and can make very sharp turns. Such climbing ability might make the vehicle dynamic characteristics time-varying, since the flight condition could change greatly within a short time relative to the plane's characteristic time. Such maneuverability might nullify the standard small disturbance assumption on which the familiar linear equations of the vehicle dynamics are based, thus introducing significant nonlinear characteristics. The failure of a time-invariant linear model of the plant is one of the most condemned features of open loop adaptive control systems.

Even though response to one particular input might
be acceptable, response to another input might not. This
means that designers would have to work with almost infinite
numbers of combinations among the disturbance and command
inputs and the internal conditions of the plant, case by case.

A.2   Principles of Known Self-Adaptive Control Systems

The above discussion may be sufficient to justify
the need for more versatile, flexible and easily produced
self-adaptive control systems. With aircraft application in
mind, a variety of self-adaptive control systems have been
proposed, and some have been installed in actual aircraft.[13,23]
Each system has an indirect and implicit scheme for envir-
onmental identification. According to the basic technique
employed, the available self-adaptive control systems can be
roughly classified into three groups.

The first group includes those systems to which small
test signals are fed.[23] The signal is usually impulse or
sinusoidal. The response is monitored at a certain station
in the loop and is kept invariant by an adjusting mechanism.
In the Sperry Self-Adaptive Control System, for instance,
narrow, small amplitude pulses are fed to the servo actuator,
and the response of the servo is measured. If the system is
linear, the impulse response may also be obtained by applying
white noise and evaluating the cross-correlation function of
the output and input with appropriate electronic circuitry.[6,13]

The second group includes those systems which have a precisely defined mathematical performance index. In the model reference self-adaptive control system, which was proposed originally by the M.I.T. group, the command input signal is fed to both the adaptive loop and the model simultaneously.[14,22,24] The performance index is a quadratic function of the error between the output of the actual plant and that of the model. In addition, the index may contain the error time derivatives. The parameters of the controller are continuously adjusted to minimize the index by the parameter influence technique.

The perturbation parameter tracking self-adaptive control systems, which were originally studied for aircraft engine cruise control, may also belong to this category.[6,15] In these systems, each adjustable parameter or the control input itself is periodically perturbed about its present average value by either a linear or sinusoidal sweep with an amplitude large enough to catch the values that extremize the performance index. Assuming that the average value of the parameter is not far from the optimum and that a parabolic relationship exists between the performance index and the parameter, the average fundamental components of the error signals in the index are used to drive the average value closer to the optimum through appropriate filtering and network techniques.

The third group consists of those systems which contain a relay in the main adaptive loop as an important element.[16,17] Two well-known systems are the Minneapolis-Honeywell Self-Adaptive System and the MG-90 Adaptive Flight Control System,

also developed by Minneapolis-Honeywell. Despite the fact

that both of the two utilize a relay and are described by the

same basic block diagram (fig. A.2) with the model as input

filter, the two are operationally entirely different from

each other, making use of different relay characteristics.

As mentioned earlier in connection with the system in fig.

A.2, a very high forward gain would yield a self-adaptive

control system only when (a) this high gain is produced in

the controller and (b) there is no risk of instability. In

no linear system will both (a) and (b) be true at the same

time.

The use of relays in the controller, however,

improves the situation. First, an infinitely high gain is

theoretically obtainable by relay. Second, although this high

gain tends to cause instability in the loop, this instability

is not a rapidly diverging one as in linear systems, but

rather a virtually constant oscillation called a limit cycle

(presumably a stable limit cycle). Last, the magnitude and

frequency of this limit cycle are controllable, and while

maintaining a relatively high gain, one can remove this limit

cycle entirely.

Keeping these advantages of the relay in mind, let us

look first at the principle behind the Minneapolis-Honeywell

Self-Adaptive Control System.[6,20,21] Fig. A.3 shows the block

diagram when the system operates as a pich-rate command system.

The fundamental goal of the system is to keep the effective

forward gain high enough to maintain a small error rate, e,

while eliminating a possible limit cycle in the loop. Note that the switching logic circuit is simply a proportional plus derivative circuit.

The A-C dither signal is fed to the electronic relay along with the output of the switching logic circuit. This external dither signal is B sin 2πft. where the amplitude B is constant and the frequency f is 2000 cps. The role of the dither signal is to alter the relay characteristics as shown in fig. A.4. A represents the average magnitude of the input to the relay. Since the contribution of the dither signal will be averaged out, A actually represents the average magnitude of the switching logic circuit output which is a linear combination of e and $\dot{e}$. The solid curve represents the normalized equivalent gain $K_{eq}(A,B)$ obtained by the dual input describing function technique for the perfect relay when the dither signal is present.[6] For comparison, the normalized equivalent gain when no dither signal is present is shown (dotted curve). The important feature of the alteration is the fact that K_{eq} is kept finite, while for the conventional describing function, K_{eq} goes to infinity for small input signals.

Now let G(s) be the open loop transfer function excluding the dual input describing function. Suppose that there is no dither signal so the K_{eq} can take any value from zero to infinity, regardless of the switching level M. As seen in fig. A.5, there is always an intersection between the

$-\dfrac{1}{K_{eq}}$ segment and the plot of G(jw) in the complex plane. This clearly indicates that the limit cycle is unavoidable.

Now let us introduce a dither signal so that there is a maximum finite value kM for K_{eq} where k is a constant (see fig. A.4). Since the $-\dfrac{1}{K_{eq}}$ segment is thus shifted to the left, it is now possible to eliminate the intersection and avoid the limit cycle as shown in fig. A.6a. Fig. A.6b shows the Nyquist plot for the overall open loop transfer function and indicates that the system is stable according to the Nyquist criterion as well. Further, for adaptability, the incremental Nyquist plot must be stationary in the complex plane with a certain stability margin. For this purpose, the switching level M is adjusted as follows: M is assigned its maximum value to make K_{eq} as great as possible, since a large average error implies that the gain for the overall open loop transfer function $K_{eq}G(jw)$ is insufficient. Next, if the average error starts to decrease significantly, due perhaps to an increasing G(jw), M should be decreased to reduce the possible values for K_{eq} and to avoid any possibility of a limit cycle.

The system was flight tested in a F94c. The performance was reported to be excellent except at the extreme ranges of the flight envelope.

The MH-90 Adaptive Flight Control System (fig. A.7) does not try to eliminate the limit cycle. The basic aim of the system is to maintain a limit cycle with an amplitude

small enough to be tolerable for a pilot and passengers, as well as for hardware components.[13,16,23] The limit cycle is fed through a narrow band filter which is tuned to 25 rad/sec, the ideal limit cycle frequency. The output of the filter is rectified and compared to a set point of the limit cycle amplitude. The difference is used to regulate the forward loop gain through the switching level control so as to reduce the difference. The aircraft for which this system has been equipped are the experimental aerospace vehicle X-15, the supersonic delta-wing VTOL prototype fighter Hawker P 1127, and the F-102A interceptor. It was announced that the Dyna Soar vehicle was also to be equipped with such a system. Although this limit cycle adaptive flight control system has only been tested in such small aircraft, it appears to be highly successful, thus far. For large vehicles, which ordinarily have a structural characteristic frequency in the range 5 to 10 c/s, some improvement would be necessary to avoid a catastrophic resonance, for the limit cycle frequency is likely to be in this same range.

A.3   Comparison with the Proposed System

Both of the Minneapolis-Honeywell systems employ both the concept of a prefilter representing the model and the principle of a follow-up servo. In the proposed system, on the other hand, the model is cast ahead of the bang-bang element as the switching function. The switching level adjustment logic can greatly reduce the chatter frequency and

even halt the chatter, if properly designed. In the Minneapolis-Honeywell Self-Adaptive System, elimination of the limit cycle (substantially the same phenomenon as chatter) is accomplished with the help of the externally introduced dither signal. In the other Minneapolis-Honeywell system, the limit cycle is regulated more explicitly by the auxiliary loop containing the amplitude setting and the filter tuned to the ideal frequency.
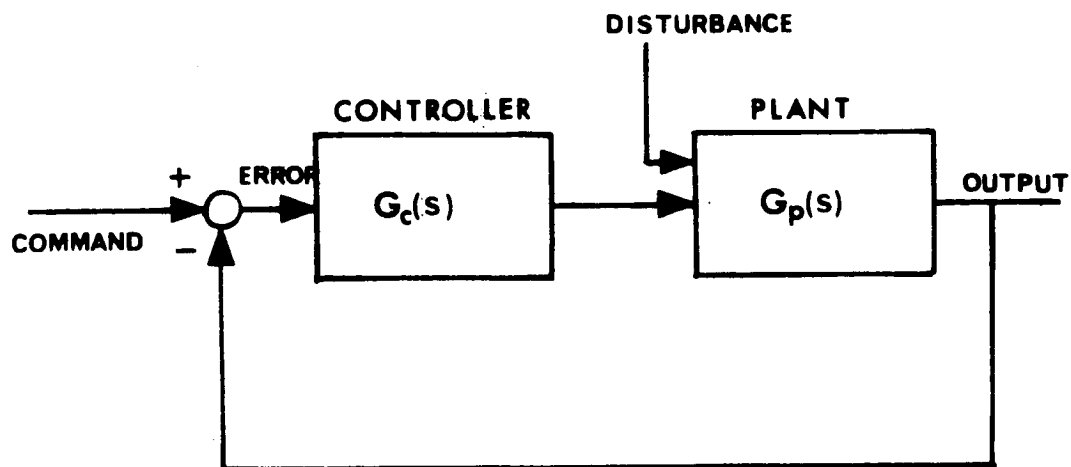
Fig. A.1 Follow-Up Servo System
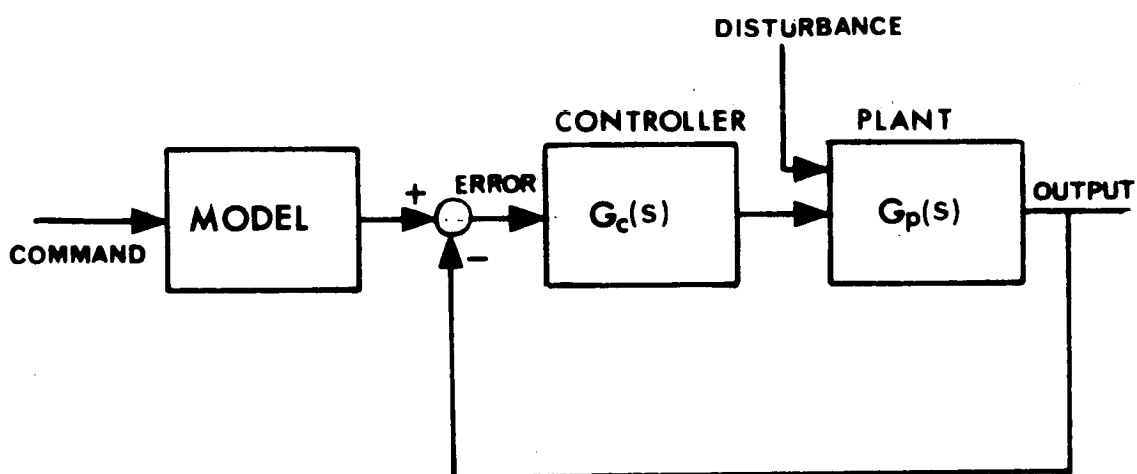
Fig. A.2 Linear Self-Adaptive Control System Based
on the Follow-Up Principle
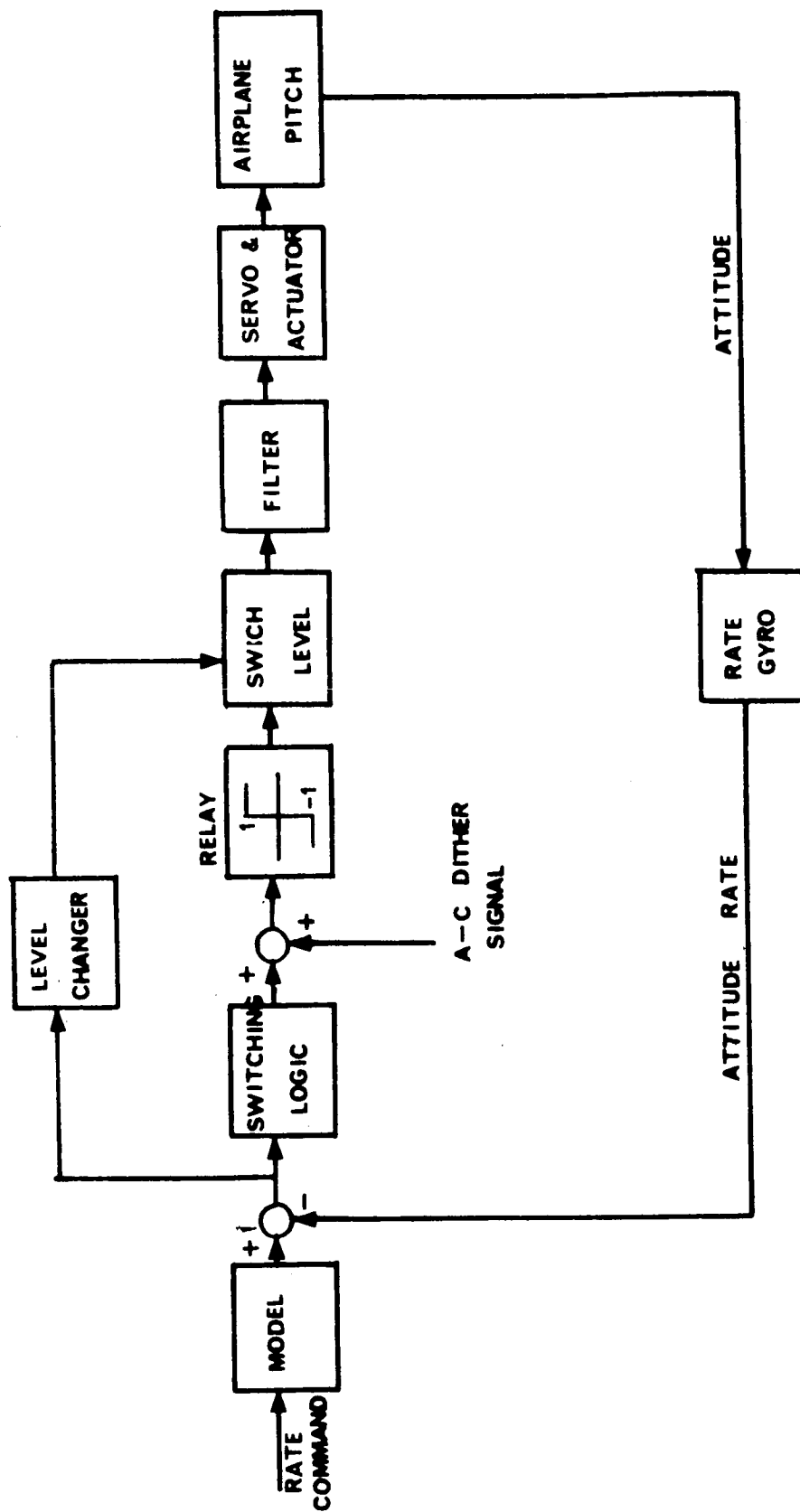
Fig. A.3 Functional Block Diagram of the Minneapolis–Honeywell
Self-Adaptive Control System
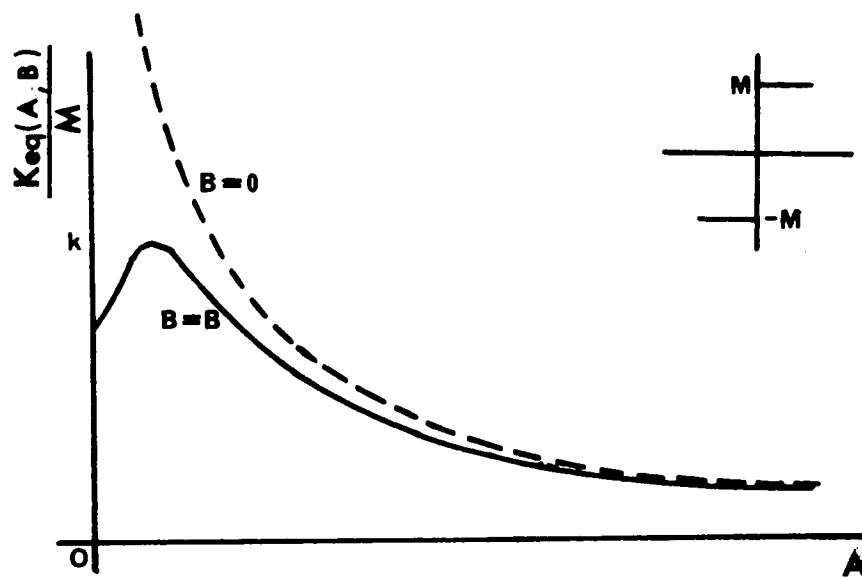
Fig. A.4   Sketch of the Dual Input Describing Function
for the Perfect Relay
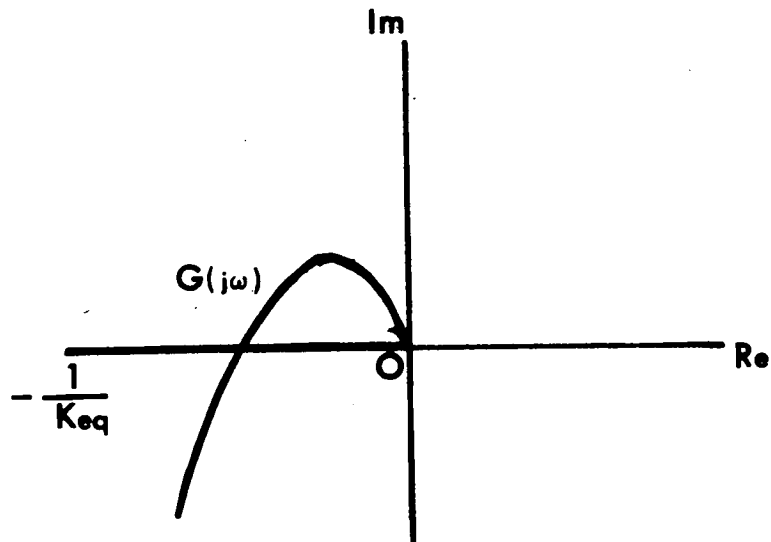
Fig. A.5   Unavoidable Existence of Limit Cycle

for the Conventional Perfect Relay
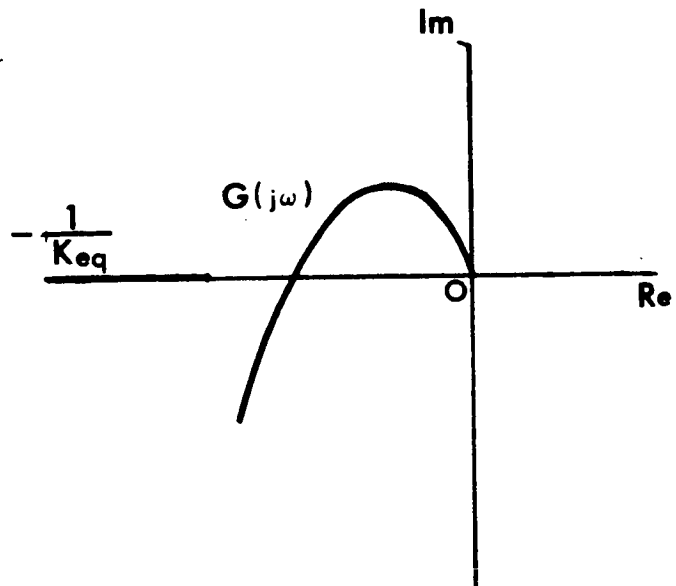
Fig. A.6a Elimination of Limit Cycle
by the Dither Signal
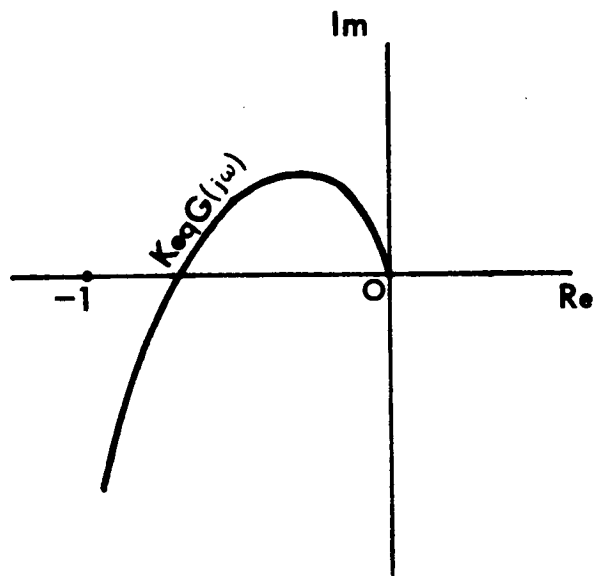
Fig. A.6b Incremental Nyquist Plot

90
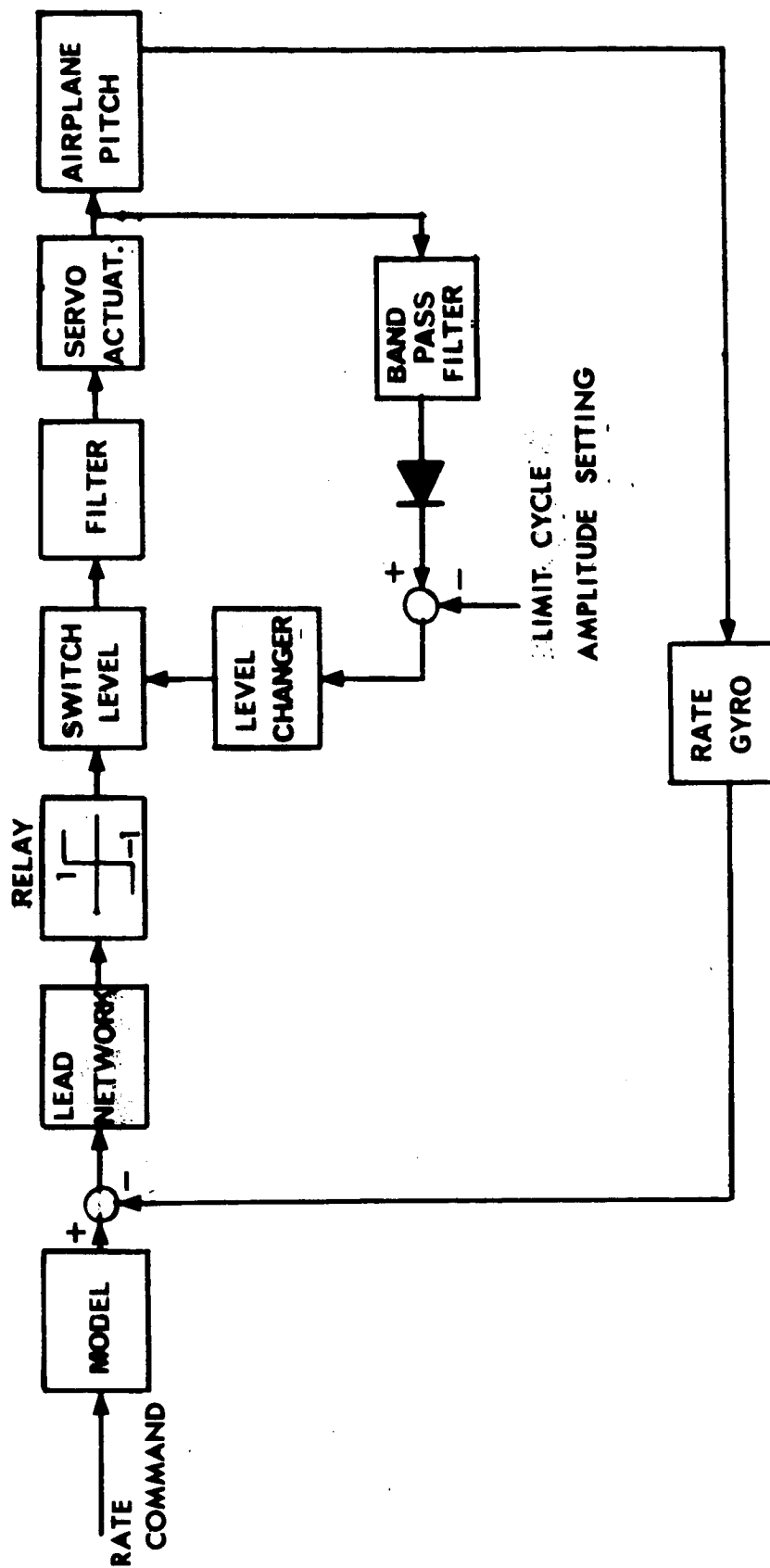
Fig. A.7 Block Diagram of the MH-90 Adaptive
Flight Control System

APPENDIX B

SOME CONSIDERATIONS ON

DISTRIBUTED PARAMETER SYSTEM APPLICATION

B.1   Current Studies on Distributed Parameter Control

Systems

A distributed parameter system is one whose para-
meters are distributed in space. Mathematically, such a
system is usually governed by a partial differential equation
or integral equation, while a lumped parameter system is gov-
erned by a set of ordinary differential equations. Many
energy converters such as chemical reactors, nuclear reactors,
furnace systems, fluid transport systems, and heat exchangers
are regarded as distributed parameter systems. In the design
of attitude control systems for an aerospace vehicle with
distinct structural flexibility or fuel sloshing, a distributed
paramter model of the vehicle is used.

One possible approach to distributed parameter systems
design is to employ the spatial quantization technique that has
been used to obtain a numerical solution of partial differential
equations. With this technique, the original equation is
approximately converted to a set of ordinary differential-
difference equations. The design problem could then be handled
using the well-developed feedback control techniques for lumped

92

parameter systems. This so-called modal approach can be found in ref. 30, where distributed feedback is introduced, leading in practice to multiple feedback loops. Generally speaking, however, such an approach might be erroneous, since the actual system does not always register satisfactory performance, or, at worst, it might become unstable. This would probably happen if the partition for the quantization is not thick enough. Suitable partitioning, on the other hand, would require dozens of feedback loops.

The recent trend has been to focus directly on the original partial or integral equation itself in dealing with design problems concerning performance and stability. In particular, there is increasing interest in optimal control with regard to distributed parameter systems. Study in this area is particularly important from an economic point of view. In the chemical industry, for example, a 1% cutdown on some engineering performance index might result in saving millions of dollars, far more than the initial cost of the extra machines.

In 1960, Butkovskii and Lerner initiated the theoretical study of optimal control of distributed parameter systems.[26] Shortly thereafter, in a series of papers[27,28] Butkovskii developed a general problem formulation and derived the maximum principle for distributed parameter systems, which is analogous to the maximum principle for lumped parameter systems derived by Pontryagin, et al.

Theoretical contributions following these pioneer works can be found in papers by Wang,[33] Sakawa,[31,32] Yeh and Ton,[34]

Axelband[25] and Chandhuri.[29] To date, considerable work has been done on various types of linear partial differential equations, although the mathematics involved in the process of analysis is in such difficult and abstract fields as functional analysis and semi-group theory. In most of the works, a norm of a certain functional in Banach space is taken as the performance index to be minimized. The resulting control law is governed by an integral equation or integro-differential equation.

Particularly if the control force is limited in magnitude, control has proven to be of the bang-bang type, while the governing equation becomes a non-linear integral equation involving the sign function. Such governing equations are almost impossible to solve analytically, as is the Hamilton-Jacob partial differential equation governing the optimum control law for lumped parameter systems.

Some other procedures for obtaining the numerical version of the optimum control law for distributed parameter systems have been suggested. Wang has developed a bang-bang type quasi-time-optimum control scheme for a fairly general class of distributed parameter systems for which the corresponding uncontrolled systems are stable. This method is simple and practical, and the idea is basically analogous to quasi-time-optimum control with linear switching functions for lumped parameter systems. Extension of such an idea would lead to the application of the chatter mode adaptive policy for distributed parameter systems.

B.2   Analysis of the Application to Parabolic Systems

Let D be a bounded, open, simply connected subset of a Euclidian space, which is assumed for simplicity to have at most three dimensions. The boundary of D will be denoted by ∂D, and the time interval $[0,+\infty]$, by T. Let the problem be a boundary value control type, so that the boundary ∂D consists of two subsets, the controlled boundary ∂D_c and the uncontrolled boundary ∂D_u. Further, ∂D_u may be divided into the prescribed boundary ∂D_p and the free boundary ∂D_f. These boundaries are not necessarily connected. The general form of the governing equation for the distributed parameter systems under consideration takes the partial differential equation of the parabolic type:

$$\frac{\partial q}{\partial t} = \mathcal{L} \, q \qquad (B.1)$$

for all

$$(t,\underline{x}) \in T \times D$$

where the independent scalar variable q is a function of time t and the spatial vector $\underline{x}$, i.e.,

$$q = q(\underline{x},t)$$

and the notation $\mathcal{L}$ stands for a linear spatial differential operator of the elliptic type:

$$\mathcal{L} = a \, \nabla^2 + \underline{b} \, \nabla + c \qquad (B.2)$$

or if the divergence form is used

$$\mathcal{L} = a^* \nabla + \nabla \underline{b}^* + c^* \qquad \text{(B.3)}$$

where, as usual, ∇^2 represents the Laplacian operator, ∇(scalar) the gradient vector of the scalar, and ∇(vector) the divergence of the vector. Each of the parameters a, $\underline{b}$, c, and their asterisked form may be a function of both t and $\underline{x}$. There are the following relations between the asterisked and un-asterisked forms:

$$a = a^*$$
$$\underline{b} = \nabla a^* + \underline{b}^* \qquad \text{(B.4)}$$
$$c = \underline{b}^* \nabla + c^*$$

Let the initial distribution $q(\underline{x},0)$ be $q_0(\underline{x})$

$$q(\underline{x},0) = q_0(\underline{x}) \qquad \text{for all } \underline{x} \in D \qquad \text{(B.5)}$$

Let the prescribed boundary condition be $q_p(\underline{x},t)$

$$q(\underline{x},t) = q_p(\underline{x},t) \qquad \text{for all } \underline{x} \in \partial D_p \qquad \text{(B.6)}$$

The bang-bang control function u is assumed to be homogeneous over the controlled boundary, and it makes the boundary condition the Dirichlet type, the Neumann type, or the general type, namely

$$u(t) = B(t) \text{ sgn } S(t) = \begin{cases} q(\underline{x},t) & \text{Dirichlet type} \\ \dfrac{\partial q(\underline{x},t)}{\partial n} & \text{Neumann type} \\ \alpha q(\underline{x},t) + \beta\dfrac{\partial q(\underline{x},t)}{\partial n} \end{cases} \quad \text{(B.7)}$$

general type

$$\alpha, \ \beta = \text{constants}$$

for all $\underline{x} \in \partial D_c$

where $\frac{\partial q}{\partial n}$ represents the normal derivative of q or the component of ∇q in the direction of the outer normal vector $\underline{n}$ at the boundary. If q represents temperature, for instance, the control function may be the temperature itself at the boundary for the Dirichlet type, the heat flow rate through the boundary for Neumann type, and the temperature of the surrounding medium for the general type.

Let

$$e(\underline{x},t) = q(\underline{x},t) - q_d(\underline{x}) \quad \text{(B.8)}$$

for all $\underline{x} \in D$

where $q_d(\underline{x})$ represents the desired steady distribution.

It is now desired to drive the system from the initial state so as to make $e(\underline{x},t)$ eventually remain null for all $\underline{x} \in D$. Let $2y(t)$ be the squared Euclidean norm for $e(\underline{x},t)$, namely

$$y(t) = \tfrac{1}{2} ||e(\underline{x},t)||^2 = \tfrac{1}{2} \iiint_D e^2(\underline{x},t) \ d\tau \quad \text{(B.9)}$$

where dτ represents the elementary volume. Clearly, if $y(t)$ is kept identically zero, so also is $e(\underline{x},t)$ for all $\underline{x} \in D$. Keeping this in mind, let us establish the switching function such that

$$S = y(t) - g(t) \qquad (B.10)$$

where $g(t)$ presumably has the following properties:

$$g(t) > 0 \qquad \text{for } 0 < t < \infty$$

$$\qquad (B.11)$$

$$\lim_{t \to \infty} g(t) = 0$$

In addition, $g(t)$ is differentiable at least once. The specific form is to be determined for a particular case. Now $\dot{S}$ becomes

$$\dot{S} = \dot{y}(t) - \dot{g}(t) \qquad (B.12)$$

$\dot{y}(t)$ can be evaluated as follows. From eq. (B.9)

$$\dot{y}(t) = \iiint_D e \frac{\partial e}{\partial \tau} \, d\tau \qquad (B.13)$$

Using eq. (B.1), (B.2), and (B.8)

$$\dot{y}(t) = \iiint_D [a \, q \, \nabla^2 q + q \, \underline{b} \, \nabla q + c \, q^2 - a \, q_d \, \nabla^2 q$$

$$- q_d \, \underline{b} \, \nabla q - c \, q_d \, q] \, d\tau \qquad (B.14)$$

98

But Green's theorem says

$$\iiint_D a\,q\,\nabla^2 q\,d\tau = \iint_{\partial D} a\,q\,\frac{\partial q}{\partial n}\,d\sigma$$

$$- \iiint_D (\nabla a\,q)\,\nabla q\,d\tau \tag{B.15}$$

where $d\sigma$ represents the elementary surface area.
Hence $\dot{S}$ takes the form

$$\dot{S} = \iint_{\partial D_c} a\,q\,\frac{\partial q}{\partial n}\,d\sigma \;+\; \gamma(t) \tag{B.16}$$

where

$$\gamma(t) = \iint_{\partial D_n} a\,q\,\frac{\partial q}{\partial n}\,d\sigma + \iiint_D [q\,\underline{b}\,\nabla q - (\nabla aq)\,\nabla q$$

$$\tag{B.17}$$

$$+\, c\,q^2 - a\,q_d\,\nabla^2 q - q_d\,\underline{b}\,\nabla q - c\,q_d\,q]\,d\tau$$

If the control is Dirichlet type, we obtain from eq. (B.7) and (B.16)

$$\dot{S} = B\,\text{sgn}\,S \iiint_{D_c} a\,\frac{\partial q}{\partial n}\,d\sigma + \gamma(t) \tag{B.18}$$

In order for the above expression to take the form of (3.1a), B must be

$$B = -\,M\,\text{sgn}\,\mu \tag{B.19}$$

99

where

$$\mu = \iint_{\partial D_c} a \frac{\partial q}{\partial n} \, d\sigma \qquad \text{(B.20)}$$

and the switching level M is normally positive.
$\dot{S}$ can now be rewritten as

$$\dot{S} = -\mu M \, \text{sgn} \, \mu \, \text{sgn} \, S + \gamma(t) \qquad \text{(B.21)}$$

and the control force u is

$$u = -M \, \text{sgn} \, \mu \, \text{sgn} \, S \qquad \text{(B.22)}$$

In most physical systems the solution to the partial differential equation can be expressed as

$$q(\underline{x},t) = k_0(\underline{x},t) + \int_0^t k_1(\underline{x},t-\tau) u(\tau) \, d\tau \qquad \text{(B.23)}$$

for $\underline{x} \in D$

where the concrete expressions for k_0 and k_1 are determined by the specific form of the partial differential equation (B.1) and the prescribed initial and boundary conditions. In spite of the bang-bang behavior of the control force u, $q(\underline{x},t)$ for $x \in D$ will be continuous in time, owing to the convolution integral in eq. (B.23). The same is also true for ∇q and $\nabla^2 q$. Thereby, $\gamma(t)$ will not register any undesirable discontinuous phenomena directly coupled with u given in eq. (B.22). A certain appropriate switching level adjustment would thus be

possible in order to sustain the chatter mode or to keep S

near zero, and consequently to drive $q(\underline{x},t)$ eventually to the

desired distribution $q_d(\underline{x})$.   Fig. B.1   shows the mathematical

block diagram for the Dirichlet type control discussed.   The

case for the Neumann or general type control can be similarly

analyzed.
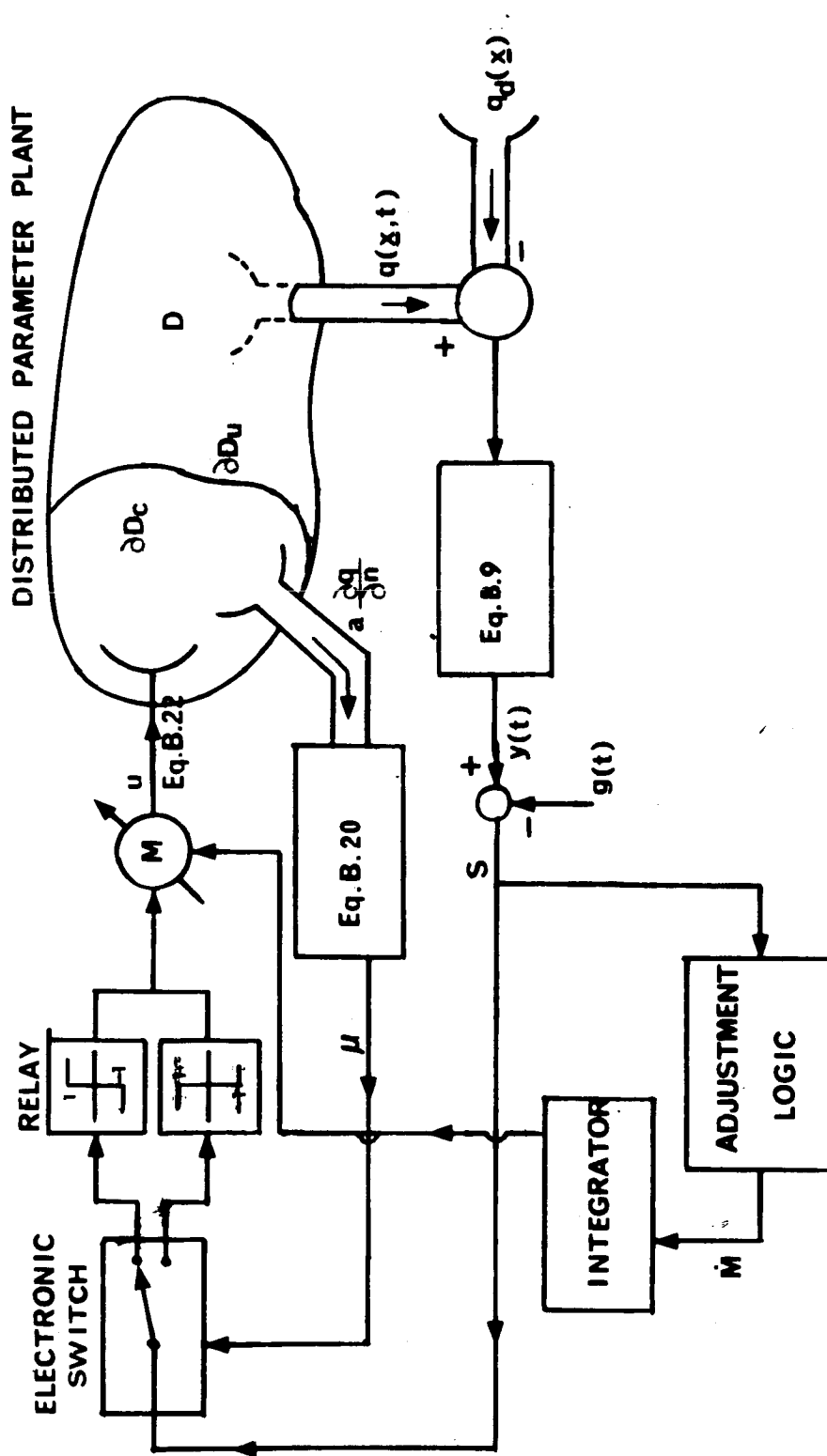
Fig. B.1 Block Diagram of a Distributed
Parameter Control System

APPENDIX C

AN APPLICATION OF THE CHATTER MODE:
NUMERICAL SOLUTION OF ORDINARY DIFFERENTIAL EQUATIONS

As a byproduct of this study, a new method for obtaining the numerical solution of ordinary differential equations has been discovered. Once the chatter mode is reached, as mentioned in the body of this thesis, the average dynamic behavior of the system is completely described by the equation of the switching function and is independent of the plant's characteristic equation.

Given an ordinary differential equation to solve, we can think of it as a switching function. First, we create an analytically solvable differential equation involving this switching function and assign a suitable initial condition to this secondary equation. Then we achieve a continuous chatter mode with switching levels of great magnitude. The output from the auxiliary equation will be the solution to the original equation. The following paragraphs present the concrete description of this method.

In general, an ordinary differential equation of n'th order can be written in the form

$$x^{(n)} - f \{ x^{(n-1)}, x^{(n-2)}, \ldots, \dot{x}, x, t \} = 0 \quad (C.1)$$

The equation may be linear or nonlinear, time-variant or time-invariant, and either homogeneous or not. The initial condition for the above equation is assumed to be given

at t=0 $\qquad$ (C.2)

$$x = x(0) \qquad \dot{x} = \dot{x}(0) \quad . \ . \ . \quad x^{(n-1)} = x^{(n-1)}(0)$$

The state variable representation is

$$x = x_1$$
$$\dot{x} = \dot{x}_1 = x_2$$
$$\ddot{x} = \dot{x}_2 = x_3 \qquad\qquad\qquad (C.3)$$

$$. \ . \ .$$

$$x^{(n)} = \dot{x}_n = x_{n+1}$$

The left hand side of eq. (C.1) is rewritten, and is now regarded as the switching function S

$$S = x_{n+1} - f(x_n, x_{n-1}, \ . \ . \ ., x_2, x_1, t) \qquad (C.4)$$

The initial condition (C.2) is also converted

at t=0

$$x_1 = x_1(0) \quad x_2 = x_2(0) \quad . \ . \ . \quad x_n = x_n(0) \qquad (C.5)$$

Next, let us draw up a new differential equation of n+1'th order

$$x^{(n+1)} = u \qquad\qquad\qquad (C.6a)$$

or

104

$$\dot{x}_1 = x_2$$

$$\dot{x}_2 = x_3$$

$$\cdot \ \cdot \ \cdot$$

$$\dot{x}_n = x_{n+1}$$

$$\dot{x}_{n+1} = u$$

(C.6b)

where u represents the "bang-bang* control force" expressed by

$$u = -M \ \text{sgn} \ S$$

and where M is the switching level and is positive. Using eq. (C.4), (C.6b), and (C.7), $\dot{S}$ becomes

$$\dot{S} = \dot{x}_{n+1} - \frac{\partial f}{\partial t} - \sum_{i=1}^{n} \frac{\partial f}{\partial x_i} \dot{x}_i$$

(C.8)

$$= -M \ \text{sgn} \ S - \frac{\partial f}{\partial t} - \sum_{i=1}^{n} \frac{\partial f}{\partial x_i} x_{i+1}$$

where the function f has been assumed to be differentiable at least once for each of its arguments.

The form of eq. (C.8) certainly indicates a potential chatter mode for large values of M. The initial condition associated with the auxiliary differential equation (C.6b) should be selected to match the given initial condition (C.5) of the original differential equation (C.1). $x_{n+1}(0)$, which is necessary in the initial condition of the auxiliary equation but missing in that of the original equation, should be arti-

ficially specified in such a way that the initial value of the switching function, S_0, is essentially zero. If u is given, the auxiliary equation is solvable analytically, and no numerical integration is needed.

Now suppose that the chatter mode has been continuous from t=0 to the present time, t, and the control polarity has reversed j times, or, in other words, the digital computer has found the sign of S changed j times. Let t_j be the time when the last reversal occurred (fig. C.1). Let us define the following:

$$\Delta t \equiv t - t_j \qquad\qquad j = 0, 1, \ldots \qquad\qquad (C.9)$$

$$\Delta t_\ell \equiv t_{\ell+1} - t \qquad\qquad \ell = 0, 1, \ldots, j-1 \quad (C.10)$$

$$S_j \equiv s(t_j) \qquad\qquad\qquad\qquad\qquad\qquad (C.11)$$

$$u_j \equiv u(t_j{}^+) \qquad\qquad\qquad\qquad\qquad\qquad (C.12)$$

In eq. (C.10, t_ℓ represents the time of the ℓ'th reversal, $t_0 = 0$. By definition,

$$u(t) = u_j = -M\ \text{sgn}\ S_j = (-1)^j\ u_0 \qquad\qquad (C.13)$$

But u(t) may not necessarily be -M sgn S(t) because the computation time is discrete as indicated in fig. C.1.

The equation describing the present state can be readily obtained by integrating the auxiliary equation (C.6b) from t_j to t with u_j such that

106

$$x_{n+1}(t) = x_{n+1}(t_j) + u_j \Delta t$$

$$x_n(t) = x_n(t_j) + x_{n+1}(t_j) \Delta t + \frac{u_j}{2} \Delta t^2 \qquad\qquad \text{(C.14)}$$

. . . .

$$x_1(t) = x_1(t_j) + x_2(t_j) \Delta t + \ldots + \frac{x_{n+1}(t_j)}{n!} \Delta t^n$$

$$+ \frac{u_j}{(n+1)!} \Delta t^{n+1}$$

where the initial value of j is 0. For each value of t after t_j, the state is computed according to the above equation. If the sign of S has been changed according to eq. (C.4), t becomes the new t_j, the control force changes its polarity, and the old $x_1(t_j)$, $x_2(t_j)$ . . ., $x_{n+1}(t_j)$ are replaced by new values. The switching level M should be great enough to maintain the chatter mode throughout a run.

Since no numerical integration is involved in this method, there is no accumulated truncation error, which is a disadvangage of other methods, such as the Runge-Kutta method, especially when the size of the time steps is too small. In the proposed method, the smaller the size of these steps, the more accurate the solution, because extremely small steps permit the computer to find the sign change before the state point deviates significantly from the switching surface. The variables to be stored in the memory are essentially the state variables at the last switching time, $x_1(t_j)$, $x_2(t_j)$, . . . $x_{n+1}(t_j)$. This will require considerably less storage than the Rugne-Kutta method. Fig. C.2 shows the flow chart illustrating the proposed procedure.
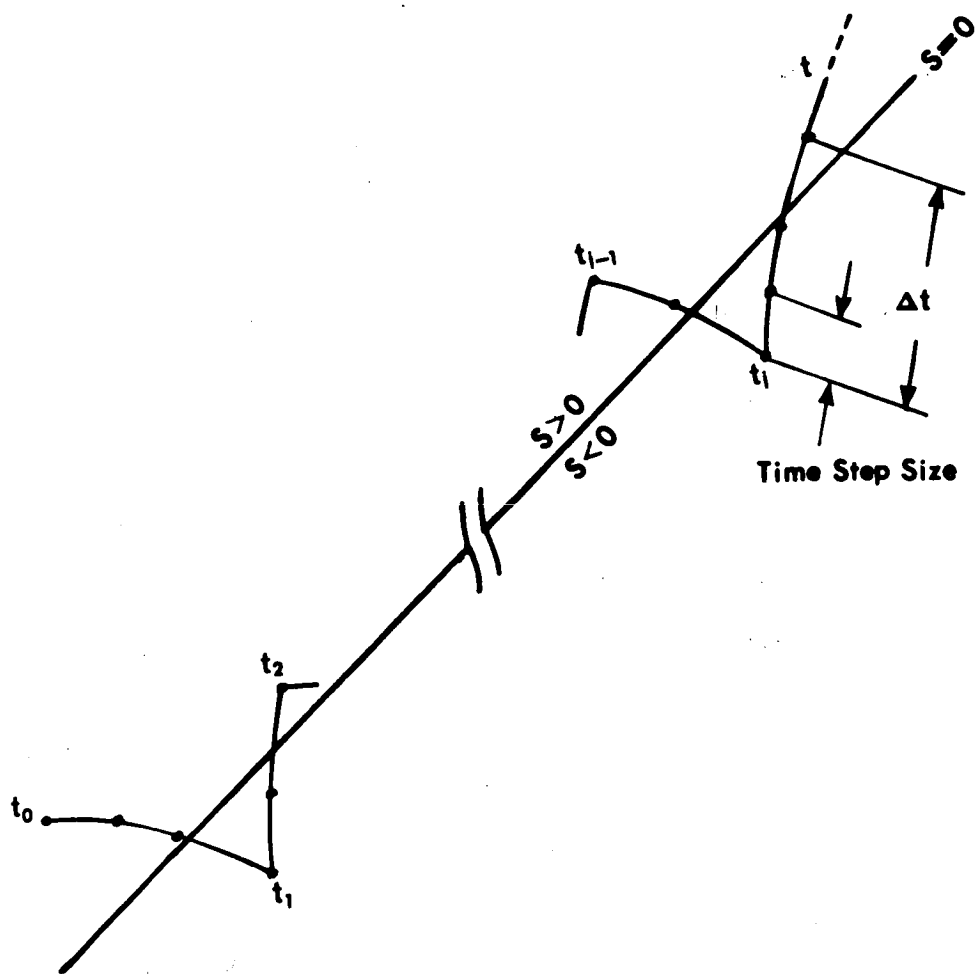
Fig. C.1 State Space Representation of the Numerical
Solution to an Ordinary Differential Euqation
by the Proposed Method
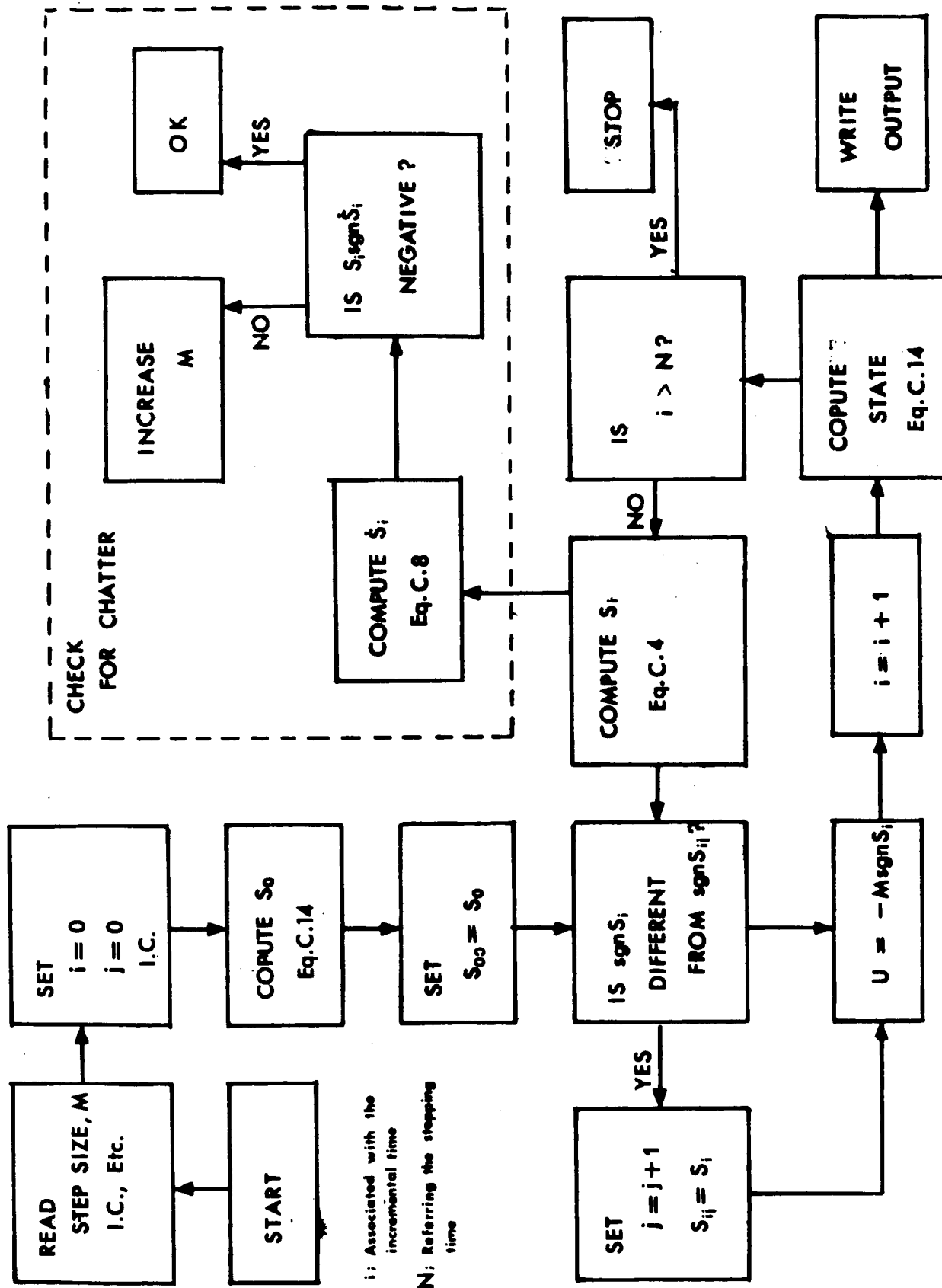
Fig. C.2 Flow Chart for the Proposed Method of Solving
Ordinary Differential Equations

START

READ
STEP SIZE, M
I.C., Etc.

SET
i = 0
j = 0
I.C.

COPUTE S₀
Eq.C.14

SET
S₀₃ = S₀

IS sgnSᵢ
DIFFERENT
FROM sgnSᵢⱼ?

SET
j = j + 1
Sᵢⱼ = Sᵢ

U = −MsgnSᵢ

COMPUTE Sᵢ
Eq.C.4

i = i + 1

COPUTE
STATE
Eq.C.14

WRITE
OUTPUT

IS
i > N ?

STOP

COMPUTE Ṡᵢ
Eq.C.8

IS SᵢsgnṠᵢ
NEGATIVE ?

INCREASE
M

OK

CHECK
FOR CHATTER

i; Associated with the
incremental time

N; Referring the stopping
time

109

REFERENCES

1. du Pressis, J. J., "An Investigation of Chatter Reduction Schemes of a Linear Switching Control System," S.M. Thesis, M.I.T., September 1966

2. Flugge-Lotz, I., Discontinuous Automatic Control, Princeton University Press, Princeton, N.J., 1953

3. Flugge-Lotz, I, and Lindberg, H. E., "Studies of Second- and Third- Order Contactor Control Systems," NASA TN D-107, October 1959

4. Flugge-Lotz, I., and Ishikawa, T., "Investigation of Third-Order Contactor Control Systems with Two Complex Poles without Zeros," NASA TN D-428, June 1960

5. Flugge-Lotz, I., and Ishikawa, T., "Investigation of Third-Order Contactor Control Systems with Zeros," NASA TN D-719, January 1961

6. Gibson, J. E., Nonlinear Automatic Control, McGraw-Hill, New York, 1963, Chapters 9 and 11

7. Johnson, G. W.,"Synthesis of Control Systems with Stability Constraints via the Direct Method of Liapunov," IEEE Trans. on Automatic Control, Vol. AC-9, No. 1, July 1964

8. Kalman, R. E., and Bertran, J. E., "Control System Analysis and Design via the Second Method of Lyapunov," Part I and II, Trans. of ASME, Vol. 82, Series D, June 1960

9. Tsien, H. S., Engineering Cybernetics, McGraw-Hill, New York, 1954, Chapter 15

10. Weissenberger, S., "Stability Analysis of Relay-Controlled Systems via the Direct Method of Lyapunov," NASA CR-320, 1965

11. Weissenberger, S., "Stability-Boundary Approximations for Relay-Controlled Systems via a Steepest Ascent Construction of Lyapunov Functions," Trans. of ASME, Series D., June 1966

12. Yasui, S., and Young, L. R., "Manual Time Optimal Control for High Order Plants," USC-NASA Conference on Manual Control (in press) March 1967

For Appendix A:

13. Blakelock, J. H., Automatic Control of Aircraft and Missiles, Wiley & Sons, Inc., New York, 1965, Chapter 6

14. Donalson, D. D., and Leondes, C. T., "A Model Reference Parameter Tracking Technique for Adaptive Control Systems I - The Principle of Adaptation," IEEE Trans. on Automatic Control, Sept. 1963

15. Draper, C. S., and Li, Y. T., "Principles of Optimalizing Control Systems and an Application to the Internal Combustion Engine," ASME Publication, New York, 1951

16. Gelb, A., "The Analysis and Design of Limit Cycling Adaptive Automatic Control Systems," Sc.D. Thesis, M.I.T., August 1961

17. Li, Y. T., and Vander Velde, W. E., "Philosophy of Non-Linear Adaptive Systems," Proceedings of the First International Congress of IFAC, Moscow, USSR, June 1960

18. Li, Y. T., and Whitaker, H. P., "Performance Characterization for Adaptive Control Systems," Proceedings of the First International Symposium on Optimizing and Adaptive Control, IFAC, Rome, Italy, April 1962

19. Li, Y. T., Young, L. R., and Meiry, J. L., "Adaptive Functions of Man in Vehicle Control Systems," IFAC Symposium, Teddington, England, September 1965

20. McClean, J. D., and Schmidt, S. F., "On the Design of a High-Gain Saturating Control System for Use as an Adaptive Autopilot," NASA TN D-305, February 1960

21. McNeil, D. H., McClean, J. D., Hegarty, D. M., and Heinle, R. H., "Design and Flight Tests of an Adaptive Control System Employing Normal Acceleration Command," NASA TN D-858, April 1961

22. Hersh, R. S., and Watts, G. L., "Model Reference Adaptive Control System for a Supersonic Transport," M.S. Thesis, M.I.T., June 1964

23. Noton, A. R. M., "The Case for Adaptive Autostabilization of Aircraft," Control, May 1963

24. Osborn, P. V., Whitaker, H. P., and Kezer, A., "New Developments in the Design of Model Reference Adaptive Control Systems," Presented at the IAS 29'th Annual Meeting, New York, January 1961 or IAS Paper No. 61-39

For Appendix B:

25. Axelband, E. E., "An Approximation Technique for the Optimal Control of Linear Distributed Parameter Systems with Bounded Inputs," IEEE Trans. on Automatic Control, January 1966

26. Butkovskii, A. G., and Lerner, A. Y., "Optimal Control of Systems with Distributed Parameters," Automation and Remote Control, December 1960

27. Butkovskii, A. G., "Optimum Process in Systems with Distributed Parameters," Automation and Remote Control, January 1961

28. Butkovskii, A. G., "The Maximum Principle for Optimum Systems with Distributed Parameters," Automation and Remote Control, Vol. 22, October 1961

29. Chandhuri, A. K., "Concerning Optimum Control of Linear Distributed Parameter Systems," International Journal of Automatic Control, July 1965

30. Gould, L. A., "On the Modal Control of Distributed Systems with Distributed Feedback, IEEE Trans, on Automatic Control, October 1966

31. Sakawa, Y., "Solution of an Optimal Problem in a Distributed Parameter System," IEEE Trans. on Automatic Control, Vol. AC-9, October 1964

32. Sakawa, Y., "Optimal Control of a Certain Type of Linear Distributed Parameter System," IEEE Trans. on Automatic Control, Vol. AC-11, No. 1, January 1966

33. Wang, P. K. C., "On the Feedback Control of Distributed Parameter Systems, International Journal of Control, 1966 Vol. 3, No. 3

34. Yeh, H. H., and Ton, J. T., "Optimum Control of a Class of Distributed Parameter Systems," IEEE Trans. on Automatic Control, Vol. AC-12, No. 1, Feb. 1967